A CRYSTALLOGRAPHIC AND THEORETICAL STUDY OF HALOGEN···HALOGEN AND HALOGEN···HALIDE SYNTHONS

By

FIRAS FANDI AWWADI

A dissertation submitted in partial fulfillment of
the requirements for the degree of

DOCTOR OF PHILOSOPHY

WASHINGTON STATE UNIVERSITY
Department of Chemistry

August 2005

To the faculty of Washington State University:

The members of the committee appointed to examine the dissertation of FIRAS FANDI AWWADI find it satisfactory and recommend that it be accepted

_____

Chair

_____

_____

_____

ACKNOWLEDGEMENTS

I have many colleagues and friends I would like to thank. First and foremost I want to express my gratitude to my mentor and professor, Roger Willett. Without his support and help I would not have reached this achievement. I would like to thank Brendan Twamley. I would like to express my appreciation to the Committee, Dr. Jim Satterlee, Dr. Kirk Peterson and Dr. Chulhee Kang, whose help and assistance has also made this possible.

I would like to thank my friends and colleagues Adrienne Thorn and Ben Shepler for their help.

My family has also been supportive, especially my sister-in-law, Rehan.

A CRYSTALLOGRAPHIC AND THEORETICAL STUDY OF HALOGEN···HALOGEN AND HALOGEN···HALIDE SYNTHONS

ABSTRACT

by Firas F. Awwadi, Ph. D.
Washington State University
August 2005

Chair: Roger D. Willett

The physical nature of halogen···halogen and halogen···halide interactions has been investigated using both *ab initio* calculations and crystallographic studies. Both studies show that halogen···halogen and halogen···halide interactions are electrostatic in nature. An electrostatic model is proposed to explain these interactions. This model is based on two main ideas; (a) the presence of a positive electrostatic cap on the halogen atom (except for fluorine), (b) the electronic charge is anisotropically distributed around the halogen atom. Halogen···halogen contacts in organic molecules can be represented as C-Y_1···Y_2-C [where θ_1= C-Y_1···Y_2, θ_2 = Y_1···Y_2-C; Y = Cl, Br, I]. Halogen···halogen interactions are characterized by a Y_1···Y_2 separation distance less than the sum of van der Waals radii (r_{vdW}) of the halogen atoms. According to the electrostatic model, two preferred arrangements are possible; (a) θ_1= θ_2 = ca. 150°; (b) θ_1 =180° and θ_2 = 90°. The second arrangement is not investigated during our study due to the fact that at this geometry, other interactions interfere with these contacts. A population analysis of the Cambridge Structural Data Base and *ab initio* calculations

confirm the existence of the former geometry. Closely examining this geometry shows that these contacts are influenced by three factors; (a) the type of the halogen atom; (b) hybridization of the *ipso* carbon; (c) the nature of the other atoms that are bonded to the *ipso* carbon atom apart from the halogen atom.

Halogen···halide interactions are represented by C-Y···X (X = F^-, Cl^-, Br^-, I^-). These interactions are characterized by a Y···X distance less than sum of the r_{vdW} of the halogen atom and the ionic radius of halide anion, as well as a linear C-Y···X angle. This arrangement is expected from the electrostatic model - the halide anion should confront the positive electrostatic potential cap of the halogen. Two types of halogen···halide interactions are studied; (1) simple halogen···halide interactions. Results show that these interactions are influenced by four factors; (i) the type of the halide anion; (ii) the type of the halogen atom; (iii) the hybridization of the *ipso* carbon; (iv) the nature of the functional groups; (2) C-Y···X-Cu (Y = Cl, Br; X = Cl^-, Br^-). These interactions are studied in complexes of the type $(n\text{CP})_2\text{CuX}_4$ ($n\text{CP}^+$ = *n*-chloropyridinium; *n* = 2, 3, or 4; X = Cl^- or Br^-) and $\text{Cu}(n\text{bp})_2\text{X}_2$, (nbp = *n*-bromopyridine; *n* = 2 and 3). A comparison of the role of these synthons in these and previously published $(n\text{BP})_2\text{CuX}_4$ structures (nBP = *n*-bromopyridinium cations; X = Br^- or Cl^-; *n* = 2) shows that; (a) the heavier the halogen atom, the stronger these interactions; (b) the lighter the halide anion, the stronger these interactions and; (c) these interactions are stronger in the complexes of the $(n\text{BP})_2\text{CuX}_4$ in comparison to $\text{Cu}(n\text{bp})_2\text{X}_2$. All of these observations fit the electrostatic model. These studies show that halogen···halide interactions are directional in nature. This implies that this synthonic interaction can act as a potential crystal engineering tool in the directed architecture of supramolecular species.

TABLE OF CONTENTS

LIST OF TABLES

LIST OF FIGURES

DEDICATION

To the memory of my mother

CHAPTER ONE

INTRODUCTION

(a) Literature Review

Designing novel materials, either organic, inorganic or hybrid, with important properties, have resulted in the birth of a new discipline in solid-state chemistry, specifically crystal engineering.[1] Crystal engineering is concerned with the forces that hold and arrange the structural units inside the lattice, therefore understanding the forces will help in designing new materials. In contrast to molecular bonding, bonds connecting structural moieties in the lattice (*viz.* intermolecular interactions) are, in most cases, weak non-covalent interactions or, as named recently, supramolecular synthons.[1] The most widely studied types of these interactions are classical hydrogen bonds; where both the proton donor and acceptor are highly electronegative atoms such as oxygen, nitrogen and fluorine,[2] as well as aromatic-aromatic interactions.[1,3] These interactions are not only important to crystal engineering, but also to molecular recognition, protein stability and function.[1a] Other types of interactions, e.g. weaker non-classical hydrogen bonds (where either or both the proton donor and acceptor are of moderate electronegativity[4]) and halogen···halogen contacts,[5] have been found to play an important role in crystalline structural architecture. Therefore, the role of these supramolecular interactions must be thoroughly understood before *a priori* crystal structure prediction.

In our study, we are investigating the nature of halogen···halogen and halogen···halide synthon and also their potential as crystal engineering tools. The halogen···halogen contacts can be represented by R-Y1···Y2-R (Y = Cl, Br, I). Previous reports have shown that, crystallographically, there are two preferred geometries for halogen···halogen contacts (Scheme 1).[5] The first arrangement is where $\theta_1 = \theta_2$, (θ_1 and θ_2 are the R-Y1···Y2 and Y1···Y2-R angles respectively); the second geometry arises when $\theta_1 \sim 180°$ and $\theta_2 \sim 90°$ (called the perpendicular arrangement).[5] Halogen···halide contacts are characterized by a halogen···halide distance less than the sum of the van der Waals radius (r_{vdW}) of the halogen atom and the ionic radius of the halide anion and also with a linear C-Y···X^- angle (Y = Cl, Br, I; X = F, Cl, Br, I).

Scheme 1. Schematic drawing of the two preferred geometries for the halogen-halogen contacts; a) $\theta_1 = 180°$, $\theta_2 = 90°$. b) $\theta_1 = \theta_2$.[5]

a)

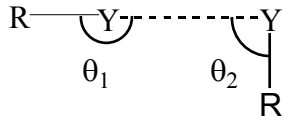

b)

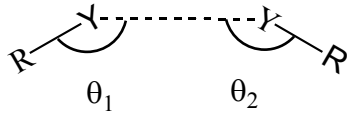

Halogen···halogen Interactions

In solid state structures of halogenated compounds, the general trend is that the halogen···halogen distances are less than the sum of their r_{vdW}.[5,6] Halogen···halogen contacts have already been used to design new materials. Matsumuto *et al.* used chlorine···chlorine

interactions to prepare highly stereoregular polymers (Figure 1).[7] Only the introduction of a *para* chloro substitution on dibenzyl Z,Z-mucanoate enabled solid state photopolymerization in this case. Based on these intermolecular chlorine···chlorine contacts, the monomer molecules aligned in a suitable arrangement to undergo polymerization to yield crystalline organic polymers. In another example, halogen···halogen contacts were used to prepare supramolecular networks from 2,4,6-tris(4-chlorophenoxy)-1,3,5-triazine[8] and its bromine analogue.[9] Furthermore, Broder *et al*.[10] used these networks as hosts for tribromobenzene, where the host complex is stabilized by C-Cl···Cl-C synthons as well as many other weak interactions (Figure 2).

The physical nature of halogen···halogen contacts has been a matter of interest and also debate. Some research groups consider these contacts to exist as a result of attractive forces.[5,6] Initially, in this context these interactions were considered an example of a donor-acceptor interaction,[5c,6] where one of the halogen atoms acts as a donor while the other acts as an acceptor. Another study showed that electrophiles tend to approach the halogen atom of the C-Y bond (Y = Cl, Br, I) at an angle of ~100°, while nucleophiles approach the halogen atom at an angle of ~165°.[5c] These results were interpreted as a charge transfer between the HOMO of the donor to the LUMO of the acceptor. Desiraju *et al.*, based on a statistical analysis of the structure of halogenated hydrocarbons, found that the number of contacts between the halogen atoms (chlorine, bromine, iodine excluding fluorine) is greater than the expected number of contacts from the exposed area of the halogen atom alone.[5a] Moreover, the heavier halogens (Cl_2, Br_2, I_2), are isomorphous and isostructural, while F_2 is completely different.[11] These studies support the idea that halogen···halogen contacts are a result of attractive forces in the heavier halogens.

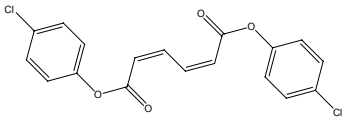

diparachlorobenzyl
(Z,Z)-muconate

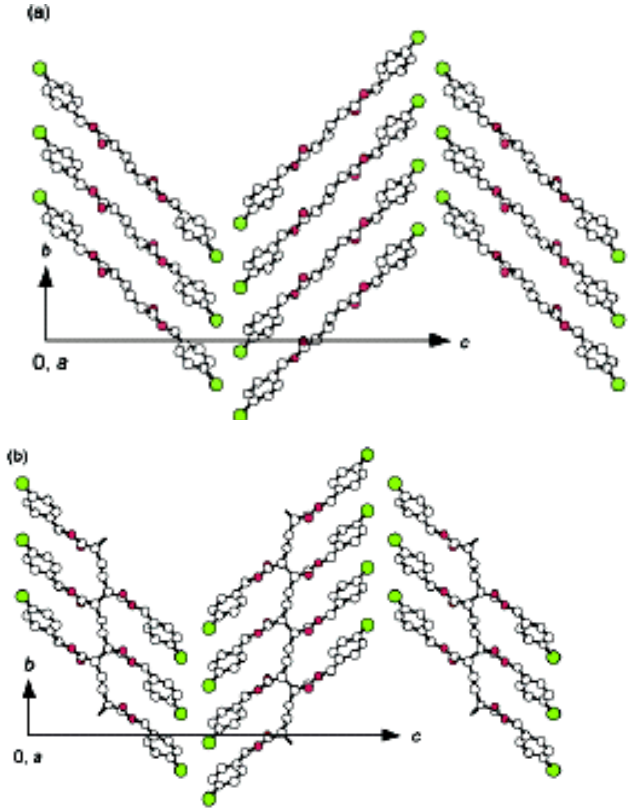

Figure 1. Packing diagram of (a) di(4-chlorobenzyl(Z,Z)-muconate and (b) the poly di(4-chlorobenzyl (Z,Z)-muconate: the view along the crystallographic a axis. Hydrogen atoms are omitted for clarity. Ref. 7.

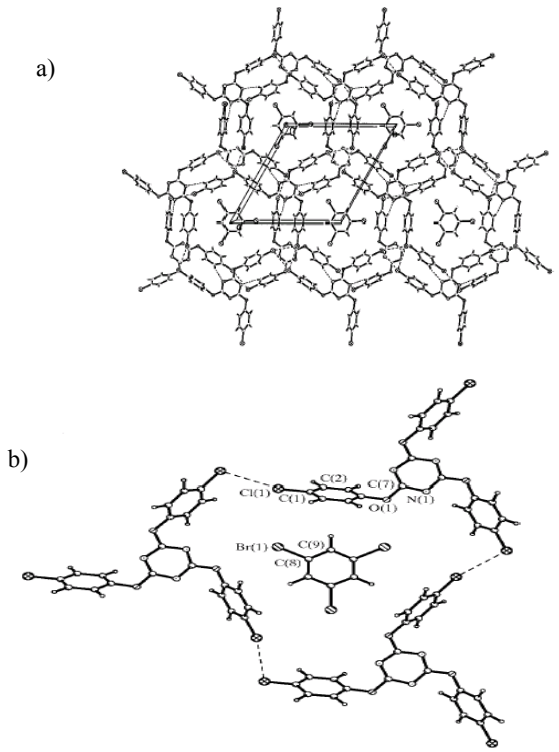

Figure 2. a) View of the 1,3,5-tribromobenzene: 2,4,6-(4-chlorophenoxy)-1,3,5-trizane inclusion complex along the *c* axis. b) Illustration of the chlorine-chlorine interactions. This Figure was taken from ref. 10.

In contrast, others claimed that halogen···halogen contacts, specifically in the chlorine···chlorine case, are due to the packing of anisotropic atoms inside the crystal.[12] The directionality of the chlorine···chlorine interaction is a result of a decrease in the exchange repulsion rather than an attractive force. Their calculations showed that the electronic charge is anisotropically distributed around the chlorine atom. Accordingly, the halogen atom has an elliptical shape. In another study, *ab initio* calculations indicated that the Y···El contacts (El = N, O and S) are mainly due to electrostatic interactions. But, other interactions (polarization, charge transfer and dispersion) contribute to the attractive nature of the contacts as well.[13] Recently, theoretical calculations on iodobenzene showed that the charge around the iodine atom is distributed anisotropically, where a partial positive charge is located along the σ bond axis and a partial negative charge in the π region of the atom.[14] This model was used to explain the structure of the trihalomesitylene compounds (Figure 3).

Halogen···halide Interactions

Halogen···halide contacts have not been studied in as much detail as halogen···halogen interactions. These synthons, recently named 'charge assisted halogen···halide interactions', $(R\text{-}Y)^{+}\cdots X^{-}$, were found to play an important role in the crystal structure of halogenated pyridinium salts.[15] It was found that bromine···bromide contacts are fairly strong based on the distance reduction, while chlorine-chloride contacts are weaker. In contrast, chlorine···chloride interactions were found to stabilize the structure of diphenyldichlorophosphonium trichloride-chlorine solvate, which has several short chlorine···chloride distances (ranging from 3.171-3.300 Å).[16] We and others found that C-Y···X-M synthons play a crucial role in influencing the structures of L_2MX_4 and ML_2X_2 (M = Cu(II), Co(II), Pd(II), Pt(II) ; X = F, Cl^-, Br^- or I^-; L = *n*-halopyridine).[17]

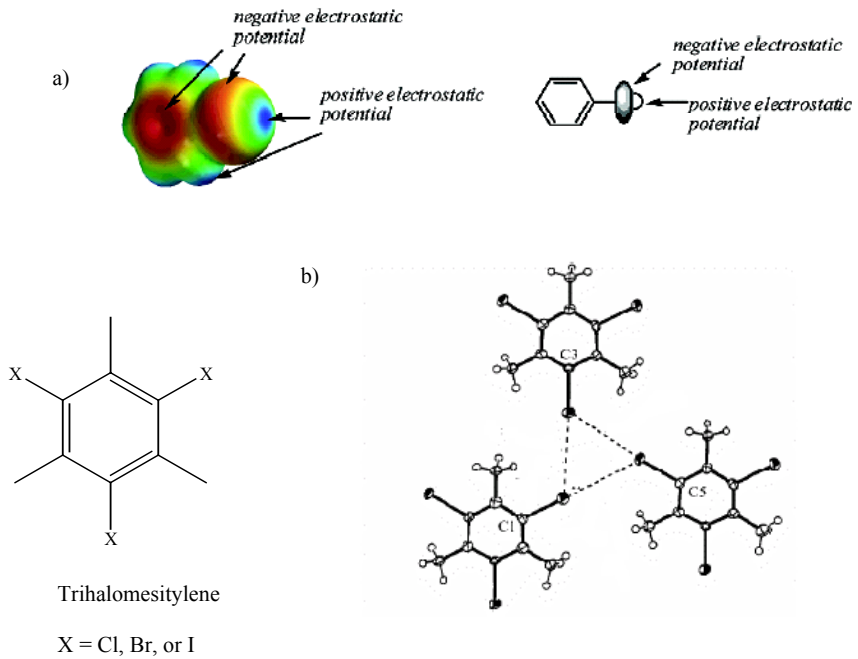

Figure 3. a) View showing the distribution of the electronic charge in iodobenzene. b) Illustration of halogen-halogen contacts in the trihalomesitylene structure. This figure, both a and b, was taken from ref. 14.

Much effort has been carried out to develop new materials with useful properties based on these synthons.[18] Yamamoto *et al.* and others used these synthons to develop organic based conducting materials.[18a,b] Their study also showed that the synthon was fundamental to the conducting property as well as helping to shape the internal architecture of the lattice. In another study, Farina *et al.* used the bromine···bromide synthon for the resolution of racemic 1,2-dibromohexafluoropropane.[18c] More recently, we have also found that the bromine-metal bromide synthons, along with hydrogen bonding interactions, could be used to dissect infinite bibridged chains in cupric bromide into decamers of ($Cu_{10}Br_{22}^{2-}$) stoichiometry, the longest known copper halide oligomeric species.[17c]

The physical nature of the halogen…halide interaction has not been investigated in depth. Several previous studies state that these synthons are a result of HOMO-LUMO charge transfers.[5c] Recently, Zordan *et al.* showed that these synthons involve electrostatic attractions, based on calculated electrostatic potentials.[17e]

(b) Motivations.

The controversial arguments on the nature of the halogen···halogen and halogen···halide contacts imply the necessity of a more thorough investigation on the role of these contacts, which help determine the three dimensional structure, and are important in supramolecular synthesis. The second motivation is to determine the relative strength of the halogen···halogen contact (Y···Y; Y = F, Cl, Br, and I). Also, the relative strength of the halogen···halide synthons has not been studied in detail ($Y\cdots X^-$; Y = F, Cl, Br, and I; and X = F, Cl, Br, and I). The third motivation is to investigate the synthons potential use as crystal engineering tools in hybrid organic-inorganic materials. Strengthening intermolecular forces is one main foci of

crystal engineering. We also have investigated several factors that would increase the relative strength of these contacts.

Three methods are used to investigate these contacts; (a) the relative strength and their physical nature are investigated using *ab initio* calculations; (b) model crystal structures are determined to characterize their role in structural architecture and their relative strength as well;(c) the Cambridge Structural Database (CSD) is investigated for halogen···halogen and halogen···halide contacts to support methods a and b.

(c) Theoretical Background.

Theoretical Method.

The electronic Hamiltonian in general for a molecule can be written as

$$H = \sum_{i=1}^{n} h_i + \sum_{i} \sum_{j>i} \frac{1}{r_{ij}}$$

h_i, this operator includes the 1-electron operators for the kinetic energy and attractive forces to the nuclei in the molecule for each electron.[19] The second term in the above equation is the repulsion operator between electrons. Unfortunately, due to the presence of the electron-electron repulsion term in the overall Hamiltonian equation, the Schrödinger equation is not exactly solvable. One of the proposed ways to approximate for this term is through using perturbation theory. In perturbation theory, in general, the overall Hamiltonian for any system can be written as

$$H = H_0 + \lambda H'$$

H_0 is a Hamiltonian for an unperturbed system (i.e. unperturbed system = known Hamiltonian, eigenfunctions, and eigenvalues). Calculating the change in the eigenvalues and

eigenfunctions due to a small perturbation in the Hamiltonian (H`), λ is a scalar quantity. Similarly, the wave function and the energy can be written as:

$$\Psi_n = \Psi_n^{(0)} + \lambda\Psi_n^{(1)} + \lambda^2\Psi_n^{(2)} + ... + \lambda^k\Psi_n^{(k)} + ...$$

$$E_n = E_n^{(0)} + \lambda E_n^{(1)} + \lambda^2 E_n^{(2)} + ... + \lambda^k E_n^{(k)} + ...$$

where $\Psi_n^{(0)}$ is the unperturbed wavefunction for the state *n*, $\Psi_n^{(k)}$ is the k^{th} order correction to the wave function (the above equations was taken from ref. 19b). Similarly, $E_n^{(k)}$ is the k^{th} order correction to the energy for the state *n*.

In this research, second-order Møller-Plesset (MP2) perturbation theory will be used to calculate the energy of halogen···halogen and halogen···halide interactions. In MP theory, the unperturbed Hamiltonian, H_0, equals the sum of Fock operators, F_i, for electrons in a molecule, and the zeroth order wavefunction is the Hartree Fock wavefunction, Φ_0

$$H_0 = \sum_{i=1}^{n} F_i$$

where

$$F_i = h_i + \sum_{j=1}^{n}\left(J_j - K_j\right)$$

where;

J_i is called the coulomb operator and K_j is called the exchange operator.

For multielectron systems, the Hamiltonian includes electron-electron repulsion term, J_i. It is hard to interpret the exchange operator since it has no classical analogy. It arises from the fact that the wavefunction must be antisymmetric with respect to electron exchange. Ignoring the scalar value λ therefore:

$$H' = \sum_i \sum_{j>i} \frac{1}{r_{ij}} - \sum_{i=1}^{n} \sum_{j=1}^{n} \left(J_j(i) - K_j(i) \right)$$

According to perturbation theory, the zero order energy term is given by:

$$E_0^{(0)} = \left\langle \Phi_0 \middle| H_0 \middle| \Phi_0 \right\rangle = \sum_i \varepsilon_i$$

which is the sum of single electron orbital energies, ε_i. Also

$$E_0^{(1)} = \left\langle \Phi_0 \middle| H' \middle| \Phi_0 \right\rangle$$

$$E_0^{(0)} + E_0^{(1)} = \left\langle \Phi_0 \middle| H_0 \middle| \Phi_0 \right\rangle + \left\langle \Phi_0 \middle| H' \middle| \Phi_0 \right\rangle = \left\langle \Phi_0 \middle| H_0 + H' \middle| \Phi_0 \right\rangle = \left\langle \Phi_0 \middle| H \middle| \Phi_0 \right\rangle$$

This integral is a Hartree-Fock variation integral. Therefore, $E_0^{(0)} + E_0^{(1)}$ is equal to the Hartree-Fock energy. $E_0^{(1)}$ corrects for the electronic repulsion in a way that the electron moves in an average smeared out electron density all over atomic space. In reality, the electrons dynamically repel each other and avoid being close to each other. The error in Hartree-Fock energy due to this factor is called correlation energy. The second order correction in the energy corrects for this electronic correlation. According to perturbation theory, the second order correction in the energy is given by:

$$E_0^{(2)} = \left\langle \Phi^{(0)} \middle| H' \middle| \Phi^{(1)} \right\rangle$$

where $\Phi^{(1)}$ is the first order correction to Hartree-Fock wavefunction. For details of derivation of the equations for calculating the value $E_0^{(2)}$, see ref. 19a.

It is relevant to compare the Møller-Plesset theory with intermolecular perturbation theory (IMPT), the previously used theory to model these contacts. MP perturbation theory treats two interacting molecules A and B as one molecule. Thus, $H_0 = H_{AB}$ is used as the unperturbed operator (i.e. sum of Fock operators). In contrast, in IMPT, the unperturbed Hamiltonian equals to the sum of the Hamiltonian of two separate molecules. $H_0 = H_A + H_B$. The first order

correction in energy gives the correction for electrostatic interaction between the undistorted charges of the two molecules.[12a] The second order correction gives the stabilization energy due to other factors (polarization and dispersion energy).

Basis Sets.

Basis sets are the mathematical description of orbitals.[19c] For representative accurate calculations, the right basis set should be used. The electron has a finite probability of existing in space, anywhere. Therefore, the larger the basis set (less constraints on electronic motion), the better the description of the electrons and thus the electronic cloud distribution and energy. Basis sets are classified based on the type of the basis function they use; there are two types of basis functions; (a) Slater type orbitals (STOs), these orbitals are not mathematically convenient to be used for polyatomic molecules; (b) Gaussian-type functions (GTFs). GTFs have the general formula:[19a]

$$g_{ijk} = NX_b^i Y_b^j Z_b^k e^{-\zeta r^2}$$

i, j and k are positive integers, ζ is a positive orbital exponent, X_b, Y_b, Z_b are the Cartesian coordinates with the origin at nucleus b and N is the normalization constant.

Basis sets are a linear combination of these Guassian functions. Each Gaussian function is called a primitive. Basis functions can consist of a single primitive Gaussian or a linear combination of many primitive Gaussians. The latter are called contracted Gaussian functions.

The energy of halogen···halogen and halogen···halide interactions will be calculated at different basis sets level, correlation consistent polarized valence split double zeta (cc-pvdz), correlation consistent polarized valence split triple zeta (cc-pvtz) and correlation consistent polarized valence split quadruple zeta (cc-pvqz).[20] Correlation consistent basis sets include all the functions with similar contribution to the correlation energy at the same stage,

independently of the function type.[19a] This implies the addition of polarization functions to the basis sets. For example, the contribution of the first d-orbital to the correlation energy is large, while the contribution of the second d-orbital is similar to that of f-orbital. Therefore, f-function should be added to the basis set. Due to the addition of such f-orbital, which is beyond the orbitals needed to describe the ground state, the basis set called polarized basis set. The main advantage of using polarized functions is that these polarized functions allow the orbital to change its shape. [19d]

The above basis sets (cc-pvdz, cc-pvtz and cc-pvqz) are classified as split valence basis sets.[19d] Split basis sets have two or more basis functions of different radial extent "sizes" for each valence orbital. The cc-pvdz basis set is a linear combination of two basis functions of different sizes for the valence orbitals. Basis sets vtz and vqz use three and four functions of different radial extent respectively. For example, in vdz basis set, carbon is represented as

C:1s, 2s, 2s', 2px, $2p_x$', $2p_y$, $2p_y$', $2p_z$, $2p_z$'

In each basis function consists of seven primitives. The 2s and 2s' can be written as

$$2s = \sum_{i=1}^{7} \mathrm{A_i} g^{-\zeta_i r^2}$$

and

$$2s' = \sum_{i=1}^{7} \mathrm{B_i} g^{-\zeta_i r^2}$$

g is a gaussian primitive function

The two functions have the same exponent values. The difference between the two basis functions is the values of the coefficients A_i and B_i. These types of functions allow the orbital to change its size. As our calculations will show, halogen···halogen and halogen···halide interactions are based on deformation of electronic charge on the halogen atom. Therefore,

diffuse function is added to the halogen atom and halide anion. Diffuse functions allow the orbital to occupy a larger size in space, and hence, reduce the constraints on electron motion.[19d]

In our study for heavy atoms, the relativistic effects cannot be ignored due to the fact that the core electron speed is comparable to the speed of light. Therefore, the core electrons are removed and a pseudo potential is used that has been parameterized in relativistic calculations. cc-pvdz-PP basis sets are used when iodine is present.[20]

The energy of interaction at complete basis set, E(cbs), is estimated using the formula[21]

$$E(n) = E(cbs) + Ae^{-(n-1)} + Be^{-(n-1)^2}$$

where n = 2, 3, 4 (i.e. 2 = DZ; 3 = TZ; 4 = QZ)

Basis Set Superposition Error, BSSE.

A phenomenon known as Basis Set Superposition Error, BSSE, influences the calculation of the energy of interaction of weakly interacting species.[19a] BSSE arises from the fact that the electrons around one nucleus may be described by orbitals on neighboring nuclei due to the incompleteness of the basis set used in the *ab initio* calculations. In our study, either a dimer or two different interacting species are studied. An interaction between a halide anion and halopyridine will be taken as an example to explain BSSE and how we correct for it. The energy of halogen···halide interaction, $E_{A\cdots B}$, is defined as

$$E_{A\cdots B} = E_{AB} - E_A - E_B$$

E_{AB}, is the energy of halopyridine···halide complex, E_A, is the energy of halopyridine species and E_B, is the energy of the halide anion.

The electron density on the halide anion may be described by the basis functions on the halopyridine molecule and *vice versa*. Hence, the calculated energy of the complex is overestimated, which leads to an overestimation of the energy of interaction, $E_{A\cdots B}$. In our study, the Counterpoise (CP) method is used to correct for BSSE.[22] This method is based on calculating the energy of the halide anion and the halopyridine species with the geometries they have in complex; the energy of the halopyridine species (E_{CA}) is calculated with the presence of the basis functions of the halide anion at the halide anion position in the space, but without the halide anion nucleus, these orbitals are called ghost orbitals. Similarly, the energy of the halide anion (E_{CB}) is calculated with the presence of the basis function of halopyridine located at the corresponding nuclei positions, but without the halopyridine nuclei. The CP corrected halogen···halide energy of interaction, $Ec_{A\cdots CB}$, is defined as

$$E_{CA\cdots CB} = E_{AB} - E_{CA} - E_{CB}$$

REFERENCES.

1. (a) Desiraju, G. R. *Nature* **2001**, *412*, 397-400. (b) Desiraju, G. R. *Crystal Engineering, The Design Of Organic Solids,* Elsevier Science Publishers B. V. **1989**. (c) Desiraju, R. G. *Angew. Chem. Int. Ed. Engl.* **1995**, *34*, 2311-2327. (d) Brammer, L. *Chem. Soc. Rev.* **2004.** (e) Braga, D.; Brammer, L.; Champness, N. *CrystEngComm.* **2005**, *7*, 1-19.

2. (a) Aakeröy C. B.; Beatty A. M. *Aust. J. Chem.* **2001**, *54*, 409-421. (b) Brammer, L.; Bruton, E. A.; Sherwood, P. *Cryst. Growth Des.* **2001**, *1*, 277-290. (c) Lutz, H. D. *J. Mol. Struct*. **2003**, *646*, 227-236.

3. (a) Sinnokrot, M. O.; Sherrill, D. C. *J. Am. Chem. Soc.* **2004**, *126*, 7690-7697. (b) Sinnokrot, M. O.; Sherrill, D. C. *J. Phys. Chem.* **2003**, *107*, 8377-8379. (c) Sinnokrot, M. O.; Valeev, E. F.; Sherrill, D. C. *J. Am. Chem. Soc.* **2002**, *124*, 10887-10893. (d) Hunter, Ch. A.; Sanders, K. M. *J. Am. Chem. Soc.* **1990**, *112*, 5525-5534. (e) Desiraju, G. R.; Gavezzotti, A. *J. Chem Soc. Chem.* Commun. **1989**, 621-623.

4. Braga, D.; Grepioni, F. *New J. Chem*. **1998**, *22*, 1159-1161. (b) Desiraju, G. R.; Stiener, T. *The Weak Hydrogen Bond in Structural Chemistry and Biology* (Oxford Univ. Press. Oxford **1990**). (c) Langley, P. J.; Hulliger, J.; Thaimattam. R.; Desiraju, G. R. *New J. Chem*., **1998**, *22*, 1307-1309.

5. (a) Desiraju, G. R.; Parthasarathy, R. *J. Am. Chem. Soc.* **1989**, *111*, 8725-8726. (b) Jagarlapudi, A. R.; Sarma, P.; Desiraju G. *Acc. Chem. Res.* **1986**, *19*, 222-228. (c) Ramasubbu, N.; Parthasarathy, R.; Murray-Rust, P. *J. Am. Chem. Soc.* **1986**, *108*, 4308-4314.

6. Bent A. H. *Chem. Rev.* **1968,** *68*, 587-648.

7. Matsumoto, A.; Tanaka, T.; Tsubouchi, T.; Tashiro, K., Saragai, S.; Nakamoto Sh., *J. Am. Chem. Soc.*, **2002**, *124*, 8891-8902.

8. Anthony, A.; Desiraju, G. R.; Jetti, R. K. R.; Kuduva, S. S.; Madhavi, N. N. L.; Nangia, A.; Thaimattam, R.; Thalladi, V. R. *Cryst. Engn, 1, Mater. Res. Bull. Suppl. S*, **1998**, 1-18.

9. Thalladi, V. R.; Brasselet, S.; Weiss, H. C.; Blaser, D.; Katz, A. K.; Carrell, H. L.; Boese, R.; Zyss, J.; Nangia, A.; Desiraju, G. R. *J. Am. Chem. Soc.* **1998**, *120*, 2563-2577.

10. Broder, Ch. K., Howard, A. J., Wilson, Ch. C., Allen, F. H., Jetti, R. K., Nangia A., and Desiraju, G. R. *Acta. Cryst.* **2000,** B56, 1080-1084.

11. (a) Willimas, D. E.; Hsu, Leh-Yeh. *Acta Cryst*., **1985**, *A41*, 296-301.(b) Meyer, L., Barrett, C. S.; Greer, S. C., *J. Chem. Phys.,* **1968**, *49*, 1902-1907. (c) Pauling, L.; Keavveny, I.; Robinson A. B., *J. Solid State Chem*., **1970**, *2*, 225-227.

12. Price, S. L.; Stones, A. J.; Lusca, J.; Rowland, R. S.; Thornley, A. E., *J. Am. Chem. Soc.* **1994,** 116, 4910-4918. (b) Nyburg, S. C.; Wong-Ng, W. *Proc. R. Soc. London*, **1979,** *A367*, 29-45. (c) Price, S. L.; Stone A. *J. Mol. Phys*., **1982**, *47*, 1457-1470.

13. Lommerse, J. P.; Stone, A. J.; Taylor R.; Allen F. H. *J. Am. Chem. Soc.* **1996**, *118*, 3108-3116.

14. Bosch, E.; Barnes, C. L. *Cryst. Growth Des*. **2002**, *2*, 299-302.

15. (a) Freytag, M.; Jones, P. G. *Zeit. Naturfor B: Chem. Sci.* **2001**, *56*, 889-896. (b) Freytag, M.; Jones, P. G.; Ahrens, B.; Fischer, A. K. *New J. Chem*. **1999**, *23*, 1137-1139.

16. Taraba, J. and Zak, Z., *Inorg. Chem.,* **2003**, 42, 3591-3594.

17. (a) Willett, R. D.; Awwadi, F. F.; Butcher, R.; Haddad, S.; Twamley, B. *Cryst. Growth Des.* **2003**, *3*, 301-311. (b) Brammer, L.; Espallargas, G. M.; Adams, H. CrystEngComm. **2003**, *5(60)*, 343-345. (c) Haddad, S.; Awwadi, F.; Willett, R. D. *Cryst. Growth Des***. 2003**, *3(4),* 501-505. (d) Zordan, F.; Brammer, L. *Acta Cryst*. **2004**, *B60*, 512-519. (e) Zordan, F.; Brammer, L.; Sherwood, P. *J. Am. Chem. Soc*. **2005**, *127*, 5979-5989.

18. (a) Yamamoto, H. M.; Yamaura, J.; Kato, R. *J. Am. Chem. Soc.* **1998**, 120(24), 5905-5913 and references therein. (b) Domercq, B.; Devic, T.; Fourmigue, M.; Auban-Senzier, P.; Canadell, E. *J. Mater. Chem*. **2001**, *11*, 1570-1575. (c) Farina, A.; Meille, S. V.; Messina, T. M.; Metrangolo, P.; Resnati, G.; Vecchio, G. *Angew. Chem. Int. Ed.* **1999**, *38*, 2433-2436.

19. (a) Jensen, F. *Introduction to Computational Theory,* **1999**. (b) Levine, I. N. *Quantum Chemistry, fifth edition,* **2000**. (c) Lowe, J. P. *Quantum Chemistry, second edition* **1993**. (d) Foresman, B. J.; Frisch A. *Exploring Chemistry with Electronic Structure Methods, second edition*, **1996**.

20. (a) Dunning, T. H., Jr. *J. Chem. Phys.* **1989**, *90*, 1007-1023. (b) Kendall, R. A.; Dunning, T. H., Jr.; Harrison, R. J. *J. Chem. Phys.* **1992**, *96*, 6796-6806. (c) Woon, D. E.; Dunning, T. H., Jr. *J. Chem. Phys.* **1993**, *98*, 1358-1371. (d) Wilson, A. K.;

Peterson, K. A.; Woon, D. E.; Dunning, T. H., Jr. *J. Chem. Phys.* **1999**, *110*, 7667-7676. (e) Peterson, K. A.; Figgen, D.; Goll, E.; Stoll, H.; Dolg, M. *J. Chem. Phys*. **2003**, *119*, 11113-11123.

21. (a) Peterson, K. A.; Woon, D. E.; Dunning, T. H., Jr. *J. Chem. Phys.* **1994**, *100*, 7410-7415. (b) Feller, D.; Peterson, K. A. *J. Chem. Phys.* **1999**, *110*, 8384-8396.

22. Boys, S. F.; Bernardi, F. *Mol. Phys.* **1970**, *19*, 553.

CHAPTER TWO

The Nature of Halogen···Halogen Synthons; Crystallographic and Theoretical Studies.

Firas F. Awwadi[†], Roger D. Willett[†,], Kirk A. Peterson[†] and Brendan Twamley[‡]*

[†]Department of Chemistry, Washington State University, Pullman, WA 99164 USA.

[‡]University Research Office, University of Idaho, Moscow, ID 83844 USA.

*Department of Chemistry, Washington State University, Pullman, WA 99164, USA, Tel (Office), 509 335 3925, FAX (dept.) 509 335 8867, E-mail rdw@mail.wsu.edu

ABSTRACT Halogen···halogen (halogen = fluorine, chlorine, bromine and iodine) contacts in organic compounds are investigated using crystallographic studies and *ab initio* calculations. Halogen···halogen contacts in organic molecules can be represented as C-X_1···X_2-C [(where θ_1= C-X_1···X_2, θ_2 = X_1···X_2-C; r_i = X_1···X_2 separation distance (Scheme 1)]. Crystallographic and calculations studies have indicated that these interactions are controlled by electrostatics. The distribution of contacts within the sum of van der Waals radii (r_{vdW}) *vs.* θ_i ($\theta_1 = \theta_2$) shows a maximum number of contacts at ca. 150° for X = Cl, Br and I. This maximum is not seen in the distribution for F···F contacts. This maximum is in good agreement with *ab initio* calculations that indicate the presence of a minimum in the potential energy diagram at ca. 150° in all of the halogen···halogen interaction potential energy diagrams, excluding F···F interactions. The position of the maximum varies depending on three factors: (a) the type of the halogen atom (b) hybridization of the *ipso* carbon atom and (c) the nature of the other atoms that are bonded to the *ipso* carbon atom apart from the halogen atom. Calculations show that the strength of these contacts increases in the following order: iodine···iodine > bromine···bromine > chlorine···chlorine. Their relative strength increases in the following order as a function of the *ipso* carbon atom hybridization: sp^2 > sp > sp^3. Attaching an electronegative atom to the carbon strengthens the halogen···halogen contacts. An electrostatic model is proposed based on two assumptions; (a) the presence of a positive electrostatic cap on the halogen atom (except for fluorine), (b) the electronic charge is anisotropically distributed around the halogen atom. These two assumptions are confirmed based on the calculated electron density and the electrostatic potential.

INTRODUCTION

Intermolecular forces are of particular significance in chemistry, mainly because these forces are responsible for stabilizing many important molecules, e.g., DNA, proteins,…,etc.[1a] These forces are also responsible for arranging crystallographic species within the crystalline lattice. Hence, these forces are one of the main foci of crystal engineering.[1] As well as their structural role, intermolecular forces affect the physical properties of crystalline materials, e.g., non-linear optical properties, electrical and magnetic properties, etc.[2a] Intermolecular forces have been used successfully in arranging reactants for pericyclic solid-state chemical reactions, in cyclo-addition reactions and solid-state polymerization.[1d,2b-d] The classical hydrogen bond, an example of a strong intermolecular force, has been widely studied for many years and utilized in crystal engineering as a structural member.[1,3] More recently, other weaker interactions, e.g., halogen bonds,[4] non-classical hydrogen bonds,[5] halogen···halogen interactions [6] and π-π stacking are being examined with a growing interest towards utilization for crystal engineering.[7]

Halogen···halogen (R-X_1···X_2-R) contacts are characterized by an inter-halogen distance, X_1···X_2, that is less than the sum of van der Waals radii (r_{vdW}). Studies show that there are two preferred geometries for the halogen···halogen contacts (Scheme 1); the first arrangement occurs when $\theta_1 = \theta_2$, (θ_1 and θ_2 are the R-X_1···X_2 and X_1···X_2-R angles respectively). The second geometry arises when θ_1 = ca. 180° and θ_2 = ca. 90°; the perpendicular arrangement (Scheme 1).[6] Another type of contacts, trihalogen contacts, have been observed in many structures, with an arrangement similar to the perpendicular arrangement (Scheme 1b). They have been used to develop new materials and explain the structural behavior of other

important materials.[8] One example is the use of chlorine···chlorine interactions to prepare highly stereo regular organic polymers.[2b]

Scheme 1. The two preferred geometries for halogen···halogen contacts; a) $\theta_1 = \theta_2$. b) $\theta_1 = 180°$, $\theta_2 = 90°$.

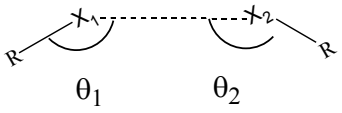

R = organic group

X= Cl, Br and I

(a)

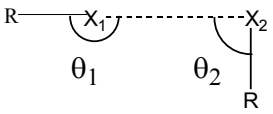

(b)

Chlorine···chlorine interactions have been a matter of interest and debate in recent years. Some research groups consider chlorine···chlorine interactions to be a result of attractive forces.[6,9,10] Initially, the interaction was considered as an example of a donor-acceptor interaction.[9] Another study showed that the electrophiles tend to approach the halogen atom of the C-X bond (X = Cl, Br, or I) at an angle of ca. 100°, while the nucleophiles approach the halogen atom at an angle of ca. 165°.[8] These results were explained based on charge transfer between the HOMO of the donor to the LUMO of the acceptor.[10] More recently, Desiraju *et al.*, based on a statistical analysis of the crystal structure of halogenated hydrocarbons, found that the number of contacts between the halogen atoms (Cl, Br, I only) is greater than the expected number of contacts from the exposed area of the halogen atom alone, which is evidence for the presence of attractive forces between the two halogen atoms involved in the halogen···halogen contact.[6a] Studies by Price *et al.* and Nyberg *et al.* using theoretical *ab initio*

quantum mechanical calculations and analysis of the crystal structure of chlorinated organic compounds indicated that Cl···Cl contacts are just a result of packing of anisotropic atoms inside the crystals, and the directionality, if any, is due only to reduction of the exchange repulsion forces rather than attractive forces. [11]

Crystallographic studies that have tackled this issue have not distinguished between the hybridization of the carbon atom bonded to the halogen atom and the nature of the other atoms that are attached to the carbon atom. The geometry and electronegativity of a sp^2 carbon is different from a sp^3 carbon. These differences are expected to have a major role on the halogen···halogen interaction. In this research, to resolve the dilemma of the exact physical nature of halogen···halogen contacts, crystallographic population analysis and theoretical studies are carried out. These studies will show that the intermolecular contacts are mainly controlled by electrostatics.

METHOD

Crystallographic Study

The Cambridge Structural Data Base (CSD), version 5.25 November 2003, was searched for halogen···halogen (F, Cl, Br and I) intermolecular contacts within the sum of r_{vdW} in room temperature structures[12] (eight filters were applied to the searches; only organic compounds,[13] crystallographic R factor < 0.075, no errors in the crystal structures, no ions, not disordered, not polymeric, 3D coordinate determined, no powder structures). Structures with the lowest R-value were selected from multiple repeat structures for analysis. Details of each search are listed in Table 1.

Scheme 2. Modeling of halogen···halogen contacts.

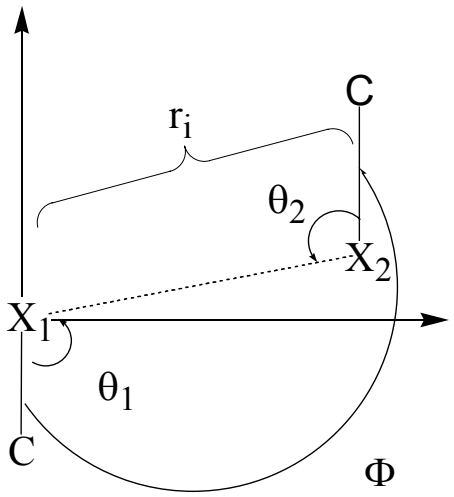

Table 1. Number of halogen···halogen contacts within the sum of r_{vdW} in the CSD.

Interaction Type	#. of Contacts	# of Contacts $\theta_1 = \theta_2$	# of Contacts $\theta_1 = \theta_2, \theta > 90°$	# of Contacts [a] $\theta_1 = \theta_2, \theta > 90°$, Φ 170°-190°	Hybridization
F···F	324	81	81	70	sp^3
	317	77	69	58	sp^2
	219	67	59	50	Aromatic
Cl···Cl	323	135	132	121	sp^3
	560	216	209	198	sp^2
	378	148	142	138	Aromatic
Br···Br	161	65	65	58	sp^3
	219	85	82	73	sp^2
	158	61	60	55	Aromatic
I···I	23	11	11	11	sp^3
	68	17	15	13	sp^2
	40	14	13	9	Aromatic

[a]Φ = torsion angle

The contacts were sorted into two categories (Scheme 2); (1) $\theta_1 = \theta_2$. (2) $\theta_1 \neq \theta_2$. We have concentrated on the former interaction, because in the latter category, other factors such as steric hindrance and interactions with the rest of the molecule play a dominant role. For X = Cl and Br, approximately 40% of the contacts fall in the $\theta_1 = \theta_2$ category, with somewhat less for X = F and I. To make this statistical analysis correlate to our calculations, as we will see later, those contacts with torsion angles Φ (C-X_1···X_2-C) (Scheme 2) between 170° to 190° are the only ones used in the statistical analysis. This represents approximately 90% of the above contacts. Contacts with θ_i < 90° were ignored, since at these θ_i values, other types of interaction are expected to play a dominant role.

Theoretical Study.

Gaussian 98 and Gaussian 03[14] was used for geometry optimization and MOLPRO[15] was used for electronic energy calculations. The structure of the molecular units of each model was optimized using Møller-Plesset second order perturbation theory (MP2) with a triple zeta basis set. The total electronic energy was computed using the cc-pVnZ basis set on C and H, aug-cc-pVnZ on Br, Cl and F, and aug-cc-pVnZ-PP on I with MP2 (n = D, T and Q for double, triple and quadruple zeta, respectively; aug. prefix denotes the presence of diffuse function on the halogen atoms).[16] This involves initially Hartree-Fock self-consistent field calculations to determine the molecular orbitals and then subsequent MP2 calculation to determine the electron correlation energy. The calculated energy of interaction is corrected for basis set superposition errors (BSSE) in models **1** and **3** (Scheme 3) using the counterpoise method.[17] With a complete basis set the corrected and uncorrected energy values are expected to converge. The minimum energy of interaction using a complete basis set E(cbs) is estimated with the following equation.[18]

$$E(n) = E(cbs) - Ae^{-(n-1)} - Be^{-(n-1)^2}$$

where n = 2, 3, 4 is the cardinal number of the correlation consistent basis set.

Halogen atoms in organic molecules are attached to carbon atoms with different hybridization (sp^3, sp^2 and sp). Halomethane (**1**), halobenzene (**2**) and haloaceteylene (**3**) molecules were used to model contacts of the types Csp^3-X···X-Csp^3, (2) Csp^2-X···X-Csp^2 and (3) Csp-X···X-Csp respectively (Scheme 3). The interaction is modeled by calculating the energy of interaction of two monomers as a function of the separation distance r_i and the angle θ_i ($\theta_i = \theta_1 = \theta_2$, Scheme 2), where θ_i was changed from 80-180° in increments of 10° with the torsion angle Φ = 180° (Scheme 2). In dimers of types **1** and **3**, the interaction is assumed to be isotropic, in the case of model **2**, the interaction is expected to be anisotropic. Therefore, the energy of interaction was modeled for two different geometries, in both cases, a dimer of the type **2** has C_s symmetry and; (a) all the atoms of dimer of **2** were located on the mirror plane; (b) the mirror plane contains the two halogen atoms and is perpendicular to the planes of the phenyl rings (Scheme 4).

Scheme 3. Structure of the modeled compounds.

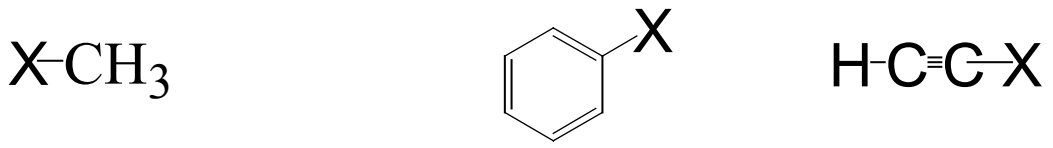

1a : X = F
1b : X = Cl
1c : X = Br
1d : X = I

2a : X = F
2b : X = Cl
2c : X = Br
2d : X = I

3a : X = F
3b : X = Cl
3c : X = Br
3d : X = I

Scheme 4. A schematic representation of modeling of the halogen···halogen contacts in an aromatic dimer for two different geometries. In both geometries, each dimer has C_s symmetry; (a) all the atoms are located on the mirror plane; (b) the mirror plane contains the two halogen atoms and bisects the aromatic planes.

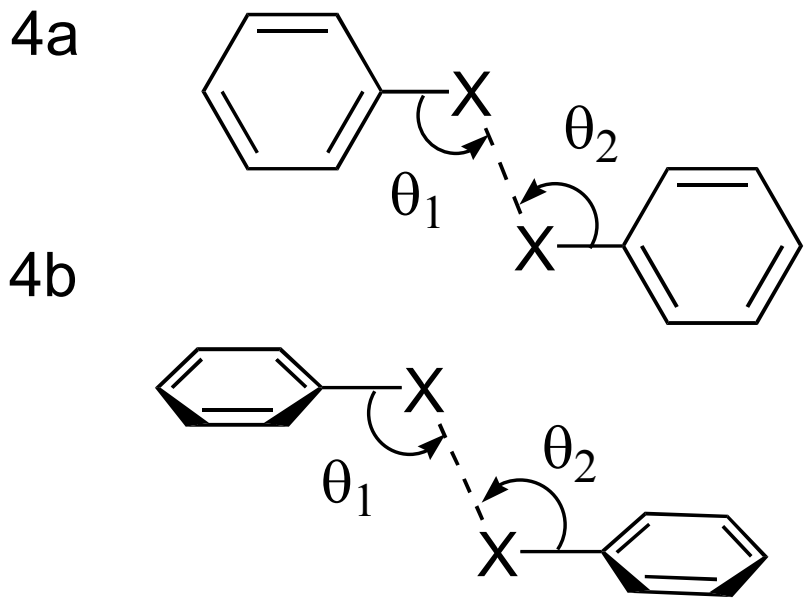

RESULTS

Crystallographic Study

Investigation of CSD shows the maximum number of reported contacts occurs for Cl···Cl interactions, with a decreasing amount of interactions in the order F > Br >> I. The histogram distribution of the number of contacts within r_{vdW} *vs.* the interaction angle θ_i ($\theta_i = \theta_1 = \theta_2$, $\theta_i >$ 90, Φ 170 – 190°) shows that the maximum number of contacts occurs between 140 and 160° (Figure 1) for all interactions except F···F. From the data there are no statistically significant trends in F···F contacts. Henceforth, F···F contacts will be omitted from our discussion in this section. The interaction angle maxima vary according to the halogen (Cl···Cl, 150-160°;

Br···Br, 140-150°; I···I, 145-155°). Closer examination of the data shows definite trends for hybridization effects.

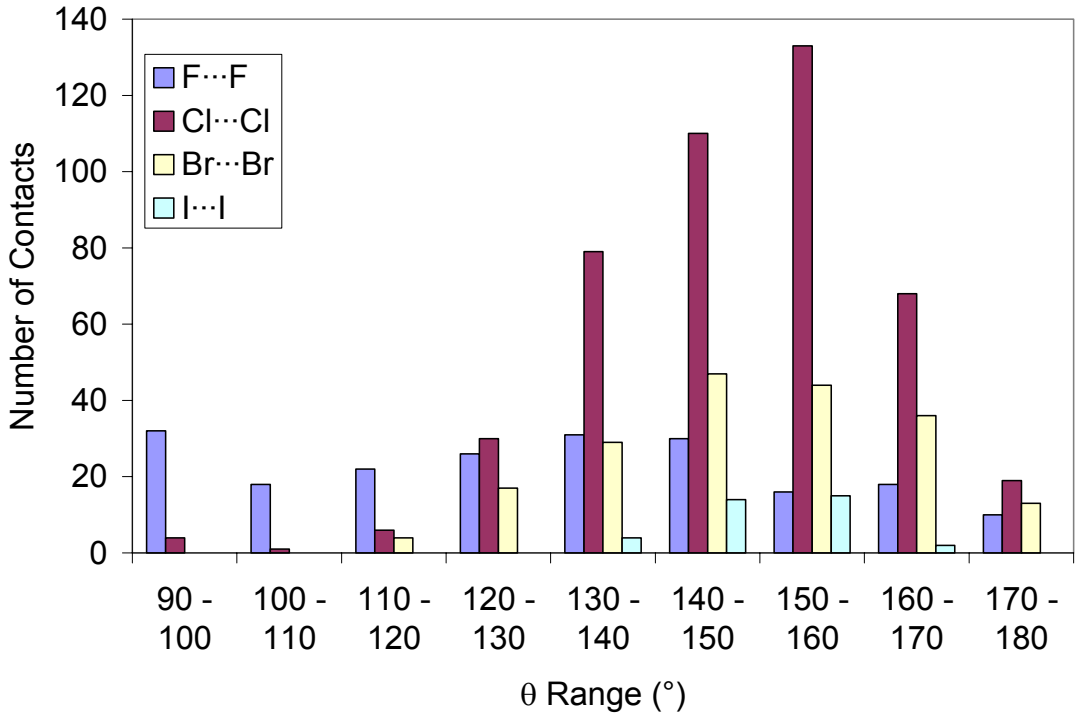

Figure 1. Histogram distribution of number of contacts *vs.* interaction angle for all halogen contacts with $\theta_i = \theta_1 = \theta_2$, $\theta_i > 90$, $\Phi = 170 - 190°$

Hybridization effects

The data were sorted according to the *ipso* carbon hybridization (Table 1). Individual histograms are shown in Figure 2 for; (a) Csp^3-X···X-Csp^3 (b) Csp^2-X···X-Csp^2 (c) C*arom*-X···X-C*arom* (X = Cl, Br, I). The latter subset, C*arom*-X, which is sp^2 hybridized has been separated as a special case from (b) Csp^2-X. Experimentally, they display distinct and different trends. There is a clear shift in the interaction angle maximum to lower θ value for all cases. This depends on both the hybridization and the halogen. The shift in the maxima occur in the order Csp^3-X···X-Csp^3 < Csp^2-X···X-Csp^2 < C*arom*-X···X-C*arom* From Figure 2c it is clear that the aromatic cases have a shifted maximum between 140-150° compared to

the total sp^2 hybridized cases (both aromatic and aliphatic), ca. 150-160°. An analysis of the data for Cl···Cl contacts between the maxima 150-160° (Csp^3-X, Csp^2-X) and 140-150° (C*arom*-X) as a function of separation distance in 0.05Å increments displays discrete maxima (Figure 3). These maxima indicate that the most frequent separation distance for Csp^3-X, Csp^2-X and C*arom*-X are 0.08Å, 0.18Å and 0.03Å respectively, shorter than the sum of r_{vdW}. The number of contacts for the other halogen···halogen contacts is not large enough to perform such statistical analysis.

Theoretical Study

Three basis sets of increasing size were used to model halogen···halogen contacts in the model compounds **1a** to **3d** (see Scheme 3). The energy of interaction was also estimated at the complete basis set level. The calculated potential energy diagram, at the double zeta basis set level (see method), indicated an energy minimum at ~150° ($\theta_1 = \theta_2$, $\Phi = 180°$) for all of the model compounds, except models containing fluorine (Figure 4). The energy of interaction at this geometry was calculated at triple and quadruple zeta basis sets and estimated, finally, at the complete basis set level (see Table 2). At the double zeta level, all energy minima occur at distances larger than the sum of r_{vdW}. Increasing the basis set level decreases the separation distance to be within the sum of r_{vdW} (for the ca. 150° geometry). The calculated energies of the interaction at the ca. 150º minimum follow the order I···I > Br···Br > Cl···Cl (Table 2). The stabilization energy was calculated as a function of the hybridization of the *ipso* carbon. The stabilization energies follow the order sp^2 > sp >sp^3. These are outlined in the following sections.

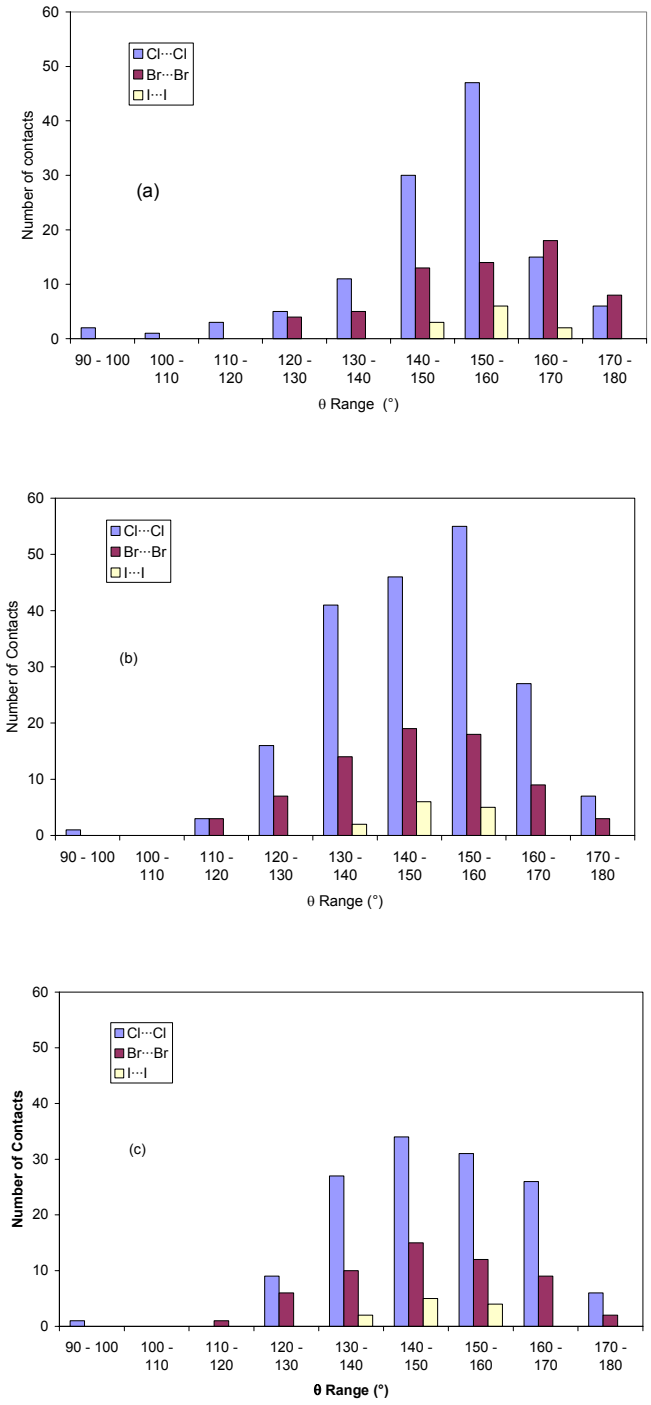

Figure 2. Histogram of the number of contacts within the sum of *vdW* radii of the type (a) Csp^3-X···X-Csp^3, (b) Csp^2-X···X-Csp^2, and (c) C*arom*-X···X-C*arom.*

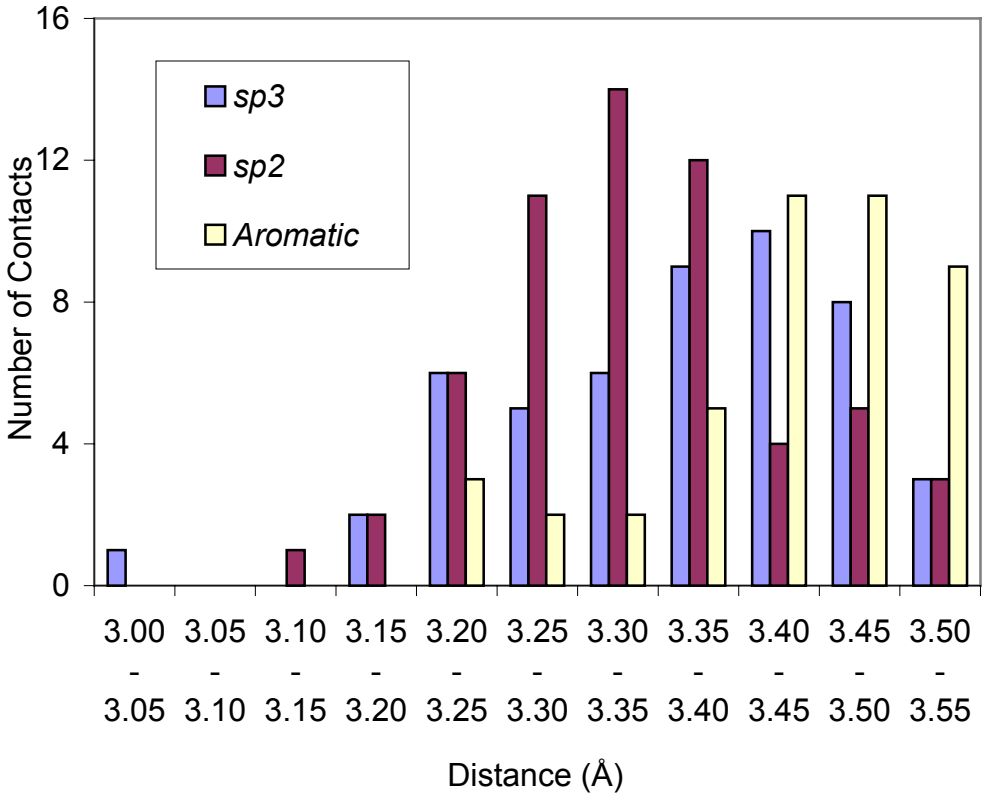

Figure 3. Histogram of the number of contacts as function of the chlorine···chlorine separation distances.

(1) Csp^3-X···X- Csp^3 Contacts

The potential energy diagram of two interacting monomers of type **1** was calculated at the double zeta basis set level, dz, for $\theta_1 = \theta_2$ geometries, and both angles were varied from 80° to 180°. The contour plot for type **1a** dimers shows only one minimum at < 80º (Figure 4a). Plots for **1b**, **1c** and **1d** show two minima; the first one ca. 150° (Figure 4b), the second again at angles less than 80°. In both minima, the separation distances are larger than the sum of the r_{vdW}. Using larger basis sets, up to, and including, an estimate of the complete basis set, moves the calculated energy minimum to within the sum of the r_{vdW} (see Table 2).

(2) Csp^2-X···X-Csp^2 Contacts.

Energy minima at ca. 150º are seen when the dimer angles are $\theta_1 = \theta_2$, $\Phi = 180°$, with atoms either on the mirror plane, or with the plane bisecting the X-aromatic plane for all halogen···halogen contacts except fluorine···fluorine (Scheme 4). These minima are shifted to lower angle values in comparison to Csp^3-X···X-Csp^3 contacts. The exact position of these minima and their energies are listed in Table 2. With the atoms on a mirror plane, the other minimum is located at ca. 90°. Conversely, when the mirror plane bisects the aromatic system, the minimum occurs at $\theta < 80º$. At these lower angles, the positions of this minimum are affected by other interactions, i.e. C-H···X hydrogen bonds, interaction with the aromatic system and the steric repulsion.

(3) Csp-X···X-Csp Contacts

Compared to interactions in types **1** and **2** compounds, type **3** compounds have an energy minimum which is shifted to lower angles, with an increase in the separation distance (Table 2).

DISCUSSION

The data, both the crystallographic and the theoretical, will be discussed in the following order; (a) proposing a model; (b) the effect of hybridization of the *ipso* carbon atom and its influence on the separation distance between the two halogen atoms and the most suitable geometry; (c) the effect of *ortho* groups in aromatic systems; (d) comparing this model with simple crystal structures; and (e) the effect of attaching an electronegative atom to the *ipso* carbon.

(a) Model.

An electrostatic model can be used to explain the theoretical and crystallographic data. An electrostatic model is based on two main ideas; (1) the calculated electrostatic potential shows

Table 2. Calculated energy of interactions, separation distances and the angle of interaction for peak ca.150° for the model compounds computed at different basis set level.

Basis set	DZ			TZ			QZ			cbs		
Compound	Angle (°)	Distance (Å)	Energy (kJ/mol)	Angle (°)	Distance (Å)	Energy (kJ/mol)	Angle (°)	Distance (Å)	Energy (kJ/mol)	Angle (°)	Distance (Å)	Energy (kJ/mol)
1b	156	3.71	-1.027	156	3.54	-1.952	156	3.47	-2.438	156	3.43	-2.770
1c	153	3.82	-2.484	153	3.68	-3.768	153	3.62	-4.413	153	3.60	-4.826
1c[a]	153	3.68	-4.373	153	3.63	-4.700	153	3.60	-5.000	153	3.58	-5.207
1d	147	4.15	-4.260	147	3.95	-6.158	147	3.89	-7.040	147	3.86	-7.585
2b	152	3.62	- 2.631									
2b[a]	152	3.46	-5.502	152	3.43	-5.041	152	3.40	-5.131	152	3.38	-5.216
2c	150	3.79	-3.663									
2c[a]	150	3.72	-6.180	150	3.68	-5.684	150	3.67	-7.506	150	3.65	-8.766
2d	148	4.1	-5.015									
2d[a]	148	3.96	-8.430	148	3.83	-8.944	148	3.82	-9.010	148	3.81	-9.029
3b	142	3.66	-2.731	142	3.55	-3.423	142	3.49	-3.843	142	3.46	-4.129
3c	140	3.85	-3.552	140	3.74	-4.453	140	3.68	-5.040	140	3.65	-5.425
3d	144	4.11	-3.745	144	4.11	-4.996	144	4.06	-5.658	144	4.04	-6.073

[a] The energy is not corrected for BSSE error.

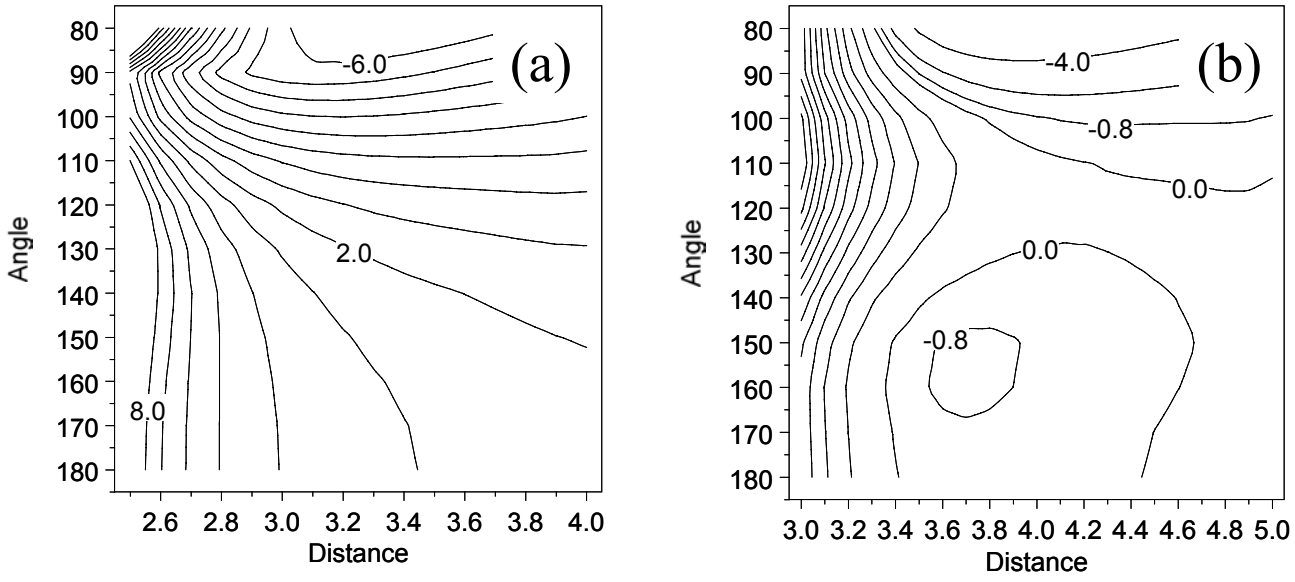

Figure 4. Potential energy diagram of two interacting type **1** molecules as a function of θ_i and distance r_i for (a) **1a** and (b) **1b**. $\theta_2 = \theta_1$. **1c** and **1d** have similar plots to **1b**. The separation distances, energies and angles are listed in Table 2.

the presence of a positive potential end cap and a negative electrostatic potential ring on the π region of the halogen for **1b, 1c** and **1d** with the exception of **1a** (Figure 5a);[8a] (2) the electron density is anisotropically distributed around the halogen atom (Figure 5b, the electron density for all atoms has been multiplied by a factor to enhance the anisotropy: comparison between molecules cannot be made).[11a,19] Therefore, the halogen atom has two different radii; a short one along the C-X bond and a longer one perpendicular to it. According to the electrostatic model, the presence of the energy minimum dictates that the negative electrostatic ring should face the positive electrostatic end cap.In view of this, two energy minima are expected between the two halogen atoms. These minima occur at the following geometries; (i) $\theta_1 = \theta_2 =$ ca. 150° and the torsion angle (C-X···X-C) Φ = 180° (Figure 6a), (ii) $\theta_2 = 180°$ and $\theta_1 = 90°$ (Figure 6b). Hereafter the former will be called type (i) and the latter type (ii) interactions. In this discussion, type (ii) interactions will be ignored due to that fact that other effects

(intermolecular interactions, steric, electronic, etc) can influence the interaction. The number of contacts within the sum of r_{vdW} agrees with our electrostatic model and the *ab initio* calculations; they display interaction maxima in the range 140-160°, except for F···F interactions (Figure 1). The calculations also indicate that, as the size of the halogen atom increases, the relative strength of the halogen···halogen contacts increase, which support the argument of deformation of the electronic charge around the halogen atom, due to the fact that heavier halogens are more polarizable.

All the calculated potential energy diagrams with $\theta_1 = \theta_2$ show another minimum at $\theta_1 = \theta_2 <$ 80º. The exception is in the type 4a model (Scheme 4). In the case, this minimum is located at ca. 90°. This minimum can be explained by *ortho* and geometry effects, i.e., the domination of C-H···X interactions and steric effects. Therefore, only the minima at ca. 150° will be used in this discussion due to minimal interactions with the rest of the molecule at this geometry.

The combination of the anisotropy in radius and the presence of the positive electrostatic potential end cap on the halogen atom can be tested by investigating the distance at which the energy minimum is located as a function of the angle θ in type (i) interactions. At $\theta_1 = \theta_2 =$ 180°, the radius of the halogen is the smallest. However, electrostatic repulsion forces the energy minimum to higher separation distances but the energy *in toto* is attractive due to the presence of other forces, e.g., dispersion. As the angle θ approaches ca. 150°, the radius is increasing and the separation distance at the energy minima decreases due to attractive forces (Figure 7). For $\theta < 150°$, the separation distance increases again due the increment in the radius and the repulsive forces. Overall, the data indicate these interactions are controlled by electrostatics.

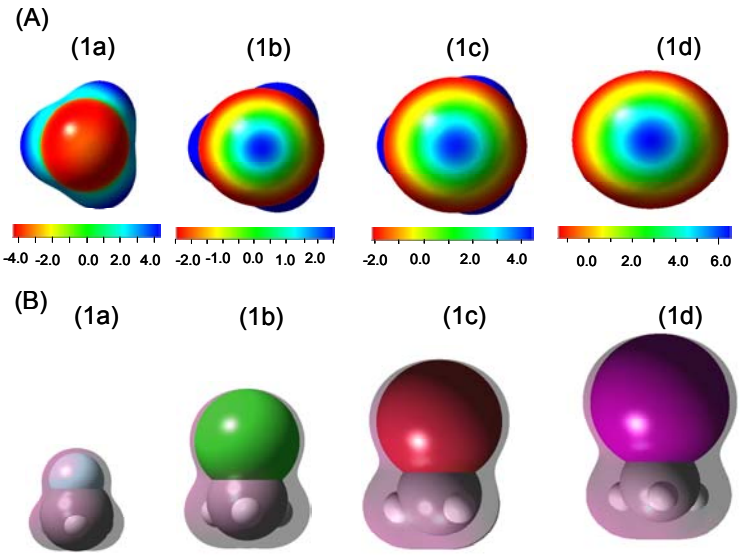

Figure 5. (a) Calculated electrostatic potential surface for **1a**, **1b**, **1c** and **1d** respectively. The energy is expressed in Hartrees and charge in electronic charge units (the scale is multiplied by 100) and (b) electron density of **1a**, **1b**, **1c** and **1d**. The anisotropy in the electronic charge distribution is represented by the *umbra* around the spherical halogen. The electron density contour isovalue is set to 0.005. The potential and electron density were calculated using MP2 and a tz basis set.

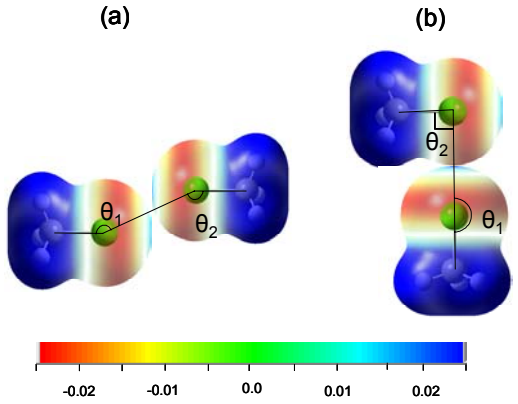

Figure 6. Geometries of the two energy minima; (a) $\theta_1 = \theta_2$ = ca. 150°, torsion angle (C-X···X-C) Φ = 180°; (b) θ_2 = 180° and θ_1 = 90°. The color indicates the value of the calculated electrostatic potential**.**

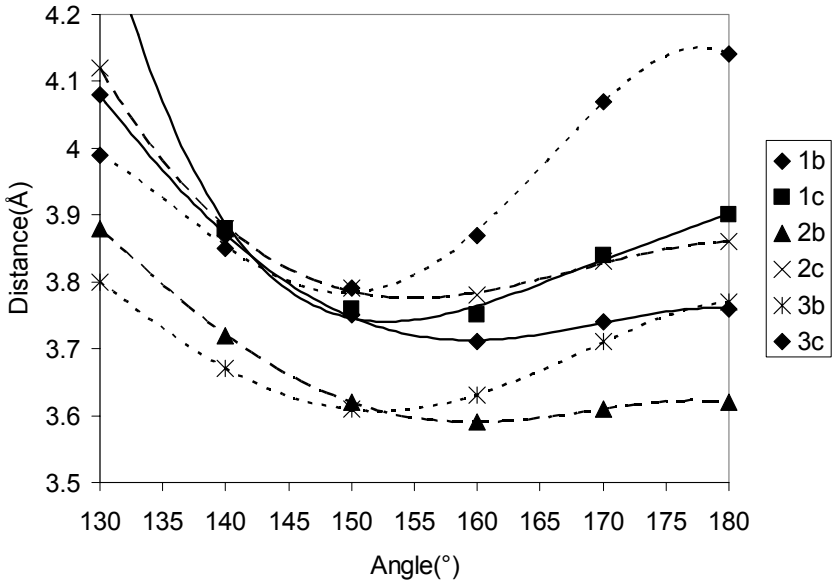

Figure 7. Plot of the angle at which the calculated energy minimum is located *vs.* the corresponding separation distance. The drawn curves are guides for the eye only.

Calculations show that the dz basis set is insufficient to model the halogen···halogen contact. For example, the dz basis set predicts the presence of energy minimum at ca. 155°. However, the model indicates that this minimum will occur at a distance longer than the sum of r_{vdW}, which disagrees with the experimental results. However, the interactions distances at the complete basis set (Table 2) are in very good agreement with experimental data. For example, for the Csp^3-X···X-Csp^3 contacts, the calculation at complete basis yields r_i = 3.43 Å, and experimentally it is found that r_i = 3.43(3) Å (Figure 3).

(b) Effect of Hybridization.

The theoretical results show that the strength of the halogen···halogen contact as a function of the *ipso* carbon atom follows the order sp^2 > sp > sp^3 (Table 2). This trend can be easily explained by the electrostatic model. The calculated electrostatic potentials of **1c**, **2c** and **3c** are shown in Figure 8. As the hybridization of the *ipso* carbon changes from sp^3 to *sp*, clearly

the positive electrostatic end cap increases. Concomitantly, there is a decrease in the negative electrostatic ring. According to the electrostatic model, the energy of interaction is governed by both the electrostatic potential end cap and also by the electrostatic negative potential ring and hence the decrease in the energy of interaction in going from sp^2 to *sp*.

This behavior parallels the electronegativity of the *ipso* carbon atom, since there is a higher s character for *sp* hybridization. Type **1** dimers have hydrogen bonded *ipso* carbon atoms, while type **2** and **3** dimers have additional carbon atoms bonded to the *ipso* carbon. This would change the electronegativity of the *ipso* carbon and, hence, the energy of interaction and the distance at which this minimum occurs. Crystallographic analysis supports this idea as indicated by the separation distance and the angle of interaction, e.g., the Cl···Cl separation distance is 0.08 and 0.18 Å less than the sum of r_{vdW} for Csp^3-X···X-Csp^3 and Csp^2-X···X-Csp^2 respectively (see Figure 3).

(c) Effect of Ortho groups.

Large *ortho* groups can have an influence on the halogen···halogen interaction. In the calculated model, with an angle of ca. 150°, the dimers are too far apart for *ortho* substituents to interact. Therefore the theoretical effects of the *ortho* substituents are not seen.

Experimentally, the effect of this interaction is obvious with substituted type **2** compounds (Figure 9), i.e., as the distance between the aromatic planes gets smaller, halogen atoms start interacting with the groups in the *ortho* positions. Therefore, θ values are spread over a wide range of values, especially at smaller contact distances. As the perpendicular distance between the two aromatic planes increases, the angles of interaction are governed by the halogen···halogen interactions. In both the F···F and Cl···Cl cases at very large separation distances, the halogen atom of one molecule interacts with the aromatic system of the other

molecule (Figure 9a and 9b). These contacts are not seen for Br···Br and I···I contacts, probably due to the size of the halogen atom and the deformation of the electronic charge.

(d) Crystal Structure of the Model Compounds.

Structures of several of the model compounds have been determined and allow comparison between the theoretical and experimental results. The structures of monohalomethanes, CH_3X, (the structure of **1a** is unknown)**,** are based on competition between hydrogen bonding and halogen···halogen contacts.[20] Hydrogen bonding is dominant in the structure of **1b**, and hence there are no Cl···Cl contacts in this example.[20a] The distance between the closest two chlorine atoms is 4.141 Å, which is outside the sum of the r_{vdW}. In contrast, the structures of **1c** and **1d** show both halogen···halogen contacts and hydrogen bonding.[20b] **1c** and **1d** are isomorphous and form chain structures based on the halogen···halogen contact. This agrees with the calculations (*vide supra*, Table 2) that Br···Br and I···I contacts are stronger than Cl···Cl contacts.

Halogen···halogen contacts play a more crucial role in the structures of type **2** models in comparison to type **1** models. The closest F···F distance in the structure of fluorobenzene is 4.727Å.[21a] The structure of **2b** displays Cl atoms directed towards each other, even though the distance between them is slightly larger than the sum of r_{vdW} (3.599Å).[21b] The contact angles are $\theta_1 = \theta_2 = 147°$, which agree well with the calculated angle $\theta_1 = \theta_2 = 152°$. This would indicate that Cl···Cl contacts are stronger when the chlorine atom is attached to sp^2 hybridized atom than sp^3 hybridized carbon.

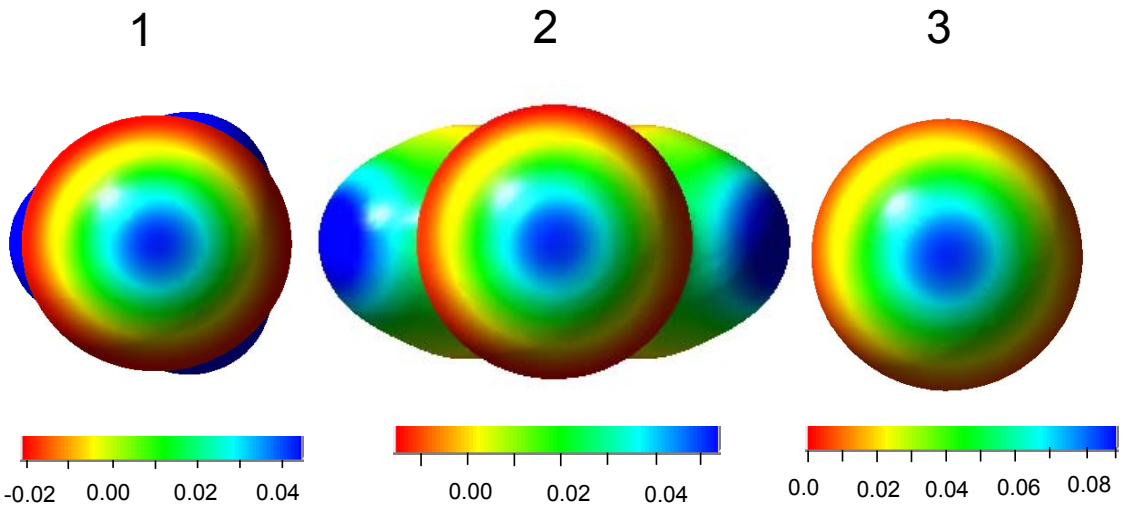

Figure 8. The calculated electrostatic potential of **1c**, **2c** and **3c**. The energy is expressed in Hartrees and charge in electronic charge units.

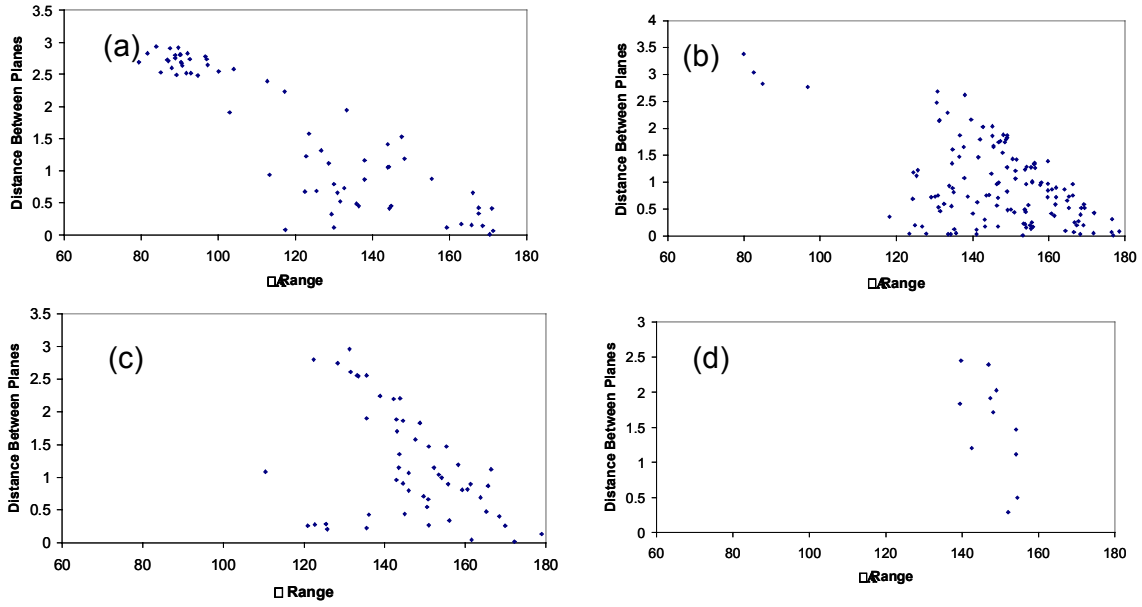

Figure 9. The angle of contacts θ *vs.* the distance between the aromatic planes for: a) F ···F, (b) Cl···Cl, (c) Br···Br and (d) I···I. with $\theta_1 = \theta_2$.

(e) Effect of Attaching an Electronegative Atom to the Ipso Carbon Atom.

The addition of a more electronegative atom to one of the model compounds will strengthen the halogen···halogen interaction. Calculations show that the addition of fluorine to **1b** and **1c** significantly increases the energy of interaction. In contrast, the addition of more atoms with the same electronegativity has only a slight effect (Table 3). This would indicate that the addition of extra electronegative atoms to the carbon atom increases the deformation in of the electronic charge and hence the positive electrostatic potential end cap.

Experimentally, examining the structures of fluorotrichloromethane and fluorotribromomethane,[22] show that the highly electronegative fluorine atoms form hetero halogen···halogen interactions (F···Cl, F···Br) rather than assisting in a stronger homo halogen···halogen interaction. In dichlorobenzene, the interaction distance is shorter than in **2b** (Table 1S), when $\theta_1 = \theta_2$. The addition of an extra Cl atom to the ring reinforces the Cl···Cl contact.[21b,23a] This follows the calculation seen for fluorohalomethane (*vide supra*).

Table 3. The calculated energies, angles and separation distances in fluorohalomethane dimers.[a]

Compound	Energy (kJ/mol)	Angle (°)	Distance (Å)
1b	-1.027	156	3.71
FCH_2Cl	-2.163	152	3.67
F_2CHCl	-2.271	149	3.69
F_3CCl	-2.334	143	3.71
1c	-2.484	153	3.83
FCH_2Br	-3.130	150	3.86
F_2CHBr	-3.088	146	3.89
F_3CBr	-3.095	141	3.91

[a] the calculations are carried out at the dz basis set level.

Other related intermolecular interactions have been shown to be electrostatic in nature. Lommerse *et al.*, based on theoretical and crystallographic studies, showed that the C-X···E interaction (X = F, Cl, Br or I, E = N, O or S) was mainly due to electrostatic factors.[24a] More recently, the electron density map of the molecular aggregation between 4,4'-dipyridyl-N,N'-dioxide and 1,4-diiodotetrafluorobenzene ,and the complex of (E)-1,2-bis(4-pyridyl)ethylene with 1,4-diiodotetrafluorobenzene revealed that I···O and I···N interactions are electrostatic in nature.[24b,c] The intermolecular perturbation calculations performed by Price *et al.* showed there is a reduction in the electrostatic repulsion that occurs at ca. 150°.[11a] In several crystallographic studies, it was found that halogen···halide interactions (C-X···X^-) prefer a linear arrangement; the negatively charged halide anion confronts the positive electrostatic potential cap on the halogen.[25] Moreover, the C-X···X-M (halogen···metal halide) synthon is again characterized by a linear C-X···X arrangement and a separation distance less than the sum of r_{vdW}.[26] Zordan *et al.* have shown that the C-X···X-M contacts involve an attractive electrostatic contribution.[26e] All of these observations agree with our electrostatic model and support it.

CONCLUSIONS

Both *ab initio* calculations and histogram distributions of halogen···halogen contacts within the sum r_{vdW} in the database structures indicate that these contacts are directive and a result of attractive forces for all halogens except fluorine. An electrostatic model can explain these interactions. The model is based on two ideas; (a) a presence of positive electrostatic potential end cap on the halogen atom, (as shown by the calculated electrostatic potential) (b) the electron density is anisotropically distributed around the halogen atom (indicated by the population analyses of the contacts and the calculated electron density). Interaction strengths

follow the order I···I > Br···Br > Cl···Cl. For X = F, the F···F interactions are weak enough that other intermolecular forces will dominate. This halogen···halogen strength trend is parallel to the polarizability of the electronic charge around the halogen atom.

The hybridization of the *ipso* carbon atom and addition of an electronegative atom to the *ipso* carbon atom also affect the strength of halogen···halogen interaction, the geometry and also the separation distance. Halogen...halogen interactions are strongest when the halogen atom is attached to sp^2 hybridized atom and the weakest when attached to a sp^3 hybridized one. Adding extra electronegative atoms to the *ipso* carbon can reinforce these contacts. The change in the interaction angle (θ) and the anisotropy in the charge distribution will affect the distance of interaction. Therefore, in order to take the separation distance as an accurate parameter for the strength of the halogen···halogen contact, the angles of the contact angles should be very similar (as the electron density is anisotropically distributed around the halogen atom). Our analyses (crystallographic and theoretical studies) show that these synthons are controlled by electrostatic factors (*in toto*), but other forces (e.g., dispersion, charge transfer) also participate in these interactions. Understanding the nature of these interactions and how to control them systematically can help design and synthesize specific supramolecular synthons for crystal engineering purposes. The addition of another simple predictable supramolecular synthonic element into the arsenal of crystal engineering techniques, e.g., hydrogen bonding, π-π, halogen bond, is a fundamental and important result.

ACKNOWLEDGEMENTS: Work supported in part by ACS-PRF 34779-AC.

Supporting Information Available: Table of interaction parameters in halobenzene structures. The complete citation of Gaussian 98 and MOLPRO programming packages. These materials are available free of charge via the Internet at http://pubs.acs.org.

REFERENCES

1 (a) Desiraju, G. R. *Nature* **2001**, *412*, 397-400. (b) Desiraju, G. R. *Crystal Engineering, The Design Of Organic Solids,* Elsevier Science Publishers B. V. **1989**. (c) Desiraju, R. G. *Angew. Chem. Int. Ed. Engl.* **1995**, *34*, 2311-2327. (d) Brammer, L. *Chem. Soc. Rev.* **2004**, *33*, 476-489. (e) Braga, D.; Brammer, L.; Champness, N. *CrystEngComm.* **2005**, *7*, 1-19.

2 (a) Yamamoto, H. M.; Yamaura, J.; Kato, R. *J. Am. Chem. Soc.* **1998**, 120(24), 5905-5913 and references therein. (b) Matsumoto, A.; Tanaka, T.; Tsubouchi, T.; Tashiro, K.; Saragai, S.; Nakamoto Sh. *J. Am. Chem. Soc.* **2002**, *124*, 8891-8902. (c) MacGillivray, L. R.;Reid, J. L.; Ripmeester, J. A. *J. Am. Chem. Soc.* **2000,** *122*, 7817-7818. (d) MacGillivray, L. R. *CrystEngComm*, **2002**, *4*, 37-41.

3 (a) Aakeröy C. B.; Beatty A. M. *Aust. J. Chem.* **2001**, *54*, 409-421. (b) Brammer, L.; Bruton, E. A.; Sherwood, P. *Cryst. Growth Des.* **2001**, *1*, 277-290. (c) Lutz, H. D. *J. Mol. Struct*. **2003**, *646*, 227-236.

4 (a) Walsh, R. B.; Padgett, C. W.; Metrangolo, P.; Resnati, G.; Hanks, T. W.; Pennington, W. T. *Cryst. Growth Des.* **2001,** *1*, 165-175. (b) Ouvrard, C.; Questel, J.; Berthelot, M.; Laurence, Ch. *Acta Cryst.* **2003**, *B59*, 512-526. (c) Forni, A.; Metrangolo, P.; Pilati, T.; Resanti, G. *Cryst. Growth Des.* **2004**, *4*, 291-295. (d) Berski, S.; Ciunik, Z.; Drabent, K.; Latajka, Z.; Panek, J. *J. Phys. Chem. B.* **2004**, 108, 12327-12332. (e) Santis, A.; Forni, A.; Liantonio, R.; Metrangolo, P.; Pilati, T.; Resnati, G. *Chem. Eur. J.* **2003**, *9*, 3974-3983. (f) Wang, W.; Wong, N.; Zheng, W.; Tian, A. *J. Phys. Chem. A*. **2004**, *108*, 1799-1805. (g) Auffinger, P.; Hays, F. A.;

Westhof, E.; Shing Ho, P., *PNAS* **2004**, *48*, 16789-16794. (h) Metrangolo, P.;Neukirch, H.; Pilati, T.; Resnati, G. *Acc. Chem. Res.* **2005**, *38*,386-395.

5 Braga, D.; Grepioni, F. *New J. Chem*. **1998**, *22*, 1159-1161. (b) Desiraju, G. R.; Stiener, T. *The Weak Hydrogen Bond in Structural Chemistry and Biology* (Oxford Univ. Press. Oxford **1990**). (c) Langley, P. J.; Hulliger, J.; Thaimattam. R.; Desiraju, G. R. *New J. Chem*., **1998**, *22*, 1307-1309.

6. (a) Desiraju, G. R.; Parthasarathy, R. *J. Am. Chem. Soc.* **1989**, *111*, 8725-8726. (b) Jagarlapudi, A. R.; Sarma, P.; Desiraju G. R. *Acc. Chem. Res.* **1986**, 19, 222-228.

7. (a) Sinnokrot, M. O.; Sherrill, D. C. *J. Am. Chem. Soc.* **2004**, *126*, 7690-7697. (b) Sinnokrot, M. O.; Sherrill, D. C. *J. Phys. Chem.* **2003**, *107*, 8377-8379. (c) Sinnokrot, M. O.; Valeev, E. F.; Sherrill, D. C. *J. Am. Chem. Soc.* **2002**, *124*, 10887-10893. (d) Hunter, Ch. A.; Sanders, K. M. *J. Am. Chem. Soc.* **1990**, *112*, 5525-5534. (e) Desiraju, G. R.; Gavezzotti, A. *J. Chem Soc. Chem. Commun*. **1989**, 621-623.

8. (a) Bosch, E.; Barnes, C. L. *Cryst. Growth Des.* **2002**, *2*, 299-302. (b) Broder, Ch. K.; Howard, A. J.; Wilson, Ch. C.; Allen, F. H.; Jetti, R. K.; Nangia A.; Desiraju, G. R. *Acta. Cryst.* **2000,** *B56*, 1080-1084.

9. Bent A. H. *Chem. Rev.* **1968,** *68*, 587-648.

10. Ramasubbu, N.; Parthasarathy, R.; Murray-Rust, P. *J. Am. Chem. Soc.* **1986**, *108*, 4308-4314.

11. (a) Price, S. L.; Stone, A. J.; Lucas, J.; Rowland, R. S.; Thornley, A. E. *J. Am. Chem. Soc.* **1994,** *116*, 4910-4918. (b) Nyburg, S. C.; Wong-Ng, W. *Proc. R. Soc. London* **1979**, *A367*, 29-45.

12. Any structure determined in the range 283-303K is considered to be a room-temperature structure.

13. Selecting this filter eliminates from the search any structure that contains a transition metal, lanthanide, actinide or any of Al, Ga, In, Tl, Ge, Sn, Pb, Sb, Bi, Po.

14. Gaussian 98, Revision A.11.2, M. J. Frisch *et. al*.

15. MOLPRO is a package of programs written by H-J. Werner *et. al.*

16. (a) Dunning, T. H., Jr. *J. Chem. Phys.* **1989**, *90*, 1007-1023. (b) Kendall, R. A.; Dunning, T. H., Jr.; Harrison, R. J. *J. Chem. Phys.* **1992**, *96*, 6796-6806. (c) Woon, D. E.; Dunning, T. H., Jr. *J. Chem. Phys.* **1993**, *98*, 1358-1371. (d) Wilson, A. K.; Peterson, K. A.; Woon, D. E.; Dunning, T. H., Jr. *J. Chem. Phys.* **1999**, *110*, 7667-7676. (e) Peterson, K. A.; Figgen, D.; Goll, E.; Stoll, H.; Dolg, M. *J. Chem. Phys*. **2003**, *119*, 11113-11123.

17. Boys, S. F.; Bernardi, F. *Mol. Phys.* **1970**, *19*, 553.

18. (a) Peterson, K. A.; Woon, D. E.; Dunning, T. H., Jr. *J. Chem. Phys.* **1994**, *100*, 7410-7415. (b) Feller, D.; Peterson, K. A. *J. Chem. Phys.* **1999**, *110*, 8384-8396.

19. Nyburg, S. C.; Faerman, C.H. *Acta Cryst*. **1985**, *B41*, 274-279.

20. (a) Burbank, R., D. *J. Am. Chem. Soc.* **1953**, *75*, 1211-1214 (b) Kawaguchi, T.; Hijikigawa, M.; Hayafuji, Y.; Ikeda, M.; Fukushima, R.; Tomiie, Y. *Bull. Chem. Soc. Jpn.* **1973**, *46(1)*, 53-56.

21. (a) Thalladi, V. R.; Weiss, H.-C.; Blaeser, D.; Boese, R.; Nangia, A.; Desiraju, G. R. *J. Am. Chem. Soc.* **1998**, *120*, 8702-8710. (b) Andre, D.; Fourme, R.; Renaud, M. *Acta Cryst.* **1971**, *B27*, 2371-2380.

22. a) Cockcroft, J. K.; Fitch, A. N. *Z. Kristallogr*. **1994**, *209(6)*, 488-490. (b) Fitch, A. N; Cockcroft, J. K. *Z. Kristallogr*. **1992**, *202*,243-250.

23. (a) Boese, R.; Kirchner, M. T.; Duntiz, J. D.; Filippini, G., Gavezzotti, A. *Helv. Chem. Acta*. **2001**, *84*, 1561-1577. (b) Croatto, U.; Bezzi, S.; Bua, E. *Acta Cryst.* **1952**, *5*, 825-829. (c) Estop, E.; Alvarez-Larena, A.; Belaaraj, A.; Solans, X.; Labrador, M. *Acta Cryst*., **1997,** *C53*, 1932-1935. (d) Housty, J.; Clastre, J. *Acta Cryst.* **1957**, *10*, 695-698. (e) Wheeler, G. L.; Colson, S. D. *Acta Cryst.* **1975**, *B31*, 911-913. (f) Fourme, R.; Clec'h, G.; Figuiere, P.; Ghelfenstein, M.; Szwarc, H. *Mol. Cryst. Liq. Cryst*. **1974,** *27*,315-323. (g) Wheeler, G. L.; Colson, S. D. *J. Chem. Phys.* **1976,** *65*, 1227-1235. (h) Panattoni, C.; Frasson, E.; Bezzi, S. *Gazz. Chim. Ital.* **1963,** *93*, 813-822.

24. (a) Lommerse, J. P.; Stone, A. J.; Taylor, R.; Allen, F. H. *J. Am. Chem. Soc.* **1996**, *118*, 3108-3116. (b) Bianchi, R.; Forni, A.; Pilati, T. *Acta Cryst.* **2004**, *B60*, 559-568. (c) Bianchi, R.; Forni, A.; Pilati, T. *Chem. Eur. J.* **2003**, *9*, 1631-1638.

25. (a) Freytag, M.; Jones, P. G. *Zeit. Naturfor B: Chem. Sci.* **2001**, *56*, 889-896. (b) Freytag, M.; Jones, P. G.; Ahrens, B.; Fischer, A. K. *New J. Chem*. **1999**, *23*,

1137-1139. (c) Logothetis, Th.; Meyer, F.; Metrangolo, P.; Pilati, T; Resnati, G. *New. J. Chem.* **2004**, *28*, 760-763. (d) Kuhn, N.; Abu-Rayyan A.; Eichele, K.; Schwarz, S.; Steimann, M. *Inorg. Chim. Acta* **2004**, *357(6)*, 1799-1804. (e) Kuhn, N.; Abu-Rayyan, N. A.; Eichele, K.; Piludu, C.; Steimann, M. *Z. Anorg. Allg. Chem.* **2004**, *630(4)*, 495-497.

26. (a) Willett, R. D.; Awwadi, F. F.; Butcher, R.; Haddad, S.; Twamley, B. *Cryst. Growth Des.* **2003**, *3*, 301-311. (b) Brammer, L.; Espallargas, G. M.; Adams, H. *CrystEngComm.* **2003**, *5(60)*, 343-345. (c) Haddad, S.; Awwadi, F.; Willett, R. D. *Cryst. Growth Des***.** **2003**, *3(4),* 501-505. (d) Zordan, F.; Brammer, L. *Acta Cryst*. **2004**, *B60*, 512-519. (e) Zordan, F.; Brammer, L.; Sherwood, P. *J. Am. Chem. Soc*. **2005**, *127*, 5979-5989.

SYNOPSIS

The Nature of Halogen···Halogen Synthons; Crystallographic and Theoretical Studies.

Firas F. Awwadi, Roger D. Willett, Kirk A. Peterson and Brendan Twamley

It is demonstrated that halogen···halogen interactions are governed by electrostatics. The two observed geometries of halogen···halogen contacts, (a) $\theta_1 = \theta_2$, (b) $\theta_1 = 180°$ and $\theta_2 = 90°$, can be explained based on the electrostatic model. The calculated electrostatic potential of halomethanes (expect fluoromethane) show positive electrostatic end caps (blue) on the halogen atoms as well as a negative electrostatic ring (red). The optimum geometry for the strongest halogen···halogen interaction is when $\theta_1 = \theta_2 \sim 150°$ and interaction strength following the order I···I > Br···Br > Cl···Cl.

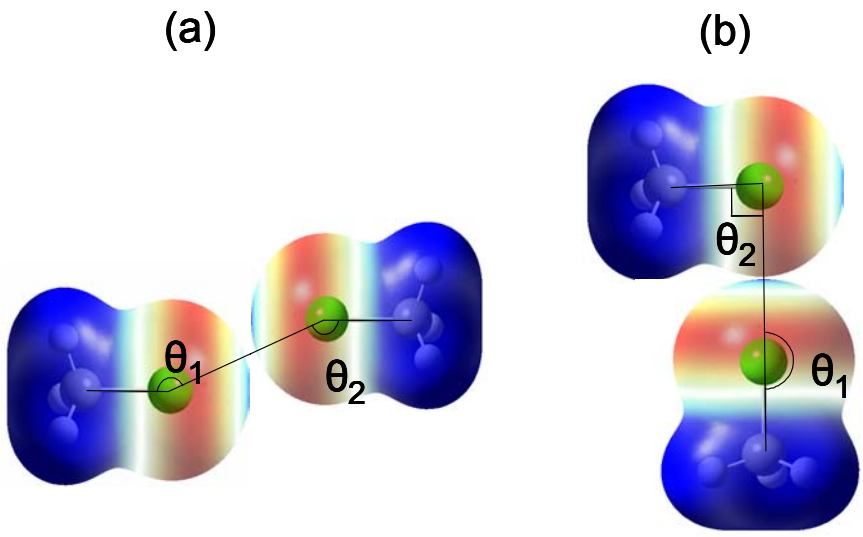

SUPPORTING INFORMATION

The Nature of Halogen···Halogen Synthons; Crystallographic and Theoretical Studies.

Firas F. Awwadi[†], Roger D. Willett[†,], Kirk A. Peterson[†] and Brendan Twamley[‡]*

[†]Department of Chemistry, Washington State University, Pullman, WA 99164 USA.

[‡]University Research Office, University of Idaho, Moscow, ID 83844 USA.

*Department of Chemistry, Washington State University, Pullman, WA 99164, USA, Tel (Office), 509 335 3925, FAX (dept.) 509 335 8867, E-mail rdw@mail.wsu.edu

Authors of Gaussian and MOLPRO programing packages

1. Gaussian 98, Revision A.11.2, M. J. Frisch, G. W. Trucks, H. B. Schlegel, G. E. Scuseria, M. A. Robb, J. R. Cheeseman, V. G. Zakrzewski, J. A. Montgomery, Jr., R. E. Stratmann, J. C. Burant, S. Dapprich, J. M. Millam, A. D. Daniels, K. N. Kudin, M. C. Strain, O. Farkas, J. Tomasi, V. Barone, M. Cossi, R. Cammi, B. Mennucci, C. Pomelli, C. Adamo, S. Clifford, J. Ochterski, G. A. Petersson, P. Y. Ayala, Q. Cui, K. Morokuma, N. Rega, P. Salvador, J. J. Dannenberg, D. K. Malick, A. D. Rabuck, K. Raghavachari, J. B. Foresman, J. Cioslowski, J. V. Ortiz, A. G. Baboul, B. B. Stefanov, G. Liu, A. Liashenko, P. Piskorz, I. Komaromi, R. Gomperts, R. L. Martin, D. J. Fox, T. Keith, M. A. Al-Laham, C. Y. Peng, A. Nanayakkara, M. Challacombe, P. M. W. Gill, B. Johnson, W. Chen, M. W. Wong, J. L. Andres, C. Gonzalez, M. Head-Gordon, E. S. Replogle, and J. A. Pople, Gaussian, Inc., Pittsburgh PA, **2001**.

2. MOLPRO is a package of programs written by H-J. Werner and P.J. Knowles with contributions from J. Almlöf, R.D. Amos, A. Bernhardsson, A. Berning, P. Celani, D.L.

Cooper, M.J.O. Deegan, A.J. Dobbyn, F. Eckert, S.T. Elbert, C. Hampel, G. Hetzer, T. Korona, R. Lindh, A.W. Lloyd, S.J. McNicholas, F.R. Manby, W. Meyer, M.E. Mura, A. Nicklass, P. Palmieri, R.M. Pitzer, P. Pulay, G. Rauhut, M. Schütz, H. Stoll, A.J. Stone, R. Tarroni, P.R. Taylor, T. Thorsteinsson.

Table 1S. X···X interaction parameters of the closest two halogen atoms in halobenzene structures.

Compound	Distance (Å)	θ_1 (°)	θ_2 (°)	Space group	Temperature K	References	REFCODE
Fluorobenzene	4.727	124.22	72.23	*P*43212	123	17a	FACFAQ
Chlorobenzene	3.599	147	147	*Pbcn*	393	17b	MCBENZ
o-dichlorobenzene	3.574	94.24	170.13	$P2_1/n$	223	23a	ABUMIT
m-dichlorobenzene	3.460	146.79	146.79	$P2_1/c$	220	23a	ABUMOZ
p-dichlorobenzene	3.847	95.68	166.49	$P2_1/a$	295	23b	DCLBEN
p-dichlorobenzene	3.806	92.48	166.69	$P2_1/a$	295	23c	DCLBEN01
p-dichlorobenzene	3.456	169.17	169.17	*P*-1	295	23d	DCLBEN02
p-dichlorobenzene	3.789	155.36	85.43	$P2_1/c$	100	23e	DCLBEN03
p-dichlorobenzene	3.778	154.52	85.32	$P2_1/a$	260	23f	DCLBEN04
p-dichlorobenzene	3.424	170.60	170.46	*P*-1	295	23g	DCLBEN05
p-dichlorobenzene	3.385	169.39	169.39	*P*-1	100	23g	DCLBEN06
p-dichlorobenzene	3.729	166.09	92.33	$P2_1/a$	100	23g	DCLBEN07
p-dichlorobenzene	3.792	166.52	93.51	$P2_1/a$	133	23h	DCLBEN11

CHAPTER THREE

The Nature of Halogen···Halide Synthons; Theoretical and Crystallographic Studies.

Firas F. Awwadi[†], Roger D. Willett[†,], Kirk A. Peterson[†] and Brendan Twamley[‡]*

[†]Department of Chemistry, Washington State University, Pullman, WA 99164 USA

[‡]University Research Office, University of Idaho, Moscow, ID 83844 USA

*Department of Chemistry, Washington State University, Pullman, WA 99164, USA, Tel (Office), 509 335 3925, FAX (dept.) 509 335 8867, E-mail rdw@mail.wsu.edu.

ABSTRACT Two types of halogen···halide synthons are investigated based on theoretical and crystallographic studies; the simple halogen···halide synthons and the charge assisted halogen···halide synthons. The former interactions were investigated theoretically (*ab initio*) by studying the energy of interaction of the halide anion with the halogen atom as a function of Y···X^- separation distance and the C-Y···X^- angle in a series of complexes (R-Y···X^-, R = methyl, phenyl, acetyl or pyridyl; Y= F, Cl, Br or I; X^- = F^-, Cl^-, Br^- or I^-). The theoretical study of the latter interaction type was investigated in only one system, the $[(4BP)Cl]_2$ dimer, (4BP = 4-bromopyrdinium cation). Crystal structure determinations, to complement the latter theoretical calculations, were performed on 13 *n*-chloropyridinium and *n*-bromopyridinium halide salts (*n* = 2, 3 and 4). The theoretical and crystallographic studies show that these interactions are controlled by electrostatics and are characterized by a linear C-Y···X^- angle and a separation distance less than the sum of van der Waals radii (r_{vdW}) of the halogen atom and the ionic radii of the halide anion. The strength of these contacts from calculations varies from weak (or absent), e.g., H_3C-Cl···I^-, to very strong, e.g., HCC-I···F^- (energy of interaction ca. -153 KJ/mol). Calculations indicate that this interaction is always absent in the C-F···X^- case. The strengths of these contacts are influenced by four factors: (a) the type of the halide anion; (b) the type of the halogen atom; (c) the hybridization of the *ipso* carbon; (d) the nature of the functional groups. Calculations show that charge assisted halogen···halide synthons have a comparable strength to simple halogen···halide synthons. These contacts are explained below based on an electrostatic model.

INTRODUCTION

Crystal engineering has been created through the systematic efforts to design new organic or inorganic materials. One of the main foci of this new field is the study of intermolecular interactions and their utilization in supramolecular synthesis.[1] These forces are important, not only due to their role in helping to arrange structural units in the crystalline lattice, but also because these forces participate in the physical properties of solid state materials, e.g., non-linear optical behavior, magnetic and electric properties, etc.[2] Intermolecular interactions have also been utilized to control solid state pericyclic reactions, e.g., dimerization and polymerization.[3,1d] These interactions range from strong forces, e.g., classical hydrogen bonds, to weaker ones e.g. halogen···halogen contacts.[4]

Initially, halogen···halogen contacts (C-Y···Y-C; Y = Cl, Br, and I) were studied using *ab initio* calculations and investigation of Cambridge Structural Data base (CSD).[4] Related synthons, halogen···halide interactions, have recently been found to be more directive in comparison to the traditional halogen···halogen synthon.[5] They are characterized by an intermolecular halogen···halide distance less than the sum of van der Waals (r_{vdW}) radii with an essentially linear C-Y···X^- angle.

These synthons have been studied crystallographically in several systems to elucidate their role in influencing the structure of crystalline materials and also their potential use as crystal engineering tools.[5] Many of the systems studied contain halide anions that carry a full negative charge. This study has been extended by bonding the halide anion to a more electropositive atom (e.g., a metal cation) thereby decreasing the negative charge on the halide, resulting in C-Y···X-M synthons.[6] These interactions play a crucial role in influencing

the structures of L_2MX_4 and ML_2X_2 (M = Cu(II), Co(II), Pd(II), Pt(II) ; X = F, Cl^-, Br^- or I^-; L = *n*-halopyridine).[6]

As a crystal engineering tool, halogen···halide synthons have been used to prepare useful materials. Yamamoto *et al.* and others synthesized organic based conducting materials using the halogen···halide synthon.[2] Their study also showed that the synthon was fundamental to the conducting property as well as helping shape the internal architecture of the lattice. Bromine···bromide synthons have been utilized in resolving racemic mixtures of 1,2-dibromohexafluoropropane by crystallizing it with enantiopure trialkylammonium hydrobromides.[7] More recently, we have used the bromine···bromide synthon to prepare a copper halide decamer, the longest ever known copper halide oligomer.[6c]

In our study, we are investigating the nature of halogen···halide synthons and also their potential as a crystal engineering tool. Several previous studies suggest that these synthons are a result of HOMO-LUMO charge transfer.[4b] Recently, Zordan *et al.* showed that these synthons involve electrostatic attractions, based on calculated electrostatic potentials.[6e] To our knowledge, there have been no published studies investigating the physical nature of these contacts. In this report, we present theoretical calculations and crystallographic studies on the physical nature of these synthons. The structures of two series of halopyridnium halide salts (*n*CP)X and (*n*BP)X (nCP^+ = *n*-chloropyridinium; nBP^+ = *n*-bromopyridinium; *n* = 2, 3, or 4; X = Cl^-, Br^- or I^-) are determined to complement *ab initio* calculations. The data will show that these synthons are controlled by electrostatics (*in toto*).

THEORETICAL METHOD AND EXPERIMENTAL SECTION.

(a) Theoretical Method

Gaussian 98 or 03[8] was used for geometry optimizations and MOLPRO[9] for electronic energy calculations. For all model compounds that are used in modeling simple halogen···halide, the structure of the molecular unit of each studied model was optimized using Møller-Plesset second order perturbation theory (MP2) with a triple zeta basis set. Similarly, (4BP)Cl, which is used to model the charge assisted halogen···halide interactions, was also optimized using MP2 and a triple zeta basis set except the N-H distance was constrained to1.014 Å, this distance was obtained by optimizing 4-bromopyridnium cation. The total electronic energy was computed with a series of cc-pVnZ basis sets (aug-cc-pVnZ on Br, Cl and F, and aug-cc-pRVnZ-PP on I, aug = presence of diffuse function on the halogen atom and halide anion) with MP2 (n = D, T and Q for double, triple and quadruple zeta, respectively).[10] This involves first Hartree-Fock, self-consistent field calculations to determine the molecular orbitals and then the subsequent MP2 calculation to determine the electron correlation energy. The calculated energy of interaction is corrected for basis set superposition error by the standard counterpoise method.[11] The energy of interaction at the complete basis set limit E(cbs) is estimated using the following equation.[12]

$$E(n) = E(cbs) + Ae^{-(n-1)} + Be^{-(n-1)^2}$$

where n = 2 (DZ), 3 (TZ), 4 (QZ) is the cardinal number of the correlation consistent basis set.

Halogen···halide interactions are classified into two types; (a) simple halogen···halide interactions. The energy of interaction of a halide anion (F^-, Cl^-, Br^- or I^-) with halogenated hydrocarbon R-Y, (R = methyl, phenyl, acetyl or pyridyl; Y = F, Cl, Br or I), Scheme 1, will

be calculated as a function of the separation distance (D) at θ = 180°. The energy of interaction will be calculated for (**1cCl**$^-$, **2cCl**$^-$, **3cCl**$^-$, **4cCl**$^-$) as a function of the distance at different values of θ. In the aromatic systems (**2cCl**$^-$ and **4cCl**$^-$), R-Y···X$^-$ has C_s symmetry and the mirror plane is located in a plane perpendicular to the plane of aromatic ring which bisects the aromatic ring at the bromine atom and the halide anion; (b) charge assisted halogen···halide interactions. The charge assisted halogen-halide synthons will be modeled by studying the energy of interaction in $[(4BP)Cl]_2$ as a function of the distance D at different values of θ. The dimer has C_S symmetry, the mirror plane bisects the dimer at the nitrogen and halogen atoms and halide anions (Scheme 1).

Scheme 1. Structure of the modeled compounds.

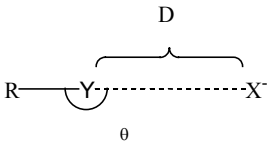

1	R = methyl	**a**	Y = F
2	R = phenyl	**b**	Y = Cl
3	R = acetyl	**c**	Y = Br
4	R = 4-pyridyl	**d**	Y = I

X = F$^-$, Cl$^-$, Br$^-$ or I$^-$

5

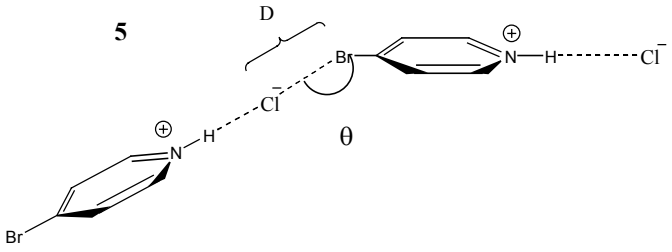

(b) Experimental Section

(1) Synthesis and Crystal Growth.

(a) (2CP)Br, (3CP)Br, (4CP)Br, (2BP)Br, (3BP)Cl and (4BP)Cl. A general procedure was followed to prepare above six compounds. About 0.2 g of the base was dissolved in

acetonitrile (2mL). The solution was acidified with concentrated acid (either hydrochloric acid or hydrobromic acid depend on the case). The solution was stirred for 10 minutes and left for slow evaporation. The next day a crystal with a suitable size for crystals structure determination formed. (b) *(2CP)I.* About 0.2 mL of the base was dissolved in 10 mL of ethanol. The solution was acidified with HI. The solution turned yellow, with time it got darker to a dark brown color. Colorless crystals formed with a suitable size for x-ray structure determination. (c) *(4CP)I.* About 0.2 g of 4-chloropyrdinium chloride was dissolved in 10 mL of absolute ethanol. The solution acidified using concentrated HI. The solution heat for 1 hour moderately and left for slow evaporation. Crystals formed with suitable size for x-ray structure determination. (d) *(3BP)I, (3CP)I and (2BP)I.* About 2 drops of 3-halopyridine was dissolved in 10 mL methanol. The solution acidified with HI and left for slow evaporation. Crystals formed with suitable size for x-ray structure determination. *(e) (4BP)I.* Small amount of (4BP)Cl was dissolved in methanol. The solution was acidified with HI, heated filtered and left for slow evaporation. (f) *(2BP)Cl.* 0.2 mL of 2-bromopyridine was dissolved in 1mL of propanol. The solution acidified with HCl (few drops). The propanol was evaporated under stream of nitrogen. The solid residue was dissolved in 5mL of methanol. The solution was left for slow evaporation. Crystals of suitable size for x-ray structure determination formed

(2) Crystallographic Experimental

The diffraction data of the studied compounds were collected at room temperature. The data of the compounds (2CP)Br, (2CP)I, (3CP)Br, (3CP)I, (4CP)Br, (4CP)I, (3BP)I, (4BP)I were collected on a Syntex $P2_1$ diffractometer upgraded to Bruker P4 specifications. The unit cell dimensions were determined from 23-40 accurately centered reflections. The data were collected and reduced using XSCANS 2.20 software.[13] Data were corrected for absorption correction utilizing ψ-scan data, using SHELXTL XPREP software, assuming ellipsoidal

shaped crystals.[14d] Data for (2BP)Cl, (2BP)Br, (2BP)I, (3BP)Cl, (4BP)Cl were collected using a Bruker/Siemens SMART APEX instrument (Mo Kα radiation, λ = 0.71073 Å) equipped with a Cryocool NeverIce low temperature device. The first 50 frames were recollected at the end of data collection to monitor for decay. Cell parameters were retrieved using SMART software and refined using SAINTPlus on all observed reflections.[14a,b] Data reduction and correction for Lp and decay were performed using the SAINTPlus software.[14b] Absorption corrections were applied using SADABS.[14c] The structures of all compounds were solved by direct methods and refined by least squares method on F^2 using the SHELXTL program package.[14d] All non hydrogen atoms were refined anisotropically. Hydrogen atoms were placed in calculated positions. Details of the data collection and refinement are given in Tables 1 and 2.

RESULTS

Theoretical Study

The contour plots of the energy of interaction *vs*. the separation distance, D, and angle, θ, for the ***n*cCl⁻** (*n* = 1, 2, 3, 4) show a global energy minimum at θ = 180° (Figure 1), and another minimum at θ < 80. This stabilization energy is anisotropic and θ dependent. The distance D, at which the energy minimum occurs, is also θ dependent. For example, in the case of **4cCl⁻**, at θ = 180°, a minimum occurs at ca. 3.1 Å. The energy minimum is anisotropically spread over θ, ranging from –32 kJ/mol at θ = 180°, crossing a saddle point at θ = 100°, ca. -7kJ/mol, and reaching ca. –8 kJ/mol at 90°, D = 3.9 Å (Figure 1d). Similarly, the contour plot of $[(4BP)Cl]_2$ shows a global energy minimum at θ = 180°(Figure 2), with comparable energy. The main difference between the contour plot of $[(4BP)Cl]_2$ (Figure 2) and **4cCl⁻** (Figure 1d), is that the 180° energy minimum is located at longer distance. Experimentally the

halogen···halide interaction are characterized by the interaction angle θ = 180°. Interactions at θ < 80° are due to other intermolecular forces which are not part of this discussion (e.g. halide-π interactions,[15] C-H···X$^-$ …etc) and we will focus directly on the energy minimum at θ = 180°.

Calculations indicated in all of the studied models that halogen···halide contacts are a result of attractive forces with several exceptions: C-F···X$^-$, **1bCl$^-$**, **1bBr$^-$** and **1cI$^-$**. Halogen···halide interaction strengths vary from very weak (**1cI$^-$**, Figure 3a) to very strong (**3dF$^-$**, Figure 3c) based on four main factors; (a) the type of the halide anion. In all of the models the energy of interaction follows the order I$^-$ < Br$^-$ < Cl$^-$ < F$^-$. In **2bX$^-$**, the energy of interaction is ca. -6.8 kJ/mol and in **2bI$^-$**, -32.1 kJ/mol for **2bF$^-$** (Figure 3b); (b) the type of the halogen atom. In contrast to halide anions, calculations show that the energy of interaction follows the order F < Cl < Br < I. In the fluorine-halide case, there is no observed energy minimum for the linear arrangement at dz basis level (i.e., there are no C-F···X$^-$ synthons). H_3C-Cl···X$^-$ synthons shows no interaction at all basis set levels except **1bF$^-$** (Figure 3a); (c) the hybridization of the carbon atom attached to the halogen atom. The strengths of halogen···halide synthons follow the hybridization: $sp > sp^2 > sp^3$. In **1bF$^-$**, the interaction strength is -7 kJ/mol, and in **3bF$^-$** ca. -68 kJ/mol; (d) the nature of the functional groups. Adding an electronegative atom on the organic moiety of the model strengthens the halogen···halide synthon, i.e., replacing the phenyl ring in chlorobenezene with a pyridyl ring reinforces the interactions, e.g., in **2bF$^-$**, -32.1 kJ/mol which increases to -58.2 kJ/mol in **4bF$^-$**.

Table 1. Summary of data collection and refinement parameters for (*n*CP)X.

Crystal	(2CP)Br	(2CP)I	(3CP)Br	(3CP)I	(4CP)Br	(4CP)I
Formula	C_5H_5BrClN	C_5H_5ClIN	C_5H_5BrClN	C_5H_5ClIN	C_5H_5BrClN	C_5H_5ClIN
Formula Weight	194.46	241.45	194.46	241.45	194.46	241.45
D_{calc} (Mg/m^3)	1.863	2.108	1.879	2.139	1.874	2.090
T(K)	295(2)	295(2)	295(2)	295(2)	295(2)	295(2)
Crystal system	Orthorhombic	Monoclinic	Triclinic	Triclinic	Monoclinic	Triclinic
Space group	$Pca2_1$	$P2_1/m$	P-1	P-1	$P2_1/m$	P-1
A (Å)	13.782(2)	6.927(2)	4.908(1)	5.128(2)	4.699(1)	5.090(1)
B (Å)	4.700(1)	6.625(2)	7.802(1)	8.224(6)	8.182(2)	8.576(1)
C (Å)	10.707(2)	8.512(2)	9.252(1)	9.276(6)	9.103(2)	9.102(1)
α (º)	90	90	83.63(1)	83.82(5)	90	83.51(1)
β (º)	90	103.19(2)	77.59(2)	74.66(5)	100.05(1)	76.39(2)
γ (º)	90	90	86.92(2)	86.82(6)	90	89.06(2)
V ($Å^3$)	693.5(2)	380.3(2)	343.7(1)	374.9(4)	344.6(1)	383.7(1)
Ind. reflections	702	716	1129	1068	632	1285
R(int)	0.0417	0.0359	0.0431	0.0662	0.0573	0.0327
Z	4	2	2	2	2	2
Goodness of fit	1.088	1.083	1.034	1.096	1.065	1.008
R_1[a] [I > 2σ]	0.0447	0.0306	0.0474	0.0514	0.0445	0.0449
wR_2[b] [I > 2σ]	0.0868	0.0695	0.1118	0.1279	0.0958	0.0761
μ mm^{-1}	6.206	4.464	6.260	4.528	6.243	4.425
Trans. range	0.190-0.456	0.469-0.469	0.117-0.573	0.344-0.660	0.454-0.574	0.472-0.666

[a] $R_1 = \sum| |F_o| - |F_c| | / \sum|F_o|$.

[b] $wR_2 = \{\sum[w(F_o^2 - F_c^2)^2] / \sum[w(F_o^2)^2]\}^{1/2}$

Table 2. Summary of data collection and refinement parameters for (*n*BP)X.

Crystal	(2BP)Cl	(2BP)Br	(2BP)I	(3BP)Cl	(3BP)I	(4BP)Cl	(4BP)I
Formula	C_5H_5BrClN	$C_5H_5Br_2N$	C_5H_5BrIN	C_5H_5BrClN	C_5H_5BrIN	C_5H_5BrClN	C_5H_5BrIN
Formula Weight	194.46	238.92	285.91	194.46	285.91	194.46	285.91
D_{calc} (Mg/m^3)	1.926	2.247	2.431	1.974	2.478	1.915	2.447
T(K)	297(2)	297(2)	299(2) K	295(2)	295(2)	295(2)	295(2)
Crystal system	Orthorhombic	Orthorhombic	Orthorhombic	Triclinic	Monoclinic	Monoclinic	Triclinic
Space group	*Pca*2$_1$	*Pca*2$_1$	*Pca*2$_1$	*P*-1	*P*2$_1$/*c*	*P*2$_1$/*m*	*P*-1
a (Å)	14.274(3)	14.273(2)	14.504(2)	4.769(1)	4.805(1)	4.392(1)	4.981(1)
b (Å)	4.440(1)	4.601(1)	4.883(1)	7.744(2)	14.391(3)	8.179(2)	8.507(2)
c (Å)	10.581(2)	10.753(2)	11.030(1)	9.153(2)	11.121(2)	9.434(2)	9.453(2)
α (º)	90	90	90	84.26(3)	90	90	80.18(2)
β (º)	90	90	90	76.91(3)	94.69(3)	95.83(3)	79.48(2)
γ (º)	90	90	90	86.06(3)	90	90	88.91(2)
V ($Å^3$)	670.5(2)	706.2(2)	781.1(2)	327.2(1)	766.4(3)	337.2(1)	388.0(1)
Ind. reflections	1538	1434	1721	1493	1263	822	1327
R(int)	0.0631	0.0348	0.0283	0.0337	0.0409	0.0513	0.0395
Z	4	4	4	2	4	2	2
Goodness of fit	0.984	1.032	1.029	1.032	1.081	1.104	1.061
R_1[a] [I > 2σ]	0.0463	0.0282	0.0235	0.0421	0.0320	0.0459	0.0436
wR_2[b] [I > 2σ]	0.0851	0.0594	0.0475	0.1084	0.0722	0.1078	0.1046
μ mm^{-1}	6.418	11.374	9.120	6.575	9.295	6.381	9.180
Trans. range	0.190-0.724	0.171-0.234	0.164-0.291	0.280-0.779	0.090-0.139	0.251-0.832	0.120-0.460

[a] $R_1 = \sum| |F_o| - |F_c| | / \sum|F_o|$.

[b] $wR_2 = \{\sum[w(F_o^2 - F_c^2)^2] / \sum[w(F_o^2)^2]\}^{1/2}$

In all of the models, the separation distance is less than the sum of r_{vdW} of the halogen atoms and the ionic radii of the halide anions, which is defined by r_{cal} (r_{cal} = [(Y···X$^-$ distance, cal.) / (Σ r_{vdW} of the halogen atom and the ionic radii of the halide anion)]×100%)[§] .These values are tabulated in Table 3. The r_{cal} value is inversely proportional to the strength of the halogen···halide synthons.

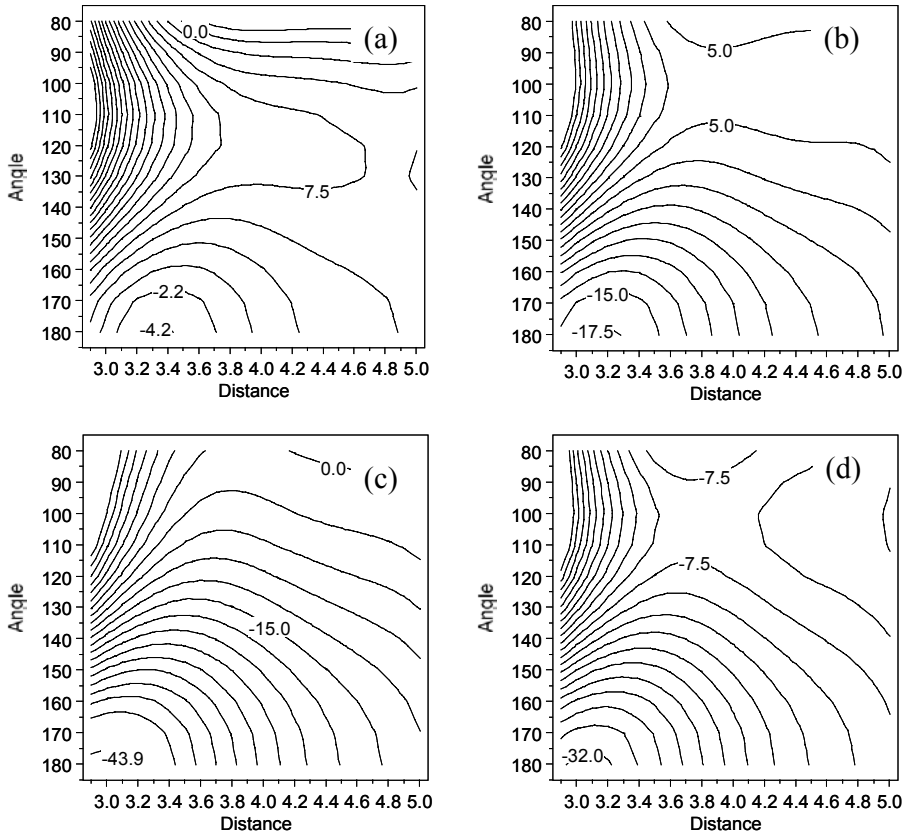

Figure 1. Potential energy diagram for the interaction of a Cl$^-$ anion with (a) bromomethane, **1c**; (b) bromobenzene, **2c**; (c) bromoacetylene, **3c**; (d) 4-bromopyridine, **4c**, as a function of θ_i and the distance D. The calculations were performed at dz basis set level. The distances are in (Å) and the angles are in (°).

[§] Ionic radii of F$^-$ = 1.33 Å, Cl$^-$ =1.81 Å, Br$^-$ = 1.96 Å, I$^-$ = 2.2 Å. r_{vdW} of Cl = 176 Å, Br = 1.86 Å, I = 1.98 Å.

Crystallographic Study

Structure Descriptions

Many of the crystals structures in (nYP)X series are isomorphous. To simplify discussion, the structures can be classified into the several structural isomorphous structures sets (Table 4).

Table 3. Calculated separation distance at which the energy minima are located.

Compound	**1bF$^-$**	**1bCl$^-$**	**1bBr$^-$**	**1bI$^-$**	**1cF$^-$**	**1cCl$^-$**	**1cBr$^-$**	**1cI$^-$**	**1dF$^-$**	**1dCl$^-$**	**1dBr$^-$**	**1dI$^-$**
D_{cbs}[a]	2.52	3.28	3.51		2.39	3.11	3.33	3.62	2.33	3.01	3.23	3.49
$r_{cal.}$[b]	85.6	91.9	94.4		74.9	84.7	87.2	89.2	70.8	80.9	82.3	84.0
Compound	**2bF$^-$**	**2bCl$^-$**	**2bBr$^-$**	**2bI$^-$**	**2cF$^-$**	**2cCl$^-$**	**2cBr$^-$**	**2cI$^-$**	**2dF$^-$**	**2dCl$^-$**	**2dBr$^-$**	**2dI$^-$**
D_{cbs}[a]	2.39	3.1	3.31	3.6	2.31	3.0	3.21	3.48	2.29	2.94	3.15	3.41
$r_{cal.}$[b]	77.3	86.8	89.0	90.1	72.4	81.7	84.0	85.7	69.6	79.0	80.3	82.0
Compound	**3bF$^-$**	**3bCl$^-$**	**3bBr$^-$**	**3bI$^-$**	**3cF$^-$**	**3cCl$^-$**	**3cBr$^-$**	**3cI$^-$**	**3dF$^-$**	**3dCl$^-$**	**3dBr$^-$**	**3dI$^-$**
D_{cbs}[a]	2.31	2.97	3.17	3.44	2.26	2.91	3.11	3.37	2.28	2.88	3.08	3.39
$r_{cal.}$[b]	74.8	83.2	85.2	86.9	70.8	79.3	81.4	83.0	69.3	77.4	78.6	81.1
Compound	**4bF$^-$**	**4bCl$^-$**	**4bBr$^-$**	**4bI$^-$**	**4cF$^-$**	**4cCl$^-$**	**4cBr$^-$**	**4cI$^-$**	**4dF$^-$**	**4dCl$^-$**	**4dBr$^-$**	**4dI$^-$**
D_{cbs}[a]	2.34	3.03	3.23	3.51	2.28	2.95	3.15	3.42	2.27	2.91	3.11	3.36
$r_{cal.}$[b]	75.7	84.9	86.8	94.7	71.5	80.4	82.5	84.2	68.6	76.8	78.9	80.4

[a] Y···X$^-$ separation distance at complete basis set level

[b] $r_{cal.}$ = [(Y···X$^-$ distance, theo.) / (Σ r_{vdW} of the halogen atom and the ionic radii of the halide anion)]×100%).

Each set of structures will be analyzed in the following sequence; (a) examination of the environment around the halide anion to identify the significant C-Y···X$^-$ synthons and the classical hydrogen bonds N-H···X$^-$; (b) description of the resultant supramolecular structures that developed based on these synthons; (c) packing of these supramolecular structures and the resultant three-dimensional structure. The dominant feature of all of the studied structures,

besides the classical N-H···X$^-$ hydrogen bonds, is the presence of the nearly linear C-Y···X$^-$ synthons and a Y···X$^-$ separation distance less than sum of r_{vdW} of the halogen atom and the ionic radii of the halide anion. The N-H···X$^-$ hydrogen bonds cooperate with C-Y···X$^-$ synthons to link the halide anions and the halopyridinium cations to form either chain structures or dimers. These chains and dimers aggregate *via*; (a) the novel N-X$^-$ synthons, this is the interaction between the nitrogen atom and the halide anion lying above it and normal to the plane of the halopyridinium cations; (b) the novel N-Y synthon, which is the interaction between the nitrogen atom and the halogen atom lying above it; (c) and the non-classical C-H···X$^-$ hydrogen bond.

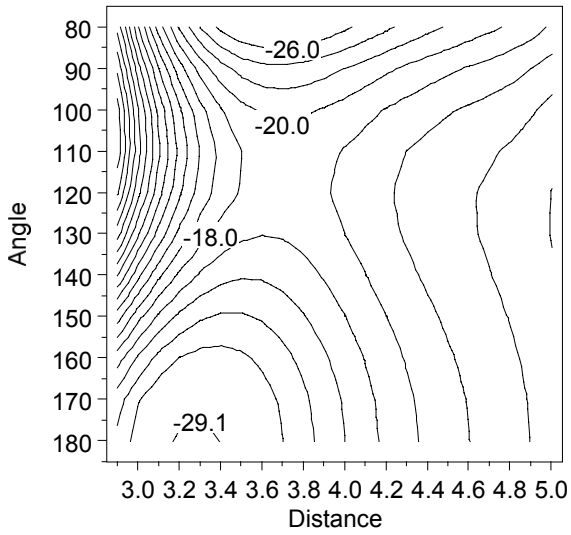

Figure 2 Contour plot of the interaction energy of $[(4BP)Cl]_2$ as function of the angle θ_i and intermolecular distance D. The distances are in (Å) and the angles in (°).

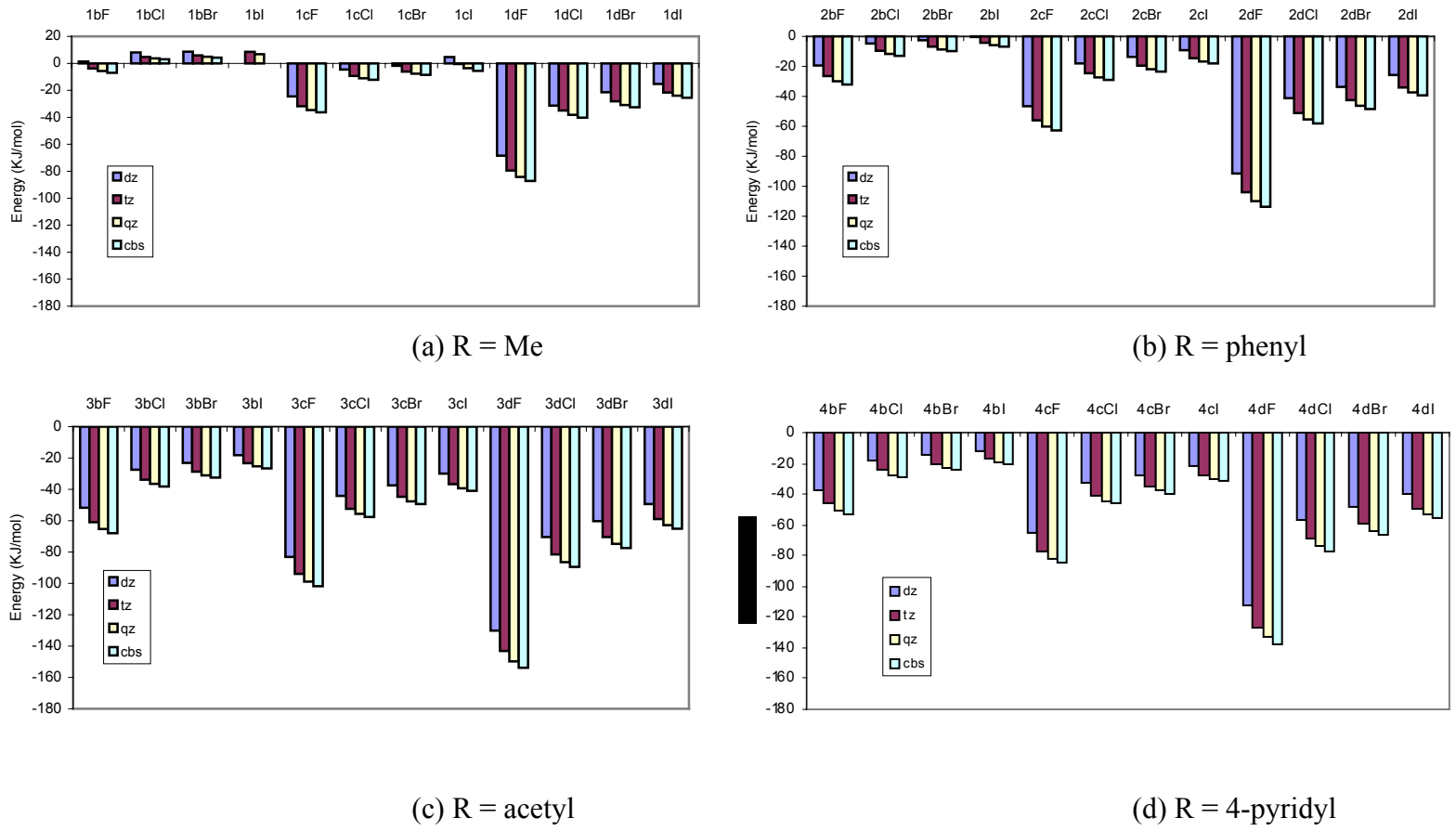

Figure 3. Calculated energy of interaction of halogen···halide synthons for, (a) type **1** model compounds, (b) type **2** model compounds, (c) type **3** model compounds, and (d) type **4** model compounds.

Table 4. Isomorphous structures sets.

Set	Space Group	Isomorphous series
(2CP)Br	$Pca2_1$	(2CP)Br, (2BP)Cl, (2BP)Br, (2BP)I
(2CP)I	$P2_1/m$	
(3CP)Br	P-1	3CP)Cl, (3CP)Br, (3BP)Br, (3CP)I, (3BP)Cl
(3BP)I	$P2_1/c$	
(4CP)Br	$P2_1/m$	(4CP)Br, (4CP)Cl, (4BP)Cl, (4BP)Br
(4CP)I	P-1	(4CP)I, (4BP)I
(2CP)Cl	$P2_1/c$	

C-Y···X⁻ and N-H···X⁻ Interactions

All of the halopyridinium cations are involved in halogen-halide contacts and N-H···X^- hydrogen bonding; geometrical arrangement of these synthons around the halopyridinium is exemplified in Figure 4. Data summarizing these synthons are tabulated in Table 5. In all of the studied structures, Y···X^- distances are less than the sum of r_{vdW} of the halogen atom and the ionic radii of the halide anion. The percent reduction in Y···X^- distances, in comparison to the sum of r_{vdW} of the halogen atom and the ionic radii of the halide anion as indicated by the r_{exp} values (Table 4), are greater in the bromopyridinium salts; r_{exp} values for the chloropyridinium cations range from 93.4%-98.2, while the analogous r_{exp} values for bromopyrdinium cations range from 87.7%-91.2%. In contrast, the C-Y···X^- angles are nearly linear in all of the studied structures; it ranges from 153.5-175.6° and 153-179.9° for the chloropyridinium and the bromopyridinium cations respectively. This would indicate that the same synthon is present in all of studied structures with variable strength, and the bromine···halide synthons are stronger than the chlorine···halide synthons. Short linear N-H···X^- hydrogen bonds are present in all of the studied structures. The H···X^- distances are

shorter in the chloropyridinium salts in comparison to the analogous H···X^- distances in the bromopyridinium salts; these distances range from 1.97-2.11, 2.29-2.38 and 2.55-2.63 Å for (*n*CP)Cl, (*n*CP)Br and (*n*CP)I respectively, while the analogous distances in the bromopyridinium salts range from 2.11-2.20 , 2.28-2.58 and 2.55-2.74 Å for (*n*BP)Cl, (*n*BP)Br and (*n*BP)I respectively (Table 5). This illustrates the competition between both interactions, strong N-H···X^- hydrogen bonding and the C-Y···X^- synthon. This also reflects the weakness of the C-Cl···X^- synthon compared to C-Br···X^- synthons. Generally, the N-H···X^- angles follow the order N-H···Cl^- > N-H···Br^- > N-H···I^-. In contrast, in the isomorphous structures the C-Y···X^- angles follow the order C-Y···I^- > C-Y···Br^- > C-Y···Cl^-. As function of the halide anion, generally, the relative reduction in halogen-halide distance follows the order I > Br > Cl (Table 5). For example, this trend can be easily seen in the three isomorphic structures ((2BP)Cl, (2BP)Br, (2BPI)) (Table 5), where the r_{exp} values are 90.2, 89.2 and 88.1 for (2BP)Cl, (2BP)Br and (2BP)I respectively. The strength of N-H···X^- hydrogen bonds follows the order Cl^- > Br^- > I^-, since a hydrogen bond is electrostatic in nature.[16] The r_{exp} values also illustrate the competition between the N-H···X^- hydrogen bond and the C-Y···X^- synthon.

Description of the Supramolecular Networks.

Attaching a halogen atom (either bromine or chlorine) transforms the halopyridinium cation from a monofunctional synthon through N-H···X^- hydrogen bond to bifunctional one through C-Y···X^- synthons and N-H···X^- hydrogen bonds (ignoring the packing interactions and the weak C-H···X^- hydrogen bonds). The C-Y···X^- and N-H···X^- synthons tie the halopyridinium cations and the halide anions in nine (2YP)X and (4YP)X structures to form chains, and the four (3YP)X structures to form dimers. These supramolecular structures pack

via nitrogen-halide synthons, nitrogen-halogen and C-H···X^- hydrogen bonds to form the three-dimensional structure.

The nine chain structures are topologically similar; the halide anions connect the halopyridinium cations *via* N-H···X^- hydrogen bonds from one side and C-Y···X^- synthons from the other side. Four of the five (2YP)X structures are isomorphic structures [(2CP)Br, (2BP)Cl, (2BP)Br and (2BP)I]. These chains run parallel to the *c* axis, they are generated from the asymmetric unit by a two fold screw axis along the chain axis (Figure 5a). In the fifth chain structure, the chains run parallel *a* axis, these chains are generated from the asymmetric unit by a translation operation along the chain axis (Figure 5b). The four (4YP)X structures are isostructural even though they are not isomorphous. In the (4CP)Br type structures, the chain network run parallel to the (-1 0 1) direction (Figure 6a), while, in the (4CP)I type structures, they structures run parallel (1 0 1) direction (Figure 6b). The main structural difference between (4CP)Br and (4CP)I types is in the symmetry of the chain structures; in the (4CP)Br structure the chains have C_s symmetry while, in the (4YP)I structures, the iodide anion lie off the chain axis, leading to the trivial C_1 symmetry for the chains. The chain structures of the (4YP)X salts have the same connectivity as the chains in the (2YP)X salts. However, the differences in geometric nature of the halopyridinium cations yield different structural characteristics. The presence of the halogen atom in the 2-position leads to short distances between the halide anions of ~6 Å, while the analogous distances in the (4YP)X structures are ~11 Å.

Table 5. C-Y···X^- and N-H···X^- synthon distances and angles in the *n*YP^+ salts.

Compound	Cl···X(Å)	C-Y···X(º)	N···X(Å)	H···X(Å)	N-H···X(º)	r_{exp}[a]	Temperature	Reference
(2CP)Cl	3.507	164	2.963	1.97	167	98.2	173	5a
(2CP)Br	3.597 (4)	170.5 (4)	3.139(9)	2.31	163.3	96.7	298	This work
(2CP)I	3.769 (2)	166.8 (2)	3.387(5)	2.55	165.2	95.2	298	This work
(3CP)Cl	3.479	156.1	2.993	2	169	97.5	173	5a
(3CP)Br	3.626 (2)	160.3 (2)	3.174(6)	2.38	154.3	97.5	298	This work
(3CP)I	3.739 (3)	165.2 (3)	3.421(8)	2.63	153.5	94.4	298	This work
(4CP)Cl	3.335	162.0	2.983	2.112	175.6	93.4	173	5a
(4CP)Br	3.506 (3)	162.6	3.147(8)	*2.29*	172.6	94.2	298	This work
(4CP)I	3.733 (3)	164.0 (3)	3.418(8)	2.60	159.0	94.5	298	This work
(2BP)Cl	3.310(3)	171.4 (2)	2.950(6)	2.11	165.4	90.2	298	This work
(2BP)Br	3.407 (1)	172.4 (1)	3.130(4)	2.30	163.3	89.2	298	This work
(2BP)I	3.575 (1)	174.0 (1)	3.381(4)	2.55	163.4	88.1	298	This work
(3BP)Cl	3.359 (1)	162.2 (1)	2.995(3)	2.20	152.9	91.2	298	This work
(3BP)Br	3.407	174.3	3.213	2.28	153	89.2	173	5a
(3BP)I	3.589 (1)	179.6 (2)	3.482(5)	2.74	145.0	88.4	298	This work
(4BP)Cl	3.313 (2)	166.4 (2)	3.016(7)	2.16	178.9	90.3	298	This work
(4BP)Br	3.350	167.4	3.184	2.575	179.9	87.7	143	5b
(4BP)I	3.648 (1)	163.5 (3)	3.434(7)	2.63	155.7	89.9	298	This work

[a] r_{exp} = [(Cl···X distance, exp) / (Σ r_{vdW} of the halogen atom and the ionic radius of the halide anion)]×100%

In the (3YP)X structures, the presence of the halogen atom at the 3 position makes the formation of the dimer favorable over the chain network. However, two asymmetric units dimerize based on the classical N-H···X^- hydrogen bond and the novel C-Y···X^- synthon (Figure 7). The two bromopyridinium cations of (3BP)I dimer lie in the same plane, therefore, the dimer has C_{2h} symmetry. In contrast, in (3BP)Cl type structures, the two cations

of the dimer are not located in the same plane, hence, this reduces the symmetry to C_1 symmetry.

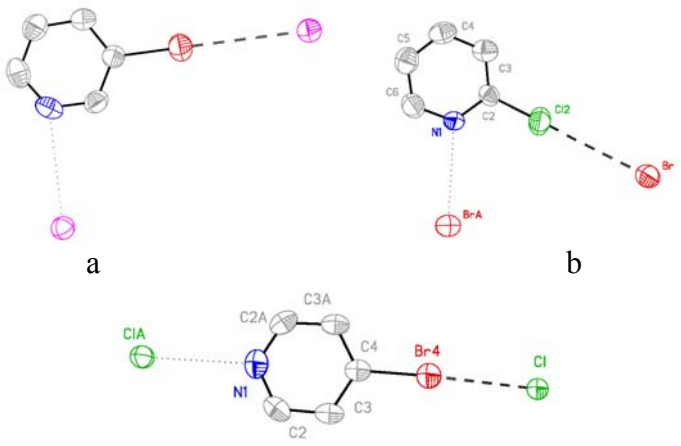

c

Figure 4. Synthonic interactions in (a) (2CP)Br, (b) (3BP)I, (c) (4BP)Cl. Hydrogen bonds and halogen-halide synthons are represented by dotted and dashed lines respectively. Thermal ellipsoids are shown at 50% probability.

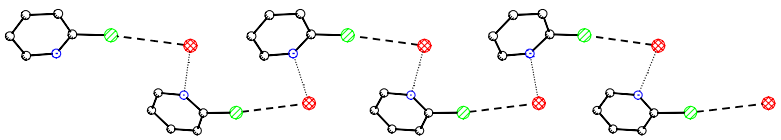

(a)

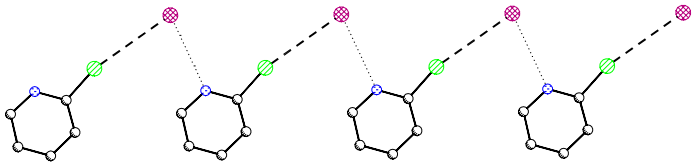

(b)

Figure 5. (a) Illustration of the chain networks in (2CP)Br. The chains run parallel to the *c* axis; (b) Illustration of the chain structure of (2CP)I. The chains run parallel to the *a* axis. Hydrogen bonds and halogen-halide synthons are represented by dotted and dashed lines, respectively.

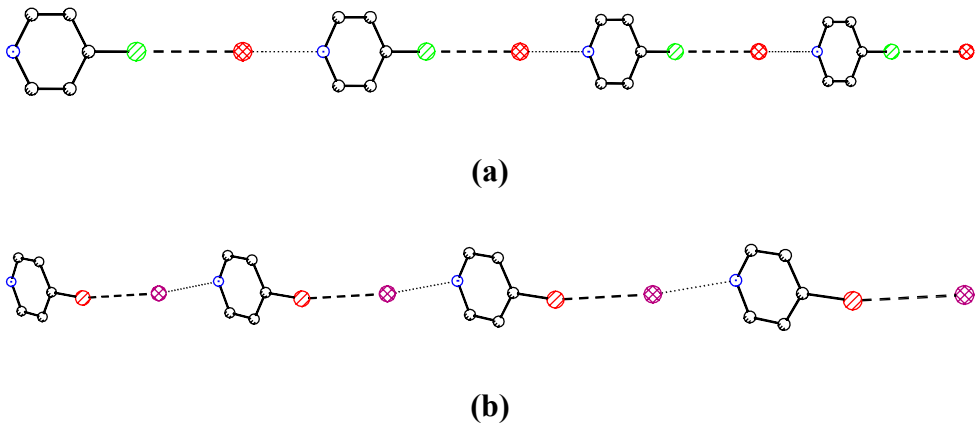

Figure 6. Chain structures of (a) (4CP)Br, chains run parallel 1 0 –1 direction; (b) (4BP)I, chain run parallel to (1 0 1). Hydrogen bonds and halogen-halide synthons are represented by dotted and dashed lines, respectively.

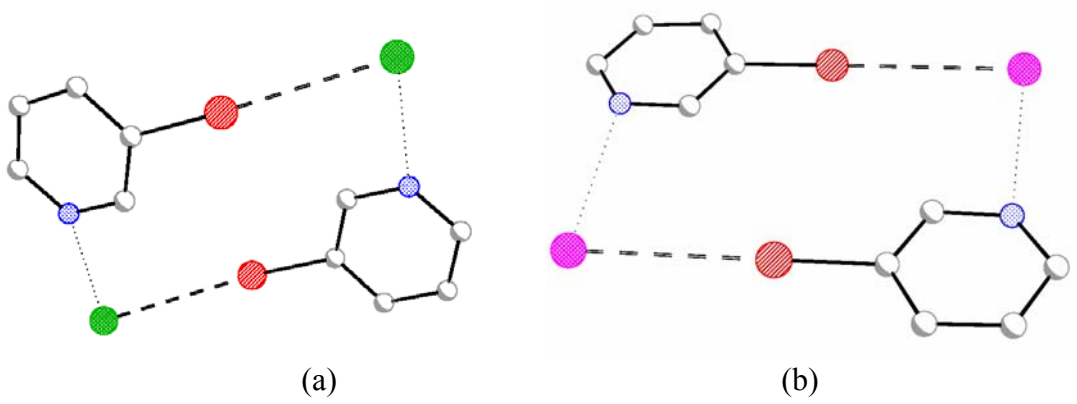

Figure 7. Dimer structures of (a) (3BP)Cl; (b) (3BP)I. Hydrogen bonds and halogen-halide synthons are represented by dotted and dashed lines, respectively.

Packing Interactions and Final Crystal Structures.

The chains and dimers described in the previous section pack *via* three different synthons; (a) the interaction between the nitrogen atom and the halide anion that is located above the plane of the aromatic ring, henceforth N-X^- synthon. This synthon is present in all structures except (2CP)I and (3CP)Cl structure. These interactions are illustrated in Figure 8; (b) the

interaction between the nitrogen atom and the halogen atom that is located above of the plane of the aromatic ring, henceforth N-Y synthon. This synthon exists in (3CP)Br, (2CP)I, (4CP)Br and (4CP)I type structures as shown in Figure 9. Recently, we found that these packing synthons play a crucial role in the crystal structures of (*n*CP)CuX_4 (*n*CP^+ = *n*-chloropyridinium; *n* = 2, 3, or 4; X = Cl^- or Br^-).[17] The data that summarize these interactions and π-π stacking interactions are listed in Table 2S. Substantial π-π overlap has not been observed in any of the studied structures. This indicates the weakness of π-π interaction in comparison to these packing interactions; (c) the C-H···X^- hydrogen bond.

Generally, the (2YP)X and (4YP)X network structures (except (2CP)I) all pack in a similar way. Nitrogen-halide synthons tie the chains together into sheets. These sheets pack *via* C-H···X^- hydrogen bonds in such a way each halide anion is located between 4 different cations, due to electrostatic forces, to form the three-dimensional structures. In (2CP)Br type structures, the sheets lie in the *bc* plane (Figure 1Sa), while, in the two isostructural sets ((4CP)Br and (4CP)I types structures), these sheets lie parallel to (0 1 0) planes (Figure 2S). In (2CP)I, the presence of the chlorine subsistent in the position 2 makes double nitrogen-chlorine synthon possible (Figure 4S), that then compete with nitrogen halide synthon. Therefore, the chain structures of (2CP)I interact *via* nitrogen-chlorine interaction to form a layer structure in the in *ab* plane. These layers interdigitate to form the three dimensional structure *via* C-H···I^- hydrogen bond. Recently, we found that this pattern of packing to play a significant role in the crystal structures of the $(2CP)_2CuX_4$ (X = Cl^- and Br^-).[17]

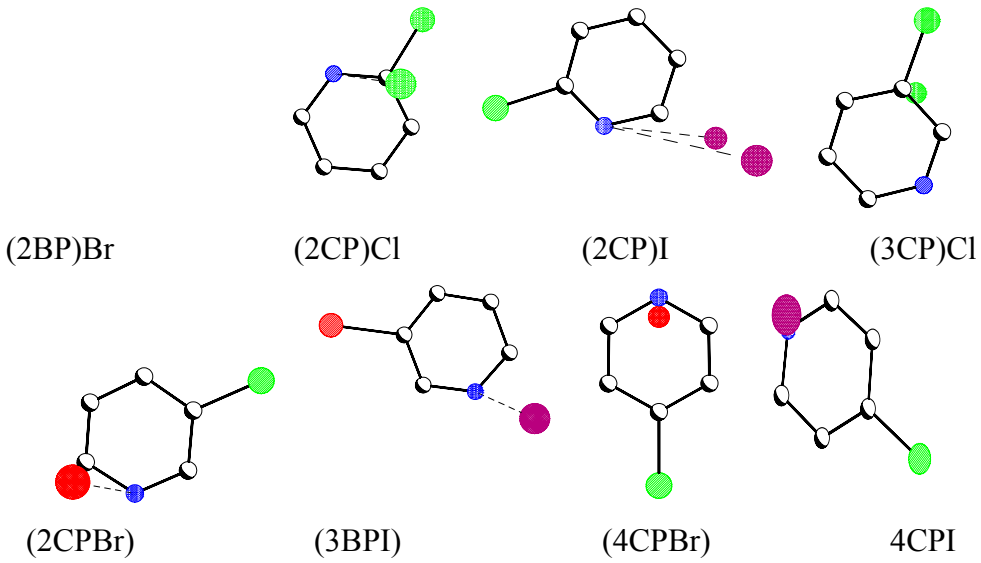

Figure 8. Illustration of nitrogen-halide synthon interactions. Views are from the normal to the planes of the cations. The dashed lines denote the nitrogen-halide connections. For each set of isomorphous structures only one example is shown.

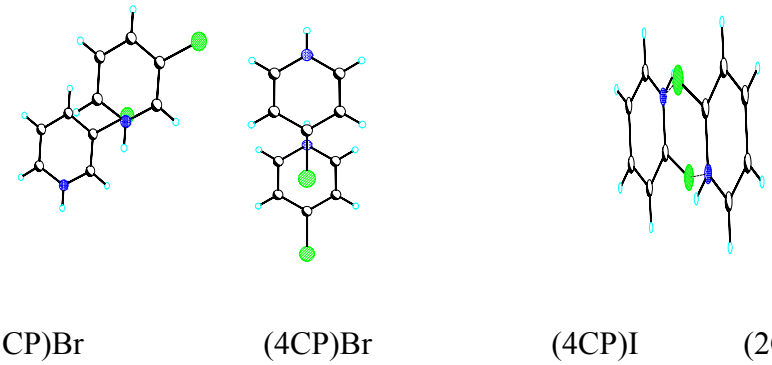

Figure 9. Illustration of nitrogen-halogen synthons. Views are from the normal to the planes of the cations. The dashed lines denote the nitrogen-halogen connections. For each set of isomorphous structures only one example is shown.

Nitrogen-halide synthons link dimers of (3CP)Br type structures together into a double chain structures run parallel to the *c* axis, with alternating halogen···halide and nitrogen-halide making up the rails and N-H···X^- defining the rungs (Figure 5Sa). Then, these chains interact

via nitrogen-chlorine synthon to form a sheet structure lies in the *ac* plane (Figure 5Sb). These chains aggregate based one the C-H···X^- hydrogen bond in such a way each halide anion confronts four chloropyridinium cations (Figure 6S). In the same manner, nitrogen-halide synthon links the dimers together to a double chains structure run parallel to *a* axis (Figure 7Sa) in (3BP)I structures. This double chain structure is topologically different from that of (3CP)Br structures. In contrast to the (3CP)Br ladders, alternating N-I^- and N-H···X^- interactions form the rails and C-Br···I^- interactions form the rungs. Moreover, the nitrogen-halogen synthons are absent in (3BP)I. Therefore, these chains aggregate to form the three-dimensional structures, based on mainly on C-H···I^- hydrogen bond (Figure 7Sb).

DISCUSSION

The results, both structurally and theoretically, show the significance of the C-Y···X^- synthons (Y = Cl, Br, I and X^-= F^-, Cl^-, Br^-, I^-) in influencing structures of crystalline materials and can be used as potential building blocks in crystal engineering *viz.* supramolecular synthesis. The strength of these synthons varies from strong forces in **3dF**$^-$ (-153.8 kJ/ mol) to nonexistent in **1bI**$^-$. Calculations indicate that the relative strength of these contacts is influenced by the following four factors: (a) type of the halogen atom; (b) type of the halide anion;(c) the hybridization of the *ipso* carbon relative to the halogen atom and ; (d) the nature of organic moiety attached to the *ipso* carbon atom.

Halogen···halide interactions, like many other intermolecular interactions, are basically electrostatic in nature. Evidence for this electrostatic nature will be presented below in the following model which is based on two main ideas; (a) the presence of a positive electrostatic potential end cap on all halogen atoms except fluorine (Figure 10);[18] (b) the electron density is anisotropically distributed around the halogen atom.[4c,18a,19] Hence halogen atoms have two

radii, a short radius along the C-Y bond and longer one perpendicular to it. According to this model, the halide anion should face the electrostatic potential end cap, and therefore a linear C-Y···X^- geometry is expected. All of the structures in this work display the C-Y···X^- linear arrangement (Table 5). Furthermore, the calculated potential energy diagram shows the presence of an energy minimum at θ = 180° (Figure 1). Experimentally, the structures presented here cover only one type of halogen···halide contact, C(sp^2)-Y···X^-. A search of the Cambridge Structural Data base (CSD),[20] for halogen···halide (F, Cl, Br and I) intermolecular contacts within the sum of r_{vdW} of the halogen atom and the ionic radius of the halide anion yielded 73 contacts.[21] The data summarizing this information is shown in Table 6. No fluorine···halide or halogen···fluoride contacts have been observed. Contacts of the type C(*sp*)-Y···X^- were observed only when Y = I.

The calculated energies show that the strength of the C-Y···X^- interaction follows the order I > Br > Cl > F for the halogen Y. The electrostatic model relies on deformation of the electronic charge. Heavier halogen atoms are softer, less electronegative and can deform more readily. This agrees with the observed trend in the strength of the C-Y···X^- interaction. Previous calculations have shown that the strength of the electrostatic potential end cap on the halogen follows the same order, I > Br> Cl > F.[18a] Experimentally, this trend is supported by crystallographic data in three different ways; (a) an examination of the r_{exp} values, e.g. R-Cl···X^- > R-Br···X^- > R-I···X^-, Table 6. The C(sp^3)-Cl···Cl and C(sp^3)-Br···Cl interactions have almost equal r_{exp} values, however, only two contacts were observed in each case; (b) the data show that changing the halogen from F to I, the C-Y···X^- arrangement becomes closer to linearity; (c) the competition between C-Y···X^- synthons and N-H···X^- hydrogen bonding in

the structures i.e. where the halogen···halide synthon is stronger, the N-H···X^- hydrogen bond is weaker (Table 5).

Table 6. Details of C-Y···X^- contacts. [a]

Interaction type	Number of contacts	$<r_{exp}>$	θ range	<θ>
C(*sp*)-I···Cl^-	5	0.81	172.6-179.7	176.4
C(*sp*)-I···Br^-	6	0.82	174.4-178.7	175.7
C(sp^2)-Cl···Cl^-	11	0.95	150.0-179.0	163.7
C(sp^2)-Cl···Br^-	5	0.97	160.1-172.9	165.3
C(sp^2)-Cl···I^-	8	0.95	149.1-174.7	163.8
C(sp^2)-Br···Cl^-	11	0.93	156.4-176.4	168.1
C(sp^2)-Br···Br^-	11	0.90	156.7-178.1	171.0
C(sp^2)-Br···I^-	3	0.89	163.5-179.6	172.4
C(sp^2)-I···Cl^-	5	0.87	166.1-173.5	169.9
C(sp^2)-I···Br^-	4	0.84	170.1-174.0	173.0
C(sp^2)-I···I^-	8	0.83	163.4-178.0	172.9
C(sp^3)-Cl···Cl^-	2	0.96	159.1 and 177.3	168.2
C(sp^3)-Br···Cl^-	2	0.97	149.0 and 173.3	161.1
C(sp^3)-Br···Br^-	2	0.94	164.7 and 169.2	167.0
C(sp^3)-I···I^-	3	0.92	166.7-174.0	170.8

[a] Both the data obtained from CSD and the structures reported in this work are used to calculate, $<r_{exp}>$ and θ range values

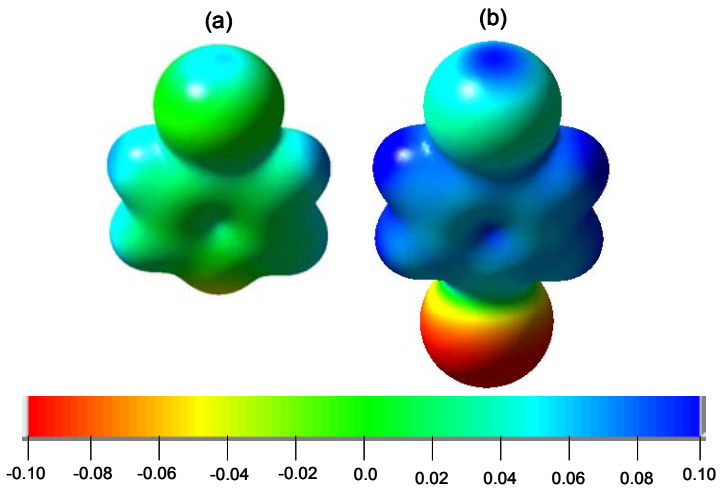

Figure 10. The calculated electrostatic potential of (a) 4-bromopyridine and (b) 4-bromopyridinium chloride. Units of the color scale are in atomic units (Energy in Hartree and charge in electronic charges). The contour electron density isovalue is set to 0.05.

The calculations show that the lighter the halide anion, the stronger C-Y···X^- contacts. This is easily described based on the electrostatic model where the smaller the anion has higher electron density on the halide anion and therefore stronger attractive electrostatic forces exist. Experimentally, the r_{exp} values show the inverse trend (smallest for iodide salts) which seems to contradict theory. These two trends can be reconciled by taking into account the presence of strong hydrogen bonding (e.g. N-H···X^-, for those structures are studied in this work) which is also electrostatic in nature.[16] Thus, the strength of the N-H···X^- hydrogen bonding follows the order N-H···Cl^- > N-H···Br^- > N-H···I^-. Therefore, due to the competition between halogen···halide contacts and hydrogen bonding, an inverted trend is observed for r_{exp} values (Table 6). This competition also describes why the calculated Y···X^- separation distance at *cbs* level is always shorter than the experimental value. In a recent study we have shown that C-Cl···Cl-Cu interaction is stronger than C-Cl···Br-Cu synthons based on the analysis of the structure of $(n\text{CP})_2\text{CuX}_4$ ($n\text{CP}^+$ = *n*-chloropyridinium; *n* = 2, 3, or 4; X = Cl^- or Br^-).[17] This

analysis showed that C-Cl···Cl-Cu synthons exist in $(n\text{CP})_2\text{CuCl}_4$, and the C-Cl···Br-Cu synthon is either absent or very weak in $(n\text{CP})_2\text{CuBr}_4$.[17] This conclusion supports our results (*vide supra*).

The theoretical calculations show that, as the hybridization of the carbon atom changes from sp^3 to *sp*, the energy of the interaction increases. The positive electrostatic end cap increases as the hybridization of the carbon atom changes from sp^3 to *sp*.[18a] This behavior parallels the electronegativity of the carbon atom, which, due to the higher s character, is higher for *sp* hybridization. Experimentally, given the limited number of data, r_{exp} values support this behavior, and r_{exp} values follow the order C(*sp*)-Y···X^- < C(sp^2)-Y···X^-< C(*sp*)-Y···X^- (Table 6).

From calculations, replacing the phenyl group with a pyridyl group increases the strength of these contacts. Similarly to the results found for the change in hybridization of the *ipso* carbon, adding an electronegative atom to the *ipso* carbon also increases the electrostatic potential end cap. Recently, we have shown that adding a fluorine atom to the *ipso* carbon strengthens contacts of the type C-Y···Y-C.[18a] This indicates that as the organic moiety has more electron withdrawing character, a stronger halogen···halide synthon can be predicted.

Calculations show that charge assisted halogen···halide interactions in the dimer $[(4\text{BP})\text{Cl}]_2$ are of comparable strength to the simple interaction in **4cCl**$^-$ (Figure 1d and Figure 2). The positive electrostatic potential cap is larger in (4BP)Cl compared to 4BP (Figure 10) , which is expected to strengthen the halogen···halide synthons. Also, this is expected to be accompanied by a reduction of the negative charge on the chloride anion in (4BP)Cl. In total, both type of interaction are of comparable strength. However, in the charge assisted halogen···halide interactions, calculations were performed on only one model dimer and the

energy minimum in the dimer occurs at a longer distance. This is probably due to competition between the halogen···halide and hydrogen bond synthons.

Several similar intermolecular synthons have been shown to involve attractive electrostatic forces. Zordan *et al*. have shown that the C-Y···X-M interaction (M = Pt(II) Or Pd(II); X = F, Cl, Br, I) involves electrostatic attraction.[6e] In another study, Lommerse *et al.* demonstrates that attractive electrostatic forces participate in determining the strength of interaction of C-X···E interactions (X = F, Cl, Br or I, E = N, O or S).[22a] The experimental electron density of the molecular aggregation between 4,4'-dipyridyl-N,N'-dioxide and 1,4-diiodotetrafluorobenzene, and the complex of (E)-1,2-bis(4-pyridyl)ethylene with 1,4-diiodotetrafluorobenzene demonstrates that I···O and I···N interactions involve attractive electrostatic forces.[22b,22c] These studies support the idea of the presence of an electrostatic potential on the halogen atom (excluding fluorine) in the C-Y bond, and therefore, these synthons involve attractive electrostatic forces.

CONCLUSIONS

Both *ab initio* calculations and crystal structures prove that halogen···halide interactions are controlled by electrostatics and can be used as crystal engineering tool - deliberately - in supramolecular synthesis. These studies show that the interactions are characterized by a linear C-Y···X^- geometry and a Y···X^- separation distance less than the sum of r_{vdW} of the halogen atom and the ionic radii of the halide anion. This geometry is explained by the presence of a positive electrostatic potential end cap on all halogen atoms except fluorine. The strength of these synthons varies from weak or non-existing (C-F···X^- and H_3C-Cl···X^-) to very strong (e.g. **3dF**$^-$, energy of interaction ca. -153kJ/mol). Four main factors are found to influence the strength of the halogen···halide contacts;

(a) the type of halogen atom (b) the type of the halide anion (c) the hybridization of the *ipso* carbon (d) addition of greater electronegative substituents to the organic group.

The calculations also show that charge assisted halogen···halide synthons are of comparable strength to the simple interaction.

Supporting Information Available: Crystal data for all the thirteen compounds in CIF format, packing Figures, π-π stacking parameters, and the energy of interaction at various basis set levels This materials are available free of charge *via* the Internet at http://pubs.acs.org.

ACKNOWLEDGEMENTS: Work supported in part by ACS-PRF 34779-AC. The Bruker (Siemens) SMART CCD diffraction facility was established at the University of Idaho with the assistance of the NSF-EPSCoR program and the M. J. Murdock Charitable Trust, Vancouver, WA, USA.

REFERENCES

1. (a) Desiraju, G. R. *Nature* **2001**, *412*, 397-400. (b) Desiraju, G. R. *Crystal Engineering, The Design Of Organic Solids,* Elsevier Science Publishers B. V. **1989**. (c) Desiraju, R. G. *Angew. Chem. Int. Ed. Engl.* **1995**, *34*, 2311-2327. (d) Brammer, L. *Chem. Soc. Rev.* **2004.** (e) Braga, D.; Brammer, L.; Champness, N. *CrystEngComm.* **2005**, *7*, 1-19.

2. (a) Yamamoto, H. M.; Yamaura, J.; Kato, R. *J. Am. Chem. Soc.* **1998**, 120(24), 5905-5913 and references therein. (b) Domercq, B.; Devic, T.; Fourmigue, M.; Auban-Senzier, P.; Canadell, E. *J. Mater. Chem*. **2001**, *11*, 1570-1575.

3. (a) Hasegawa. M. *Advances in Physical Organic Chemistry*, Academic Press: London, 1995; vol. 30, pp 117-171. (b) MacGillivray, L. R.;Reid, J. L.; Ripmeester, J. A. *J. Am. Chem. Soc.* **2000,** *122*, 7817-7818. (c) Matsumoto, A.; Tanaka, T.; Tsubouchi, T.; Tashiro, K.; Saragai, S.; Nakamoto Sh. *J. Am. Chem. Soc*. **2002**, *124*, 8891-8902.

4. (a) Desiraju, G. R.; Parthasarathy, R. *J. Am. Chem. Soc.* **1989**, *111*, 8725-8726. (b) Ramasubbu, N.; Parthasarathy, R.; Murray-Rust, P. *J. Am. Chem. Soc.* **1986**, *108*, 4308-4314. (c) Jagarlapudi, A. R.; Sarma, P.; Desiraju G. *Acc. Chem. Res.* **1986**, *19*, 222-228. (d) Price, S. L.; Stone, A. J.; Lucas, J.; Rowland, R. S.; Thornley, A. E. *J. Am. Chem. Soc.* **1994,** *116*, 4910-4918.

5. (a) Freytag, M.; Jones, P. G. *Zeit. Naturfor B: Chem. Sci.* **2001**, *56*, 889-896. (b) Freytag, M.; Jones, P. G.; Ahrens, B.; Fischer, A. K. *New J. Chem*. **1999**, *23*, 1137-1139. (c) Logothetis, Th.; Meyer, F.; Metrangolo, P.; Pilati, T; Resnati, G. *New.*

J. Chem. **2004**, *28*, 760-763. (d) Kuhn, N.; Abu-Rayyan A.; Eichele, K.; Schwarz, S.; Steimann, M. *Inorg. Chim. Acta* **2004**, *357(6)*, 1799-1804.

6. (a) Willett, R. D.; Awwadi, F. F.; Butcher, R.; Haddad, S.; Twamley, B. *Cryst. Growth Des.* **2003**, *3*, 301-311. (b) Brammer, L.; Espallargas, G. M.; Adams, H. *CrystEngComm*. **2003**, *5(60)*, 343-345. (c) Haddad, S.; Awwadi, F.; Willett, R. D. *Cryst. Growth Des***.** **2003**, *3(4),* 501-505. (d) Zordan, F.; Brammer, L. *Acta Cryst*. **2004**, *B60*, 512-519. (e) Zordan, F.; Brammer, L.; Sherwood, P. *J. Am. Chem. Soc*. **2005**, *127*, 5979-5989.

7. (a) Farina, A.; Meille, S. V.; Messina, T. M.; Metrangolo, P.; Resnati, G.; Vecchio, G. *Angew. Chem. Int. Ed.* **1999**, *38*, 2433-2436.

8. Gaussian 98, Revision A.11.2, M. J. Frisch *et al.*

9. MOLPRO is a package of programs written by H-J. Werner *et al*.

10. (a) Dunning, T. H., Jr. *J. Chem. Phys.* **1989**, *90*, 1007-1023. (b) Kendall, R. A.; Dunning, T. H., Jr.; Harrison, R. J. *J. Chem. Phys.* **1992**, *96*, 6796-6806. (c) Woon, D. E.; Dunning, T. H., Jr. *J. Chem. Phys.* **1993**, *98*, 1358-1371. (d) Wilson, A. K.; Peterson, K. A.; Woon, D. E.; Dunning, T. H., Jr. *J. Chem. Phys.* **1999**, *110*, 7667-7676. (e) Peterson, K. A.; Figgen, D.; Goll, E.; Stoll, H.; Dolg, M. *J. Chem. Phys*. **2003**, *119*, 11113-11123.

11. Boys, S. F.; Bernardi, F. *Mol. Phys.* **1970**, *19*, 553.

12. (a) Peterson, K. A.; Woon, D. E.; Dunning, T. H., Jr. *J. Chem. Phys.* **1994**, *100*, 7410-7415. (b) Feller, D.; Peterson, K. A. *J. Chem. Phys.* **1999**, *110*, 8384-8396.

13. XSCANS, Siemen Analytical X-ray Instrument, Inc., Version 2.2, Madison, WI, USA.

14. (a)SMART: v.5.626, Bruker Molecular Analysis Research Tool, Bruker AXS, Madison, WI, **2002**. (b) SAINTPlus: v. 6.36a, Data Reduction and Correction Program, Bruker AXS, Madison, WI, **2001**. (c) SADABS: v.2.01, an empirical absorption correction program, Bruker AXS Inc., Madison, WI, **2001**.(d) SHELXTL: v. 6.10, Structure Determination Software Suite, Sheldrick, G.M., Bruker AXS Inc., Madison, WI, **2001**.

15. Kim, D.; Tarakeshwar, P.; Kim, S. K. *J. Phys. Chem. A* **2004**, *108*, 1250-1258.

16. Aakeröy Ch. B.; Beatty A. M. *Aust. J. Chem.* **2001**, *54*, 409-421.

17. Awwadi, F. F.; Willett, R. D.; Twamley, B. *in preparation.*

18. (a) Awwadi, F. F.; Willett, R. D.; Peterson K. A.; Twamley, B. *in preparation*. (b) Bosch, E.; Barnes, C. L. *Cryst. Growth Des.* **2002**, *2*, 299-302. (c) Auffinger, P.; Hays, F. A.; Westhof, E.; Ho, P. S. *Proc. Natl. Acd. Sci*. U.S.A. **2004**, *10*, 16789-16794.

19. Nyburg, S. C. and Faerman, C. H., *Acta Cryst*. **1985**, *B41*, 274-279.

20. CSD, version 5.26 November 2004.

21. The CSD was searched for halogen···halide contacts in room temperature structures, where the *ipso* carbon is *sp*, sp^2 or sp^3 hybridized. Six filters were applied to the searches; only organic compounds, crystallographic R factor < 0.1, no errors in the crystal structures, not disordered, not polymeric and no powder structures. To overcome the electronegativity factor, the search was constrained to the cases were the

atoms attached to the *ipso* carbon, other than the halogen atom involved in the contacts, are either carbon or hydrogen.

22. (a) Lommerse, J. P., Anthony J. S., Taylor, R. and Allen, F. H., *J. Am. Chem. Soc.,* **1996**, 118, 3108-3116. (b) Bianchi, R.; Forni, A.; Pilati, T. *Acta Cryst.* **2004**, *B60*, 559-568. (c) Bianchi, R.; Forni, A.; Pilati, T. *Chem. Eur J*, **2003**, *9*, 1631-1638.

SYNOPSIS

The Nature of Halogen···Halide Synthons; Theoretical and Crystallographic Studies.

Firas F. Awwadi, Roger D. Willett, Kirk A. Peterson and Brendan Twamley

It is demonstrated that halogen-halide contacts are controlled by electrostatic forces. *Ab initio* calculations and experimental crystallographic results can be used to explain the linear arrangement of C-Y···X^- (Y = Cl, Br or I; X = F, Cl, Br or I), which is due to the presence of a positive electrostatic potential end cap on all halogen atoms except fluorine. The strength of these synthons varies from weak or non-existing (C-F···X^- and H_3C-Cl···X^-) to very strong (e.g. HCCI···F^-).

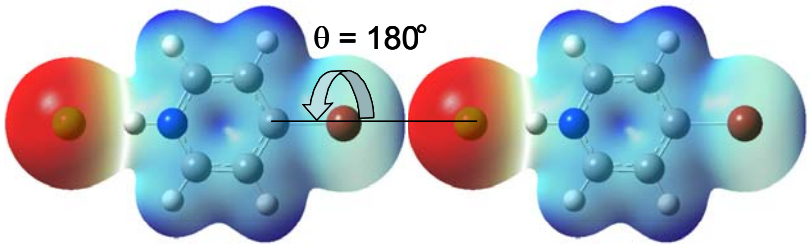

SUPPORTING INFORMATION

The Nature of Halogen···Halide Synthons; Theoretical and Crystallographic Studies.

Firas F. Awwadi[†], *Roger D. Willett*[†,*], *Kirk A. Peterson*[†] *and Brendan Twamley*[‡]

[†]Department of Chemistry, Washington State University, Pullman, WA 99164 USA

[‡]University Research Office, University of Idaho, Moscow, ID 83844 USA

*Department of Chemistry, Washington State University, Pullman, WA 99164, USA, Tel (Office), 509 335 3925, FAX (dept.) 509 335 8867, E-mail rdw@mail.wsu.edu

Authors of Gaussian and MOLPRO programing packages

1. Gaussian 98, Revision A.11.2, M. J. Frisch, G. W. Trucks, H. B. Schlegel, G. E. Scuseria, M. A. Robb, J. R. Cheeseman, V. G. Zakrzewski, J. A. Montgomery, Jr., R. E. Stratmann, J. C. Burant, S. Dapprich, J. M. Millam, A. D. Daniels, K. N. Kudin, M. C. Strain, O. Farkas, J. Tomasi, V. Barone, M. Cossi, R. Cammi, B. Mennucci, C. Pomelli, C. Adamo, S. Clifford, J. Ochterski, G. A. Petersson, P. Y. Ayala, Q. Cui, K. Morokuma, N. Rega, P. Salvador, J. J. Dannenberg, D. K. Malick, A. D. Rabuck, K. Raghavachari, J. B. Foresman, J. Cioslowski, J. V. Ortiz, A. G. Baboul, B. B. Stefanov, G. Liu, A. Liashenko, P. Piskorz, I. Komaromi, R. Gomperts, R. L. Martin, D. J. Fox, T. Keith, M. A. Al-Laham, C. Y. Peng, A. Nanayakkara, M. Challacombe, P. M. W. Gill, B. Johnson, W. Chen, M. W. Wong, J. L. Andres, C. Gonzalez, M. Head-Gordon, E. S. Replogle, and J. A. Pople, Gaussian, Inc., Pittsburgh PA, **2001**.

2. MOLPRO is a package of programs written by H-J. Werner and P.J. Knowles with contributions from J. Almlöf, R.D. Amos, A. Bernhardsson, A. Berning, P. Celani, D.L. Cooper, M.J.O. Deegan, A.J. Dobbyn, F. Eckert, S.T. Elbert, C. Hampel, G. Hetzer, T. Korona, R. Lindh, A.W. Lloyd, S.J. McNicholas, F.R. Manby, W. Meyer, M.E. Mura, A. Nicklass, P. Palmieri, R.M. Pitzer, P. Pulay, G. Rauhut, M. Schütz, H. Stoll, A.J. Stone, R. Tarroni, P.R. Taylor, T. Thorsteinsson.

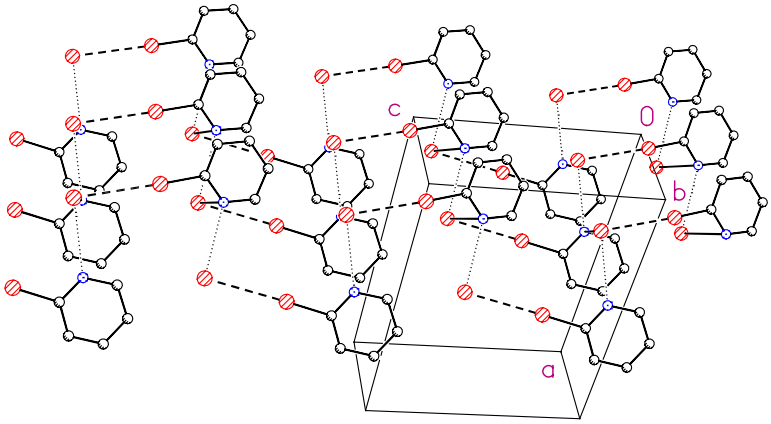

(a)

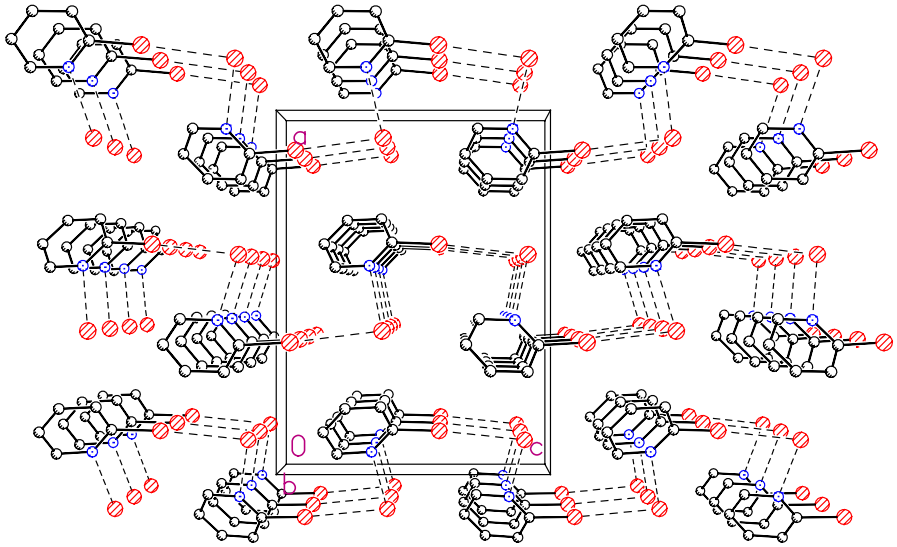

(b)

Figure 1S. (a) Illustration of packing of chains in (2BP)Br to form layers lie in *bc* plan. The chains interact *via* N-Br^- normal interaction to form a layer structure. Hydrogen bonds and halogen-halide synthons are represented by dotted and dashed lines respectively. (b) Interaction of the layers to form the three-dimensional structure *via* C-H···Br^- hydrogen bonds. Hydrogen bonds and halogen-halide synthons are represented by dashed lines.

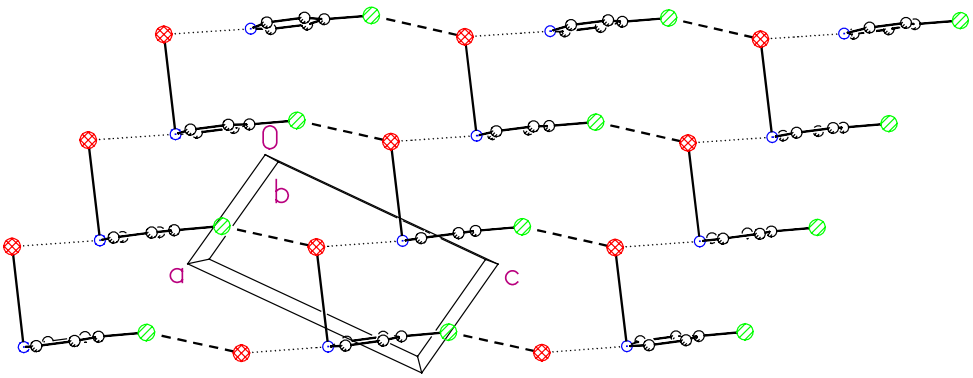

(a)

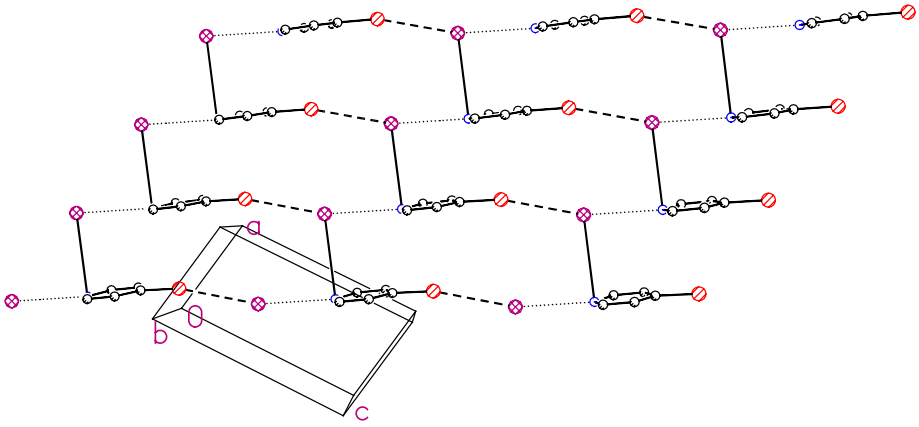

(b)

Figure 2S. Illustration of the layer structure of; (a) 4CPBr, the layers lie parallel to the (0 1 0) planes; (b) (4BP)I, the layers lie parallel to the (0 1 0) planes. Hydrogen bonds, halogen-halide and N-X^- synthons are represented by dotted, dashed and solid lines respectively.

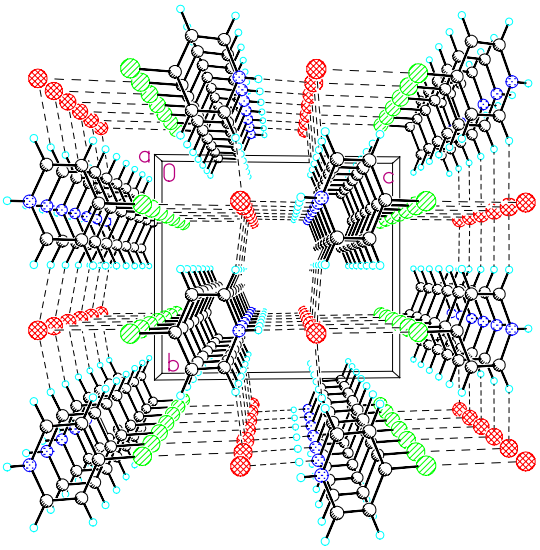

Figure 3S. Illustration of packing of layers into the three-dimensional structures of (4CP)Br.

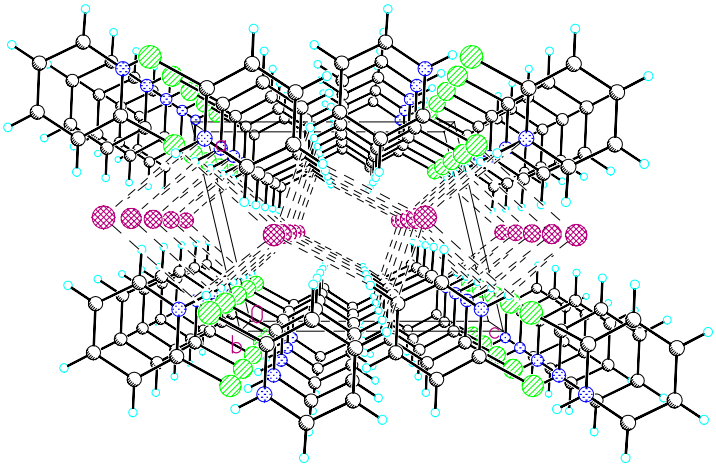

Figure 4S. Illustration of packing the chains based on N-Cl synthons into layers lie in *ac* plane in (2CP)I, these layers interact *via* C-H···I^- hydrogen bonds to form the three-dimensional structure

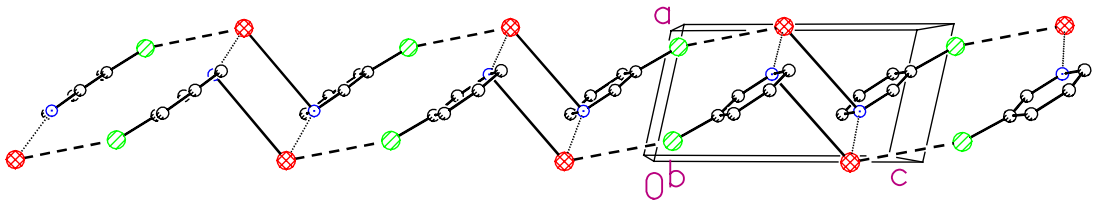

(a)

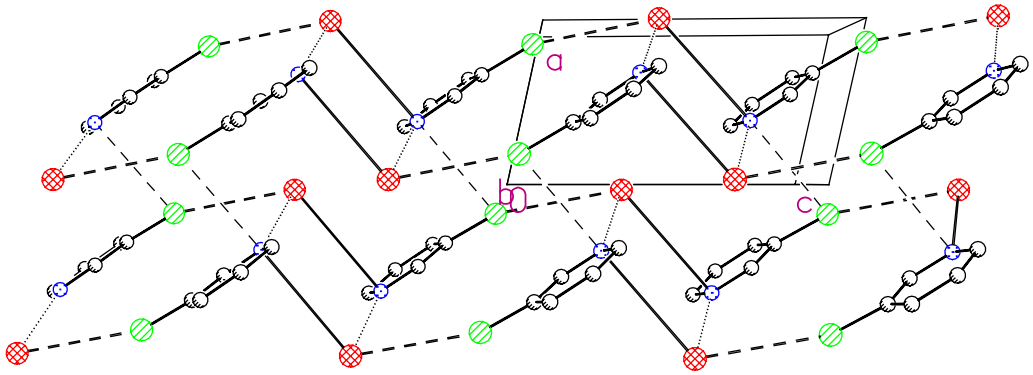

(b)

Figure 5S. (a) Ladder chain network in (3CP)Br, illustrating the N-H···Br^-, C-Cl···Br^- and N-Br^- synthonic interactions, the chains run parallel to the *c* axis. (b) Illustration of the layer structure of (3CP)Br, showing the N-Cl synthons by dashed lines. The layers lie parallel to the *ac* plane. Hydrogen bonds, halogen-halide, N-Br^- and N-Cl synthons are represented by dotted, thick dashed, solid and dashed lines respectively

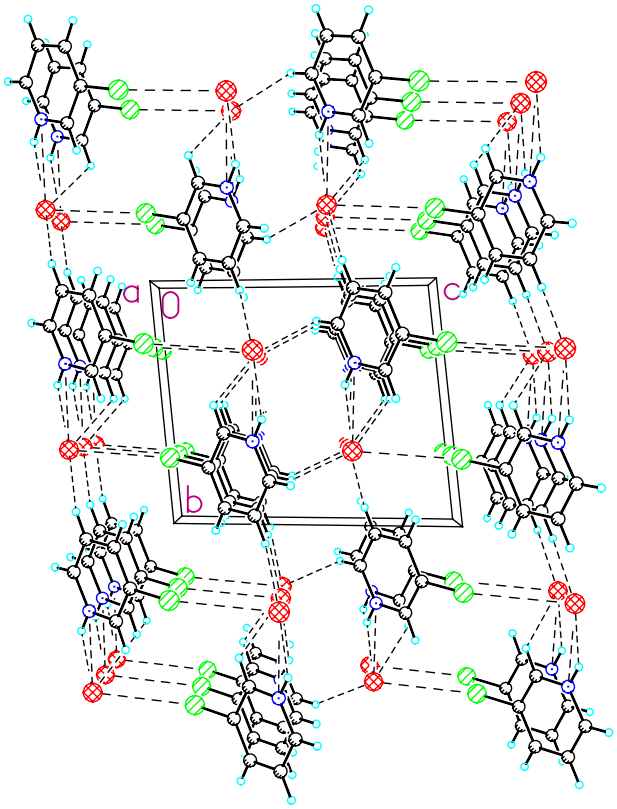

Figure 6S. Three-dimensional structure of (3CP)Br.

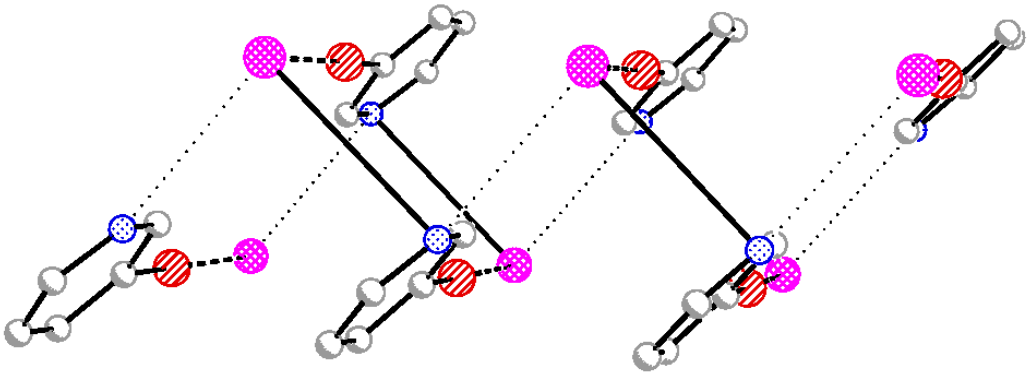

(a)

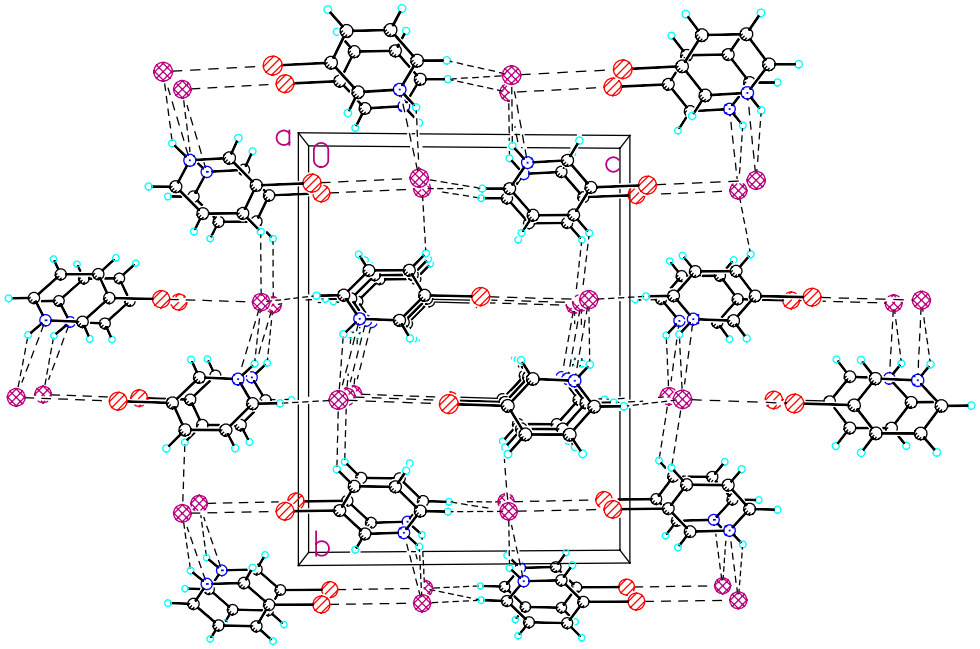

(b)

Figure 7S. (a) Illustration of double chain network in (3BP)I, showing the hydrogen bonds, halogen-halide and N-I$^-$ by dotted, dashed and solid lines, respectively. The chains run parallel to *a* axis. (b) Illustration of three-dimensional structure of (3BP)I.

Table 1S. Calculated separation distance at which the energy minima are located at different basis set levels.

Compound	**1bF$^-$**	**1bCl$^-$**	**1bBr$^-$**	**1bI$^-$**	**1cF$^-$**	**1cCl$^-$**	**1cBr$^-$**	**1cI$^-$**	**1dF$^-$**	**1dCl$^-$**	**1dBr$^-$**	**1dI$^-$**
dz[a]	2.71	3.56	3.84		2.53	3.32	3.55	4.16	2.45	3.18	3.44	3.75
tz[b]	2.61	3.39	3.63	4.32	2.45	3.18	3.41	3.75	2.38	3.08	3.29	3.57
qz[c]	2.56	3.32	3.55	3.92	2.41	3.14	3.36	3.66	2.35	3.04	3.25	3.52
Compound	**2bF$^-$**	**2bCl$^-$**	**2bBr$^-$**	**2bI$^-$**	**2cF$^-$**	**2cCl$^-$**	**2cBr$^-$**	**2cI$^-$**	**2dF$^-$**	**2dCl$^-$**	**2dBr$^-$**	**2dI$^-$**
dz[a]	2.56	3.31	3.6	3.88	2.44	3.19	3.41	3.71	2.39	3.12	3.34	3.62
tz[b]	2.47	3.18	3.4	3.7	2.36	3.06	3.28	3.56	2.33	3	3.21	3.48
qz[c]	2.42	3.13	3.34	3.63	2.33	3.02	3.23	3.51	2.3	2.96	3.17	3.43
Compound	**3bF$^-$**	**3bCl$^-$**	**3bBr$^-$**	**3bI$^-$**	**3cF$^-$**	**3cCl$^-$**	**3cBr$^-$**	**3cI$^-$**	**3dF$^-$**	**3dCl$^-$**	**3dBr$^-$**	**3dI$^-$**
dz[a]	2.46	3.13	3.37	3.67	2.37	3.08	3.28	3.57	2.36	3.05	3.25	3.53
tz[b]	2.37	3.04	3.24	3.53	2.31	2.96	3.16	3.44	2.3	2.94	3.14	3.4
qz[c]	2.33	2.99	3.2	3.48	2.28	2.93	3.13	3.4	2.28	2.9	3.1	3.36
Compound	**4bF$^-$**	**4bCl$^-$**	**4bBr$^-$**	**4bI$^-$**	**4cF$^-$**	**4cCl$^-$**	**4cBr$^-$**	**4cI$^-$**	**4dF$^-$**	**4dCl$^-$**	**4dBr$^-$**	**4dI$^-$**
dz[a]	2.48	3.23	3.45	3.75	2.4	3.13	3.34	3.64	2.36	3.08	3.29	3.57
tz[b]	2.41	3.1	3.32	3.6	2.33	3.0	3.21	3.49	2.31	2.96	3.16	3.43
qz[c]	2.37	3.05	3.26	3.54	2.3	2.97	3.17	3.45	2.28	2.93	3.13	3.38

[a] double zeta basis set.

[b] triple zeta basis set.

[c] quadruple zeta basis set.

Table 2S. Packing interactions parameters: π-π stacking and N-X$^-$and N-Y interactions.

Compound	$d_{\perp}$ (Å)[a]	$d_{c\text{-}c}$(Å)[b]	Θ (º)[c]	$D_{Y\text{-}N}$[d]	Φ(°)[e]	$d_{X\text{-}N}$[f]	Φ'(º)[g]
(2CP)Cl	Not	parallel				3.874	23.40
(2CP)Br	3.3422	4.700	44.67			3.591	6.89
(2CP)I	3.3126	4.954	44.54	3.490	18.35	4.522	42.90
(3CP)Cl	3.2453	4.648	45.71	3.602	36.16	4.181	32.81
(3CP)Br	3.3201	4.908	47.43	3.429	4.13	3.820	15.72
(3CP)I	3.3258	5.128	49.57	3.413	0	3.961	14.18
(4CP)Cl	3.3437	4.514	42.21	3.726	21.29	3.502	4.72
(4CP)Br	3.4467	4.699	42.82	3.730	18.46	3.642	4.93
(4CP)I	3.4512	5.090	47.31	3.735	19.23	3.854	6.18
(2BP)Cl	3.4173	4.440	39.68			3.616	5.86
(2BP)Br	3.3839	4.601	42.65			3.644	4.63
(2BP)I	3.3970	4.883	45.92			3.754	3.622
(3BP)Cl	3.2702	4.769	46.71	3.512	11.32	3.669	16.09
(3BP)Br	3.3440	4.426	40.93	3.996	29.86	3.569	29.37
(3BP)I	3.4025	4.805	44.92	4.494	36.70	3.737	13.69
(4BP)Cl	3.5613	4.392	35382	4.218	28.09	3.572	8.31
(4BP)Br	3.4819	4.471	38.85	4.045	25.26	3.547	8.66
(4BP)I	3.5382	4.981	44.73	4.049	25.47	3.826	6.75

[a] The perpendicular distance between the planes of two adjacent cations.

[b] The centroid to centroid distance between the adjacent pyridinium cations.

[c] The angle between the line connecting the two centroids and the normal to the plane of the cation.

[d] The distance from the nitrogen to halogen atom of the adjacent cation.

[e] The angle between the N-Cl line and the normal to the plane of pyridinium cation.

[f] The N-X$^-$ distance from the nitrogen to the halide anion.

[g] The angle between the N-X$^-$ line and the normal to the plane of the pyridinium cation.

CHAPTER FOUR

The Aryl Chlorine···Halide Ion Synthon and Its Role in the Control of the Crystal Structures of Tetrahalocuprate(II) Ions.

Firas F. Awwadi[†]*, Roger D. Willett*[†,]** and Brendan Twamley*[‡]

[†]Department of Chemistry, Washington State University, Pullman, WA 99164 USA.

[‡]University Research Office, University of Idaho, Moscow, ID 83844 USA.

*Department of Chemistry, Washington State University, Pullman, WA 99164, USA, Tel (Office), 509 335 3925, FAX (dept.) 509 335 8867, E-mail rdw@mail.wsu.edu.

ABSTRACT The role of the arylchlorine···halide (C-Cl···X^-) synthons in the development of crystal structures of the type $(n\text{CP})_2\text{CuX}_4 \cdot m\text{H}_2\text{O}$ ($n\text{CP}^+$ = *n*-chloropyridinium; *n* = 2, 3, or 4; X = Cl^- or Br^-, *m* = 0 except for $(3\text{CP})_2\text{CuBr}_4 \cdot \text{H}_2\text{O}$) are investigated. All structures consist of chloropyridinium cations and tetrahalocuprate anions. Based on detailed analysis of the synthonic interactions in these systems, it is concluded that the C-Cl···Cl^- synthon plays a more significant role as a crystal engineering tool than the C-Cl···Br^- synthon. In addition, it is shown that the C-Cl···X^- interactions are weaker than the C-Br···X^- synthons in the analogous $(n\text{BP})_2\text{CuX}_4$ salts ($n\text{BP}^+$ = *n*-bromopyridinium). For all of the $(n\text{CP})_2\text{CuCl}_4$ salts, the $n\text{CP}^+$ cations are involved in nearly linear C-Cl···Cl^- interactions with Cl···Cl^- distances less or equal to the sum of the van der Waals radii (r_{vdW}). Supramolecular chain networks, based on the C-Cl···Cl^- and N-H···Cl^- synthons, are formed with all three $n\text{CP}^+$ cations. In addition, a polymorph of the 4CP^+ salt contains two-dimensional networks based on these synthons. In contrast, the role of the C-Cl···Br^- synthons is less well defined, with only two of the five independent $n\text{CP}^+$ involved in these interactions. A supramolecular structure developed on the basis of the C-Cl···Br^- and N-H···Br^- synthons is observed only for $(4\text{CP})_2\text{CuBr}_4$. In $(3\text{CP})_2\text{CuBr}_4.\text{H}_2\text{O}$, one of the two independent cations is involved in the development of a supramolecular ladder structure on the basis of the C-Cl···Br^- and O-H···Br^- synthons. The role of two previously undescribed synthons, the N-Cl and N-X^- synthons, where the N-Cl and N-X vector lies roughly normal to the plane of the pyridinium ring, is explored in the further development of the three dimensional structures.

INTRODUCTION.

Non-covalent interactions have received much interest in the recent decades due to their importance in stabilizing many important molecules like proteins, DNA...etc, and arranging the structural units inside the crystal lattice.[1] Moreover, the physical properties (e.g. non-linear optical behavior, magnetic and electrical properties) of solid state materials depend not only on the molecular structure of the building units but also on the arrangement of these structural units inside the crystal lattice.[2] In fact, the role of these interactions in determining the supramolecular structure of crystalline materials is one of the main foci of crystal engineering.[1] Great success has been achieved in using intermolecular interactions in solid state pericyclic reactions, especially solid state polymerization and dimerization, e.g. resorcinol has been used as a template to arrange reactants *via* hydrogen bonding in a suitable arrangement for cycloaddition reactions.[3,1d] The intermolecular forces range from strong ones, e.g. classical hydrogen bond,[4,1b] to weaker ones, e.g. π-π stacking.[5] Classical hydrogen bonds and π-π stacking have been studied in much detail, while the study of other interactions, such as halogen bonds and halogen···halogen contacts,[1e] have received attention only in more recent years.

Initially, the main focus in studying halogen···halogen contacts in the solid state was on interactions of the type C-Y···Y-C.[6-9] However, our interest in halogen bonds has focused primarily on the so-called charge assisted halogen···halide ion interactions, denoted C-Y···X^-, where the C-Y portion of the synthon is incorporated into a pyridinium cation and where X^- is either a simple halide ion or incorporated into a halometallate anion. These C-Y···X^- synthons are characterized by a Y···X^- distance less than the sum of r_{vdW} and a nearly linear C-Y···X angle.[8,10,11] The rationalization for this arrangement was based on the presence of an

electrostatic potential cap along the σ region of the halogen atom, and a negative electrostatic ring in the π-region of the halogen atom.[9b] So, according to the electrostatic picture of the carbon bonded halogen atom, the halide anion is expected to confront the positive electrostatic potential cap of the C-Y bond. In this context, Freytag *et al.*, found that in the structure of 4-halopyridinium halides, the C-Y···X^- synthon compliments the role of the N-H···X^- hydrogen bond in forming a chain structure,[11b] and we have extended this study to a wider series on *n*-halopyridinium halide salts.[11f] In our studies, we have also found that the C-Br···X^- synthon competes favorably with the N-H···X^- hydrogen bond in the 2,5-dibromopyridinium halide salts.[11g]

Recently there have been several reports on the subject of C-Br···X-M contacts.[10] Replacing one of the carbon atoms with a metal atom increases the negative electrostatic charge on a halogen atom bonded to the metal ion. In fact, electrostatically, this halogen atom can be considered to be essentially equivalent to a halide anion. Therefore, this synthon is found to be more directional than the more traditional C-Y···Y-C synthon. Zordan *et al.* expanded the study of these synthons to include all carbon bonded halogen atoms. Their results showed that C-Y···Cl-M synthons (M = Pt(II) or Pd(II))[10e]. are a very valuable tool in supramolecular assembly and supramolecular synthesis when Y

= Cl, Br or I but not when X = F. Their results also pointed to the importance of the electrostatic attraction term in controlling these synthons.[10e]

Halogen···halide synthons have been utilized in developing useful new materials.[12,2] For example, molecular conductors were prepared based on halogen···halide synthons where these synthons not only play a structural role but also participate in the modification of their conducting properties.[2,12a] Farina *et al.* utilized the bromine···bromide synthon in chemical

separation and were able to resolve the racemic mixture of 1,2-dibromohexafluoropropane by crystallizing it with enantiopure trialkylammonium hydrobromides.[12b] Recently, we used the C-Br···Br-Cu synthon along with N-H···Br^- hydrogen bonding to prepare the longest ever known cupric bromide oligamer.[10c]

Hybrid organic-inorganic halocuprate salts have been studied in details due to their novel magnetic properties.[13] Therefore, understanding their structural features is of special interest. In a previous study, we have shown that C-Br···X-Cu synthons play a significant role in determining the supramolecular structure of the $(n\text{BP})_2\text{CuX}_4$ salts, ($n\text{BP}^+$ = *n*-bromopyridinum, n = 2, 3 or 4, and X = Cl^- or Br^-).[10a] This synthon was characterized by Br···X^- distance 0.3-0.4 Å less than the sum of the r_{vdW} and approximately linear C-Br···X^- angles. In this paper, we examine the crystal structure of the following $(n\text{CP})_2\text{CuX}_4$ compounds ($n\text{CP}^+$ = *n*-chloropyridnium): (**1**) $(2\text{CP})_2\text{CuCl}_4$, henceforth 2CP-Cl; (**2**) $(3\text{CP})_2\text{CuCl}_4$, henceforth 3CP-Cl; (**3**) $(4\text{CP})_2\text{CuCl}_4$ polymorph (I), henceforth 4CP-Cl(I); (**4**) $(4\text{CP})_2\text{CuCl}_4$ polymorph (II), henceforth 4CP-Cl(II); (**5**) $(2\text{CP})_2\text{CuBr}_4$, henceforth 2CP-Br; (**6**) $(3\text{CP})_2\text{CuBr}_4.\text{H}_2\text{O}$, henceforth 3CP-Br.$H_2O$; and (**7**) $(4\text{CP})_2\text{CuBr}_4$, henceforth 4CP-Br. Structural analysis of the crystals of these compounds will show that chlorine···chloride synthons play a significant role in determining the crystal structure of the compounds $(n\text{CP})_2\text{CuCl}_4$. However, the role of the chlorine···bromide synthon is less obvious. Comparing these structures with published analogues structures, $(n\text{BP})_2\text{CuBr}_4$, shows that the C-Br···$X^-$ synthons, in these examples, plays a more significant role in determining the supramolecular structure of crystalline materials than C-Cl···X^- synthons. In addition, the role of two previously undescribed synthons, the N-Cl and N-X^- synthons, where the N-Cl and N-X

vector lies roughly normal to the plane of the pyridinium ring, is explored in the further development of their three dimensional structure

EXPERMENTAL SECTION

Synthesis and Crystal Growth.

(a) *Bis(n-chloropyridinium)tetrahalocuprate(II)*; 2CP-Cl, 3CP-Cl and 3CP-Br.H_2O. A general procedure was followed to prepare the above three compounds; 2 mmol of copper dihalide ($CuCl_2.2H_2O$ or $CuBr_2$) were dissolved in 20 mL of acetonitrile acidified with 1 mL of concentrated hydrochloric acid or hydrobromic acid. 4 mmol of either 2-chloropyridine or 3-chloropyridine were dissolved in 20 mL of acetonitrile acidified with 1 mL of concentrated hydrochloric acid or hydrobromic acid. The two solutions were mixed and gently heated while being stirred for 10 minutes. The mixture was filtered and the resulting solution allowed to slowly evaporate. Crystals developed from the solution after several days. (b) *Bis(4-chloropyridinium)tetrachlorocuprate(II) – polymorph I* , 4CP-Cl(I) and bis(4-chloropyridinium)tetrabromocuprate(II), 4CP-Br. 2 mmol of the appropriate copper dihalide ($CuCl_2.2H_2O$ or $CuBr_2$) were dissolved in 20 mL of acetonitrile acidified with 1 mL of concentrated hydrochloric acid or 3 mL of concentrated hydrobromic acid. 4 mmol of 4-chloropyridinium chloride was dissolved in 20 mL acetonitrile acidified with either 1 mL of concentrated hydrochloric acid or 3 mL of concentrated hydrobromic acid. The two solutions mixed and gently heated for 15 minutes while being stirred. The mixture was filtered and the resulting solution allowed to slowly evaporate. Crystals formed within a few days. (c) *Bis(2-chloropyridinium)tetrabromocuprate(II), 2CP-Br.* 1 mmol of cupric bromide, $CuBr_2$, was dissolved in 20 mL of 2-propanol acidified with 2 mL of concentrated hydrobromic acid. 2 mmol of 2-chloropyridine were dissolved 10 mL of 2-propanol acidified with 1 mL concentrated hydrobromic acid. The two solutions mixed and gently heated for 15 minutes.

The solution was filtered and transferred to a desiccator connected to vacuum. Crystals formed within 3 days. (d) *Bis(4-chloropyridinium)tetrachlorocuprate(II),* 4CP-Cl(II) . 2 mmol of 4-chloropyridiniumchloride was added to 1 mmol of $CuCl_2.2H_2O$ dissolved in 30 mL of acetonitrile. The solution was stirred for 15 minutes with heating. The solution was left to slowly evaporate until yellow crystals formed (a few hours).

Crystal Structure determinations.

The diffraction data of the studied compounds were collected at room temperature. The data of all of the compounds except 2CP-Br were collected on a Syntex $P2_1$ diffractometer upgraded to Bruker P4 specifications. The unit cell dimensions were determined from 26-36 accurately centered reflections. The data were collected and reduced using XSCANS 2.20 software.[14] Data were corrected for absorption correction utilizing ψ-scan data, using SHELXTL XPREP software, assuming ellipsoidal shaped crystals.[15d] Data for 2CP-Br were collected using a Bruker/Siemens SMART APEX instrument (Mo Kα radiation, λ = 0.71073 Å). Data were measured using omega scans of 0.3 ° per frame for 5 seconds, and a full sphere of data was collected. A total of 2450 frames were collected with a final resolution of 0.83 Å. The first 50 frames were recollected at the end of data collection to monitor for decay. Cell parameters were retrieved using SMART software and refined using SAINTPlus on all observed reflections.[15a,b] Data reduction and correction for Lp and decay were performed using the SAINTPlus software.[15b] Absorption corrections were applied using SADABS.[15c] The structures of all compounds were solved by direct methods and refined by least squares method on F^2 using the SHELXTL program package.[15d] All non hydrogen atoms were refined anisotropically. Hydrogen atoms were placed in calculated positions except for the water molecule. Water molecule hydrogen atoms were found using Fourier difference map, and

were refined isotropically with restraints. Details of the data collection and refinement are given in Table 1.

Table 1. Summary of data collection and refinement parameters.

Crystal	**2CP-Cl**	**3CP-Cl**	**4CP-Cl(I)**	**4CP-Cl (II)**	**2CP-Br**	**3CP-Br.H_2O**	**4CP-Br**
Formula	$C_{10}H_{10}Cl_6CuN_2$	$C_{10}H_{10}Cl_6CuN_2$	$C_{10}H_{10}Cl_6CuN_2$	$C_{10}H_{10}Cl_6CuN_2$	$C_{10}H_{10}Br_4Cl_2CuN_2$	$C_{10}H_{12}Br_4Cl_2CuN_2O$	$C_{10}H_{10}Br_4Cl_2CuN_2$
Form. Wt.	434.44	434.44	434.44	434.44	612.28	630.30	612.28
D_{calc} (Mg/m^3)	1.726	1.787	1.732	1.746	2.323	2.281	2.282
T(K)	295	295	295	295	297(2)	295	295
Crystal syst.	Orthorhombic	Triclinic	Monoclinic	Monoclinic	Monoclinic	Triclinic	Monoclinic
Space group	*Pccn*	*P*-1	$P2_1/c$	*C*2/*c*	$P2_1/c$	*P*-1	*C*2/*c*
a (Å)	14.711(3)	7.313(1)	7.673(2)	16.297(4)	15.065(1)	6.980(1)	17.010(2)
b (Å)	7.818(1)	7.775(2)	27.637(7)	7.469(2)	9.087(1)	9.534(2)	7.673(1)
c (Å)	14.539(3)	15.489(3)	8.728(1)	13.738(3)	14.478(1)	14.017(3)	13.804(2)
α (º)	90	81.66(1)	90	90	90	99.49(2)	90
β (º)	90	79.76(1)	115.79(1)	98.78(3)	117.967(1)	90.77(2)	98.45(1)
γ (º)	90	69.29(1)	90	90	90	93.85(2)	90
V ($Å^3$)	1672.2(6)	807.4(3)	1666.4(7)	1652.6(7)	1750.5(2)	917.6(3)	1782.2(4)
Ind. refl.	1434	2761	2854	1403	3167	3134	1485
R(int)	0.0661	0.0300	0.0461	0.0316	0.0369	0.0563	0.0387
Z	4	2	4	4	4	2	4
goodness of fit	1.031	1.063	1.008	1.039	1.029	1.021	1.065
R_1[a] [I>2σ]	0.0581	0.0375	0.0499	0.0389	0.0240	0.0593	0.0461
wR_2[b] [I>2σ]	0.1104	0.0876	0.1006	0.0895	0.0567	0.1166	0.1142
μ mm^{-1}	2.250	2.331	2.258	2.277	10.671	10.185	10.480

[a] $R_1 = \sum | |F_o| - |F_c| | / \sum |F_o|$.

[b] $wR_2 = \{\sum[w(F_o^2 - F_c^2)^2] / \sum[w(F_o^2)^2]\}^{1/2}$

RESULTS

Structure Descriptions.

Six of the seven crystal structures studied in this research consisted of isolated, planar chloropyridnium cations and distorted tetrahedral CuX_4^- anions. In addition to these species, the asymmetric unit of 3CP-Br contains a water molecule. Polymorphism and isomorphism phenomena were observed only in $(4CP)_2CuX_4$, X = Cl and Br; 4CP-Cl crystallizes in two different monoclinic phases ($P2_1/c$ and $C2/c$). The $C2/c$ phase is isomorphous to 4CP-Br (Table 1). In addition, several of these salts are isomorphous to the corresponding $(nBP)_2CuX_4$ salts (nBP$^+$ = n-bromopyridinium).[10a] 4CP-Cl and 4CP-Br(I) are isomorphous to $(4BP)_2CuCl_4$, while 4CP-Br(II) is isomorphous to $(4CP)_2CuBr_4$. 3CP-Cl is isomorphous to 3BP-Cl. The CuX_4^- anions exhibit typical flattened tetrahedral geometry with the approximate D_{2d} symmetry, although the extent of flattening is not large (Table 2). The average *trans* X-Cu-X angles are in the range 128.5-144.4° and 126.4-138.0° for the chloride and bromide salts respectively. The smaller values of these *trans* angles are in the range normally observed for salts containing non-hydrogen bonding cations.[16] The exceptions are the larger *trans* angles in 3CP-Cl salt, where one of the pyridinium cations packs to form close contacts (ca. 3.92 Å) with the copper atom, forcing one of the *trans* angles to open further.

Table 2. Selected bond distances and angles.

Crystal	**2CP-Cl**	**3CP-Cl**	**4CP-Cl(I)**	**4CP-Cl(II)**	**2CP-Br**	**3CP-Br.H_2O**	**4CP-Br**
Trans angle 1 (°)	136.73(11)	138.32(5)	133.31(7)	128.47(4)	132.85(2)	130.75(7)	126.44(4)
Trans angle 2 (°)	130.12(11)	144.44(5)	132.42(6)		133.54(2)	137.95(7)	
Cu-X1 distance (Å)	2.256(2)	2.295(1)	2.212(2)	2.210(1)	2.400(1)	2.429(2)	2.396(1)
Cu-X2 distance (Å)	2.227(2)	2.230(1)	2.229(1)	2.272(1)	2.387(1)	2.358(2)	2.352(1)
Cu-X3 distance (Å)		2.237(1)	2.253(2)		2.340(1)	2.379(2)	
Cu-X4 distance (Å)		2.232(1)	2.275(2)		2.407(1)	2.381(2)	

A variety of supramolecular interactions tie the anions and cations together in these structures. The structures will be analyzed in the following sequence: (a) examination of the environment of the pyridinium cations and CuX_4^{2-} anions to identify the significant C-Cl···X^- and the N-H···X^- interactions; (b) description of the resultant supramolecular networks; (c) analysis of the packing interactions between the networks and (d) the resultant three-dimensional structures of the compounds. In three of the four tetrachlorocuprate crystal structures, 2CP-Cl, 3CP-Cl, and 4CP-Cl (II), a chain structure is developed based on the classical N-H···X^- hydrogen bond (both linear and bifurcated) and the novel C-Cl···Cl^- synthon. The remaining structure, 4CP-Cl(I), based on these two synthons, forms a perforated layer structure. The role of C-Cl···X^- synthon is less obvious in the tetrabromocuprate salts. 4CP-Br, isomorphous to 4CP-Cl(II), contains a chain supramolecular structure. In the 3CP-Br.H_2O structure, N-H···Br^- hydrogen bonds cooperate with the C-Cl···Br^- synthons to form dimers of copper centers, while O-H···Br^- hydrogen bonds link these dimer units into a ladder structure. The effect of the C-Cl···Br^- synthon is absent or very weak in 2CP-Br, using the chlorine···bromide distance as a parameter reflecting the strength of C-Cl···Br synthon, due to the fact that there are no chlorine···bromide contacts within the sum of r_{vdW}. These chains, ladders and monomers are aggregated into the final three-dimensional structure *via* different packing interactions between chloropyridinium cations and with either another chloropyridinium cation or tetrahalocuprate anion, and other weaker interactions like the C-H···X^- hydrogen bond.

C-Cl···X⁻ and N-H···X⁻ Interactions.

The linear geometric arrangement of the C-Cl···X^- synthons and the more varied nature of N-H···X^- hydrogen bond geometries (linear, symmetric bifurcated and asymmetric bifurcated)

that are present in the various structures are exemplified in Figure 1. The bisynthonic nature of monochloropyridinium cation is illustrated through these N-H···X^- and C-Cl···X^- interactions (ignoring secondary C-H···X^- hydrogen bond and stacking interactions). The data summarizing these contacts are listed in Table 3 for all seven compounds. In all four tetrachlorocuprate salt structures, the chloropyridinium cations are involved in chlorine···chloride contacts within the sum of r_{vdW} (ca. 3.52 Å). The Cl···Cl^- distances range from 3.30 to 3.51 Å, and the C-Cl···Cl^- angles range from 150.0 to 175.9°. In contrast, in the bromide salts, not all of the chlorine atoms are involved in chlorine···bromide contacts within the sum of r_{vdW} (ca. 3.62 Å). In the bromide salts, the contacts are observed only in 4CP-Br and one of the cations in 3CP-Br, the Cl···Br^- distances are 3.42 Å and 3.55 Å with C-Cl···Br^- angles 172.8° and 171.9° for 4CP-Br and 3CP-Br respectively. Thus, the Cl···X^- distances are 0-0.24 Å less than the sum r_{vdW}. Three types of N-H···X^- hydrogen bonds are observed in the structures: linear (2CP-Cl, 4CP-Cl(I), 2CP-Br and 3CP-Br), symmetric bifurcated (3CP-Cl and 3CP-Br) and asymmetric bifurcated (3CP-Cl, 4CP-Cl(I), 4CP-Cl(II), 2CP-Br and 4CP-Br). In the analogous methyl compounds, $(n\text{MP})_2CuX_4$, (*n*MP = *n*-methylpyridinium, *n* = 2, 3, or 4. X = Cl^- or Br^-), asymmetric hydrogen bonds have not been observed.[17a] Therefore, the presence of C-Cl···X^- synthons distorts some of the symmetric bifurcated hydrogen bond, and transforms them to asymmetric ones.

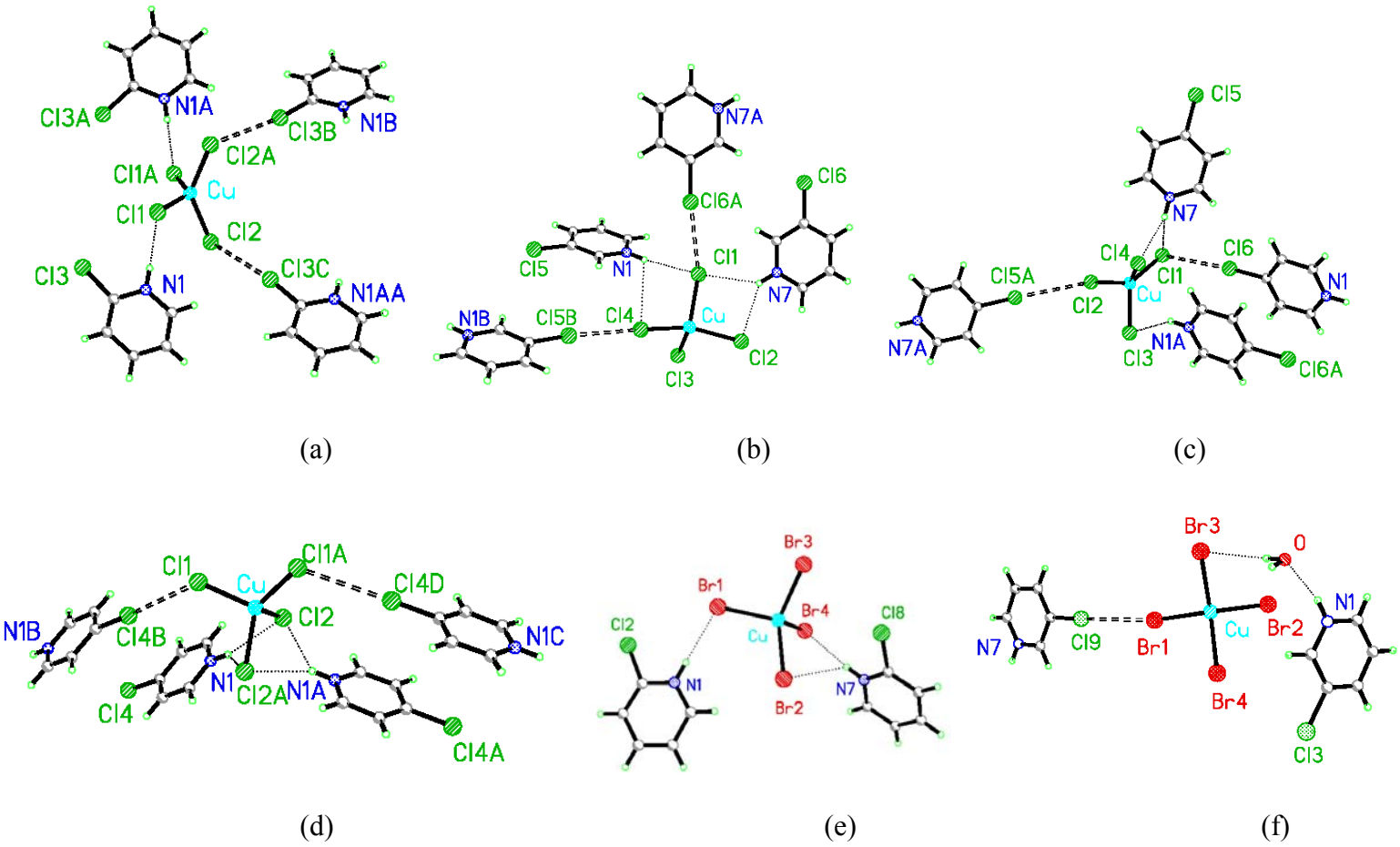

Figure 1. Synthon interactions in (a) 2CP-Cl, (b) 3CP-Cl, (c) 4CP-Cl(I), (d) 4CP-Cl(II), (e) 2CP-Br and (f) 3CP-BrH_2O. The nitrogen atom of cation 1 (cat1) is labeled N1 and that of cation 2 (cat2) is labeled N7, in cases where there are two crystallographically different cations. Dotted and dashed lines represent hydrogen bonds and chlorine···halide synthons, respectively.

Table 3. C-Cl···X and N-H···X synthon distances and angles in the *n*CP^+ salts.

Compound[a]	Cl···X(Å)	C-Cl···X(º)	Cl···X-Cu(º)	N···X(Å)	H···X(Å)	N-H···X(º)	Type of H-bond
2CP-Cl	3.303(3)	150.05(17)	115.95(08)	3.130(5)	2.27	175.3	Linear
3CP-Cl cat1	3.341(2)	175.61(15)	171.52(5)	3.139(3)	2.33	156.0	asym bifurcated
				3.320(4)	2.91	111.2	
cat2	3.277(2)	165.23(14)	157.55 (5)	3.231(4)	2.54	138.6	Bifurcated
				3.278(4)	*2.57*	140.5	
4CP-Cl(I) cat1	3.447(2)	173.40(18)	100.57(6)	3.399(5)	2.77	131.5	asym bifurcated
				3.133(4)	2.37	147.6	
cat2	3.511(2)	145.13(5)	129.55(7)	3.093(5)	2.27	160.3	Linear
4CP-Cl(II)	3.403(2)	175.95(15)	117.20(5)	3.215(4)	2.46	147.2	asym bifurcated
				3.411(4)	2.76	133.6	
2CP-Br cat1	3.696 (1)	169.09 (14)	92.04 (2)	3.264(3)	2.41	176.0	Linear
cat2	3.621 (1)	83.69 (12)	161.77 (2)	3.320(3)	2.49	161.6	asym bifurcated
				3.555(3)	3.08	116.7	
3CP-Br cat1	3.423(3)	171.9 9(35)	171.58(6)	3.429(8)	2.73	139.5	Bifurcated
				3.405(8)	2.72	137.5	
cat2[b]				2.743(11)	1.90	166.3	Linear
H_2O [c]				3.476(8)	2.65	163.1	
				3.561(8)	2.77	154.2	
4CP-Br	3.551(3)	172.87(30)	117.15(6)	3.399(8)	2.68	141.8	asym bifurcated
				3.516(8)	2.84	137.1	

[a] When two crystallographic cations are present, they are denoted as cat1 and cat2.

[b] The proton acceptor is the oxygen atom of the water molecule.

[c] The water molecule is the proton donor.

Description of the Supramolecular Networks. (a)$(nCP)_2CuCl_4$.

In these crystal structures, it is possible to identify extended structures developed based upon the combination of the N-H···Cl^- and C-Cl···Cl^- synthons. The resulted networks are illustrated Scheme 2. Of the four tetrachlorocuprate salts, three of them form chain structures (2CP-Cl, 3CP-Cl and 4CP-Cl(II)) and one forms a layer structure (4CP-Cl(I), as shown in Scheme 2. In the chain structures, the tetrachlorocuprate anions are linked *via* [CuX_4^{2-} – ($n$$CP^+$)$_2$ – CuX_4^{2-}] bibridged units. The layer structure contains both the bibridged linkage as well as [CuX_4^{2-} – ($n$$CP^+$) – CuX_4^{2-}] monobridged interactions.

The three chain networks are quite different topologically and structurally, though they are developed based on the bibridged unit. In the 2CP-Cl structure, the bibridged chains lie on two-fold axes (Figure 2). Therefore the tetrachlorocuprate anions are connected *via* a unique parallel bibridged unit, distinctive in that both bridging chloropyridinium cations are connected to one anion *via* C-Cl···Cl^- contacts and to the other one *via* N-H···Cl^- hydrogen bonds (Scheme 2a). This is in contrast to the bibridged unit observed in $(2BP)_2CuX_4$ which has the more common antiparallel arrangement.[10a] Within that unit, the cations are related by center of inversion so that one of the cations is connected to a tetrahalocuprate anion *via* a N-H···X^- hydrogen bond while the other is connected *via* C-Br···X^- contacts. This type of connection is observed in 3CP-Cl and 4CP-Cl (Scheme 2c and 2b respectively) as well as in 4CP-Br and their isomorphic structures - $(3BP)_2CuCl_4$ and $(4BP)_2CuBr_4$.[10a] The bibridged unit of 3CP-Cl is topologically different from that of 2CP-Cl and 4CP-Cl, in that one of the chloride anions is not involved in synthon formation (Scheme 2c).

Scheme 2. A schematic representation of the extended networks developed based on C-Cl···X^- and N-H···X^- synthons in $(n\text{CP})_2\text{CuX}_4$ crystal structures. The tetrachlorocuprate anion $(\text{CuX}_4)^{2-}$ and the chloropyridinium cation are designated by X and N-Cl respectively. The C-Cl···X^- synthon is represented by a solid line, while the hydrogen bonds N-H···X^- (either linear or bifurcated) are denoted by dotted lines (the lighter one denoted the weaker half of the asymmetric hydrogen bond).

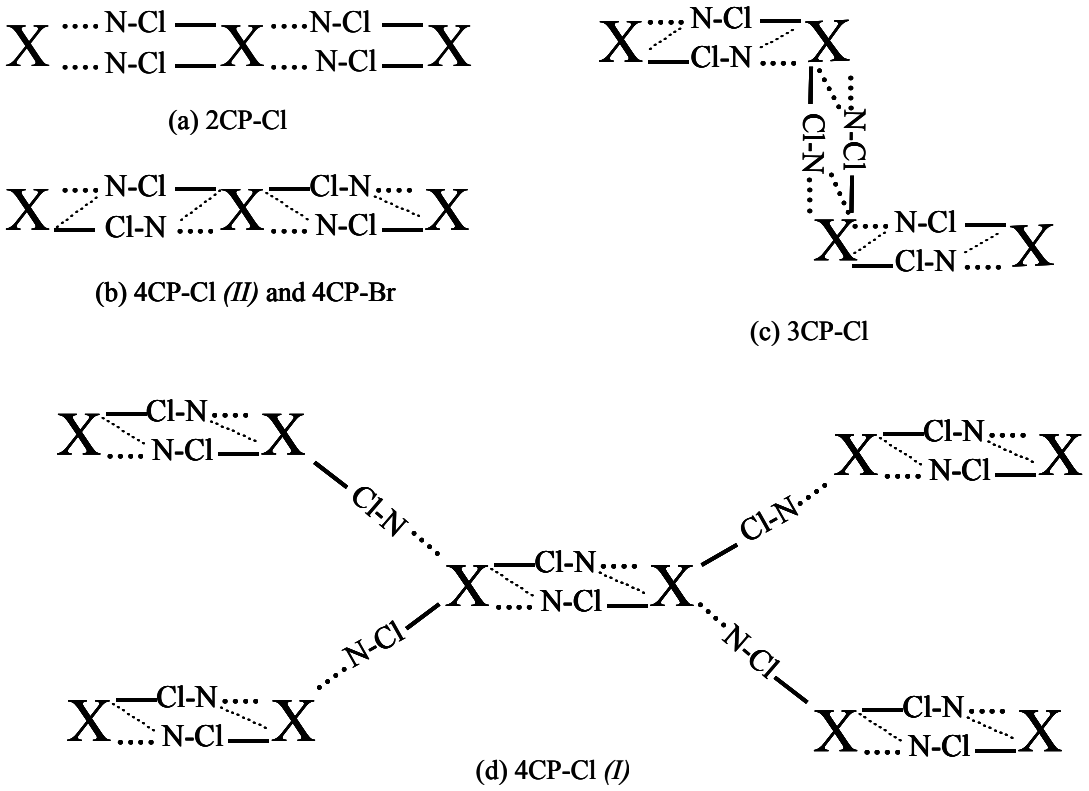

In the chain network structure of 2CP-Cl, the chains run parallel to the *c* axis (Figure 2). The presence of the chlorine atom at position 2 leads to more open chain structure and a more acute Cu – ($n\text{CP}^+$) – Cu angle, which results in a relatively short distance between the copper centers within the chain, 7.3 Å, while these separation distances are ~ 12.3 Å in the other two chains structures (3CP-Cl and 4CP-Cl(II)). This also leads to the absence of the bifurcated

hydrogen bond. In contrast, due to geometric nature of the $4CP^+$ cation compared to the $2CP^+$ cation, the two $4CP^+$ bibridged cations are involved in an asymmetric bifurcated hydrogen bond and the two cations are stacked within the chains. Thus the 4CP-Cl(II) chain forms a more compact structure. In the chain structure of 4CP-Cl(II), the exterior chloride anions are involved in the C-Cl···Cl^- contacts and the interior anions are involved in the bifurcated hydrogen bond, producing a zigzag chain structure that runs parallel to (1 0 –1) (Figure 3). The 3CP-Cl structure is different from 4CP-Cl(II) and 2CP-Cl, in that the two chloropyrdinium cations within the molecular unit are not related by symmetry. Thus, there are two different bibridged units; each bibridged unit is composed from two chloropyridinium cations related by an inversion center (Figure 4). Each cation is involved in a relatively short C-Cl···Cl^- contact and a bifurcated hydrogen bond; cation 1 is involved in an asymmetric hydrogen bond while cation 2 is involved in symmetric bifurcated hydrogen bond. These chains run parallel to the (1 1 –1) direction (Figure 4). Examination of Figure 4 shows that the environment around each chloride ion is different.

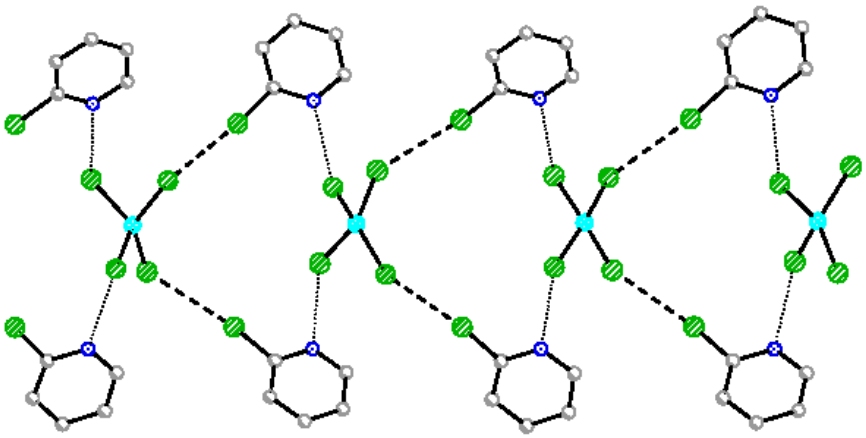

Figure 2. Chain network in 2CP-Cl, showing the C-Cl···Cl^- and N-H···Cl^- synthonic interactions. The chains run parallel to the *c* axis.

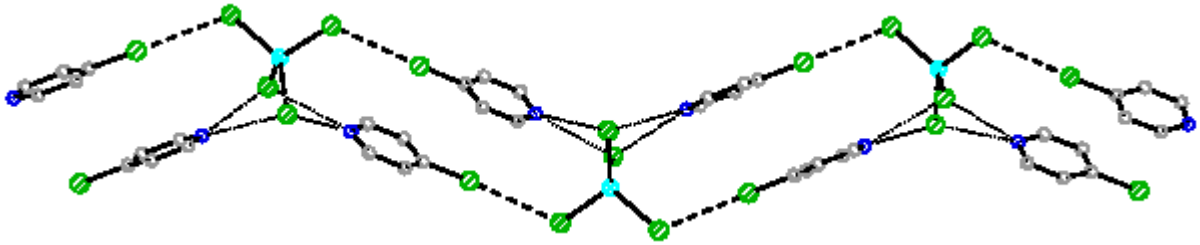

Figure 3. Chain network in 4CP-Cl(II), showing the C-Cl···Cl^- and N-H···Cl^- synthonic interactions. The chains run parallel to (1 0 –1) direction.

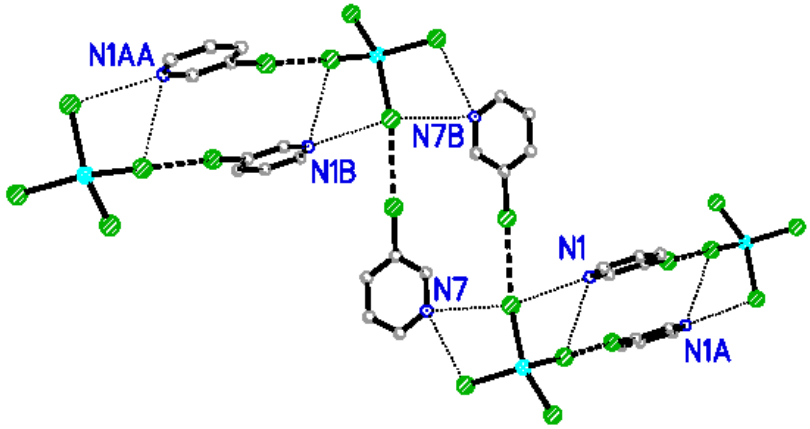

Figure 4. Chain network in 3CP-Cl.

4CP-Cl(I) crystallizes as two different polymorphs. The $P2_1/c$ phase forms a two dimensional layer structure isomorphous with $(4BP)_2CuBr_4$ (Scheme 2d and Figure 5), while the $C2/c$ forms a chain structure isomorphous with $(4BP)_2CuCl_4$. In both phases a dimer of copper centers is formed based on a similar bibridged unit. In 4CP-Cl(I), these dimers are linked *via* a monobridged unit, using almost linear N-H···Cl^- hydrogen bonds and C-Cl···Cl^- contacts to form two dimensional layer structure (Figure 5). Rotating one of the monobridged units, cation 2, 90° around the Cu-Cl bond axis converts the two monobridged units to a bibridged unit (Figure 6), and produces a chain structure analogous to that of 4CP-Cl(II). In contrast to the bibridged unit, in the monobridged unit, the N-H···Cl^- synthon exhibits a relatively short linear hydrogen bond. Also, the chlorine···chloride distance is quite large,

almost equal to the sum of r_{vdW} (3.511 Å). This reflects the competition between the hydrogen bond and chlorine···chloride synthon. It can also be a sign of the weakness of the C-Cl···Cl^- synthon compared to the N-H···Cl^- hydrogen bond but other packing interactions and C-H···Cl^- hydrogen bonding cannot be ignored.

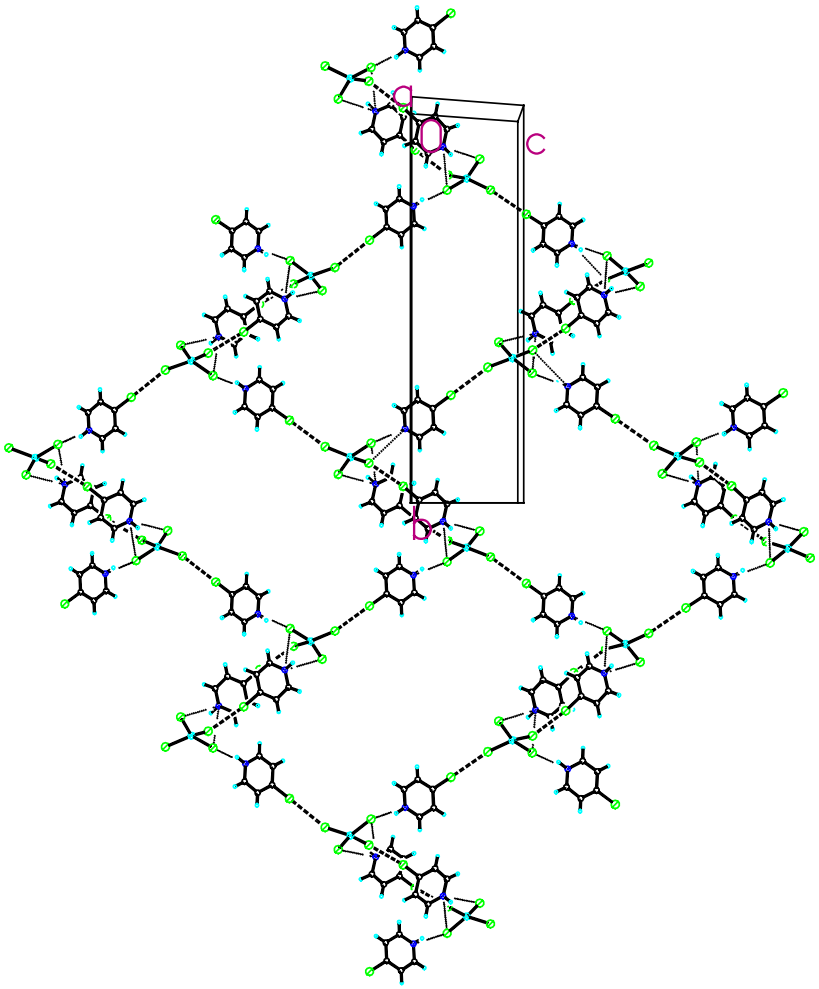

Figure 5. Layer structure of 4CP-Cl(I), showing the both monobridged and bibridged [$CuCl_4^{2-}$ - $(4CP^+)_n$ - $CuCl_4^{2-}$] synthonic interactions. The layers lie in (–3 0 2) plane.

(b) $(nCP)_2CuBr_4$.

The role of C-Cl···X^- contacts is less obvious in the structure of the $(nCP)_2CuBr_4$ salts. In these three structures, there are five crystallographically different chloropyridinium cations. Only two of them are involved in C-Cl···Br^- contacts within the sum of r_{vdW} (3CP-Br.H_2O and 4CP-Br), and one of the structures contains a water of crystallization molecule. However, the N-H···Br^- synthon exists in all of the structures with one exception, cation 2 in 3CP-Br.H_2O, where a N-H···O hydrogen bond is formed. This reveals the weakness of C-Cl···Br^- contacts with respect to the N-H···Br^- hydrogen bond as well as to other strong hydrogen bonding interactions.

Because of the apparent weakness of the C-Cl···Br^- contacts (relative to the C-Cl···Cl^- or C-Br···Br^- contacts) there are few systematics in the nCP-Br structures. In 2CP-Br, the 2-chloropyridinium cations are linked to the copper center *via* N-H···Br^- hydrogen bonds (Figure 1e). There are no chlorine···bromide contacts within the sum of r_{vdW}; the shortest Cl···Br^- distance equals 3.621 Å with an anomalous C-Cl···Br^- angle (88°). These monomers aggregate *via* packing interactions and C-H···Br^- hydrogen bonds, to form the three-dimensional structure. In 3CP-Br.H_2O, two copper centers dimerize based on a combination of N-H···Br^- and C-Cl···Br^- contacts (Figure 7). These dimers interact *via* O-H···Br^- hydrogen bonds and N-Br^- synthons (*vide infra*) to form a ladder structure (Figure 7), both cations are involved in N-Br^- synthons (Scheme 4e and 4f). The crystal structure of 4CP-Br is isomorphous to 4CP-Cl(II). Even though the two structures are isomorphous, there are significant differences in the N-H···X^- and C-Cl···X^- synthon parameters. The Cl···Cl^- and Cl···Br^- distances are 0.117 Å and 0.069 Å less than the sum of the r_{vdW} and the C-Cl···X^- angle is closer to linear a in the chloride salt. In addition, the N-H···X^- hydrogen bond is closer to symmetric bifurcated arrangement in the case of 4CP-Br when compared to 4CP-Cl(II); the

difference in N···X$^-$ distances between the two legs of the asymmetric hydrogen bond are 0.30 Å and 0.16 Å for the chloride and the bromide salt respectively. These structural differences would give indications about the relative strength of these synthons and hence their importance, the chlorine···bromide synthon is weaker than the chlorine···chloride synthon.

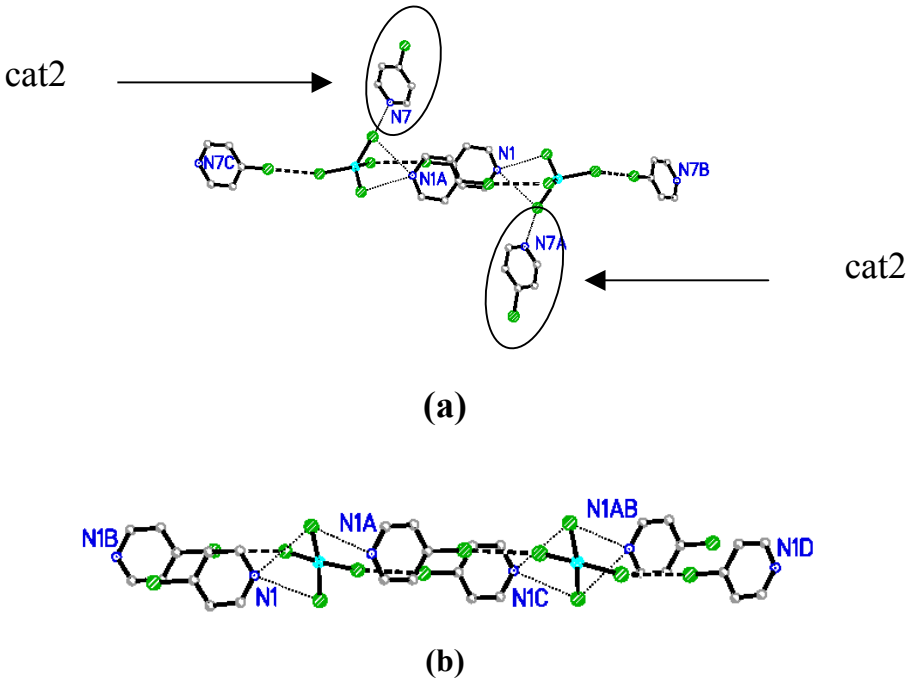

Figure 6. The connection between the bibridged copper dimer centers in 4CP-Cl polymorphs. (a) 4CP-Cl(I); (b) 4CP-Cl(II).

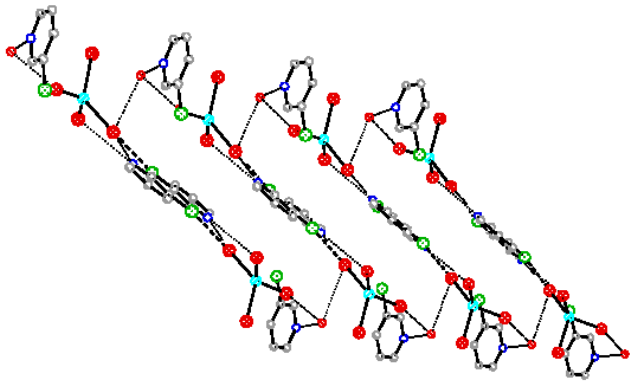

Figure 7. Ladder structure of $(3CP)_2CuBr_4.H_2O$, showing N-H···Br$^-$, N-H···O and C-Cl···Br$^-$ synthonic interactions. The ladders run parallel to *b* axis.

Packing Interactions and Final Structure.

The chains, ribbons and layer described in the previous section interact *via* three different types of packing interactions. These packing synthons are illustrated in Schemes 3 and 4. Table 3 lists these stacking interactions.

(a) π-π stacking. Of all of the studied structures, π-π overlap is only observed in two cases (3CP-Cl and 2CP-Br).

(b) The nitrogen-halide ion synthon, which is the interaction between the nitrogen atom and the halide anion that is located above the plane of the pyridinium cation. This synthon exists in all of the structures except 2CP-Cl (Scheme 4).

(c) The nitrogen-chlorine synthon, defined as the interaction between the nitrogen atom and the chlorine atom that is located above it. This synthon exists in all salts except 3CP-Cl.

In all of the *n*CP-X systems, π-π overlap is either very small or absent as the halogen···halide interaction is a preferential synthon. For significant chlorine···halide contacts, there is only one π-π overlap example, 3CP-Cl (Scheme 3c and d). In contrast, other stacking interactions are present almost in all of them. This indicates that the π-π overlaps only exist serendipitously. For 2CP-Br, where the chlorine···halide contacts are absent, both crystallographically different cations are involved in π-π overlap (Scheme 3h). The structures of $(n\text{MP})_2\text{CuX}_4$ depend on π-π overlap to develop the supramolecular architecture since no halogen···halide interactions can exist.[17a].

In the case of 2CP-Cl, where the chloropyridinium cations are accessible due to the fact that chloropyridinium cations protrude from the chains. The nitrogen-chlorine synthons and C-H···Cl^- hydrogen bonding help adjacent chains to interdigitate (Scheme 3b and Figure 1S), effectively locking the chains together. Three of the crystal structures, 3CP-Cl, 4CP-Cl(II) and

4CP-Br, pack in a similar pattern. The chain structures, which are developed *via* the C-Cl···X^- synthons and N-H···X^- hydrogen bonds, are stacked to form layer structures, based on the nitrogen-halide synthon. These layers interact *via* C-H···X^- hydrogen bonds, with the result that the tetrahalocuprate anions lie between pairs of bibridged units. In the 3CP-Cl structure, the nitrogen atoms of cation 2 interact with the tetrahalocuprate anions based on nitrogen-halide synthons (Scheme 4a and Figure 2S) to form layers. These layers interact *via* C-H···Cl^- synthons to form the three-dimensional structure (Figure 2Sb). In the compact zigzag network structure of 4CP-Cl(II) and 4CP-Br, the nitrogen-chloride synthons tie the chains together into sheets (Scheme 4d and Figure 3S). These layers aggregate to form the three-dimensional structure *via* weak C-H···Cl^- hydrogen bond between the layers. Thus, each tetrahalocuprate anion from one chain is between two bibridged units from the adjacent two layers (Figure 10).

The perforated layers of 4CP-Cl(I) stack based on the same synthons observed in 4CP-Cl(II). Both cations are involved in nitrogen-chloride synthon; three of these perforated layers interact *via* N-Cl synthon, using the monobridged unit, cation 2. This packing develops an undulating layer structure, similar to the perforated layers, they lie in the (3 0 –2) plane (Scheme 3f and ref. 10a); these layers stack atop each other *via* N-Cl^- synthon along *a* direction (Scheme 4b), the both crystallographically different cations, the monobridged and bibridged units, are involved in this synthonic interaction. Also, C-H···Cl^- hydrogen bonds cooperate with the nitrogen-chloride synthons in developing the three dimensional structure.

The C-H···X^- synthons play a dominant role in structures in the tetrabromocuprate salts where the C-Cl···X^- interaction is weak or absent. The crystal structure of 2CP-Br is developed based on the C-H···Br^- hydrogen bond and other packing interactions and there are

no chlorine···bromide contacts within the sum of the r_{vdW}. An extended chain network structure runs parallel to the *c* axis which is formed *via* C-H···Cl^- hydrogen bonds and nitrogen-halide synthons (Scheme 4e and Figure 4Sa). These chains aggregate *via* a bifurcated C-H···X^- hydrogen bond to form a layer structure in the *bc* plane (Figure 4Sb). A double layer structure is formed based on the nitrogen-chlorine synthons (Scheme 3i and Figure 5S). Even though there are no Cl···Br^- distances within the sum of the r_{vdW}, these synthons cooperate with the π-π stacking in packing these double layers to the final crystal structure (Figure 5S). The shortest Cl···Br^- distances observed in 2CP-Br, only one of the C-Cl···Br^- angles is in a suitable arrangement for a linear C-Cl···X^- contact (Table 3). In the ladder structure of 3CP-Br.H_2O, C-H···Br^- hydrogen bonds tie the ladders into the three-dimensional structure (Figure 6S).

DISCUSSION

The results of this study show that the role of C-Cl···X^- synthons is obvious and dominant when X = Cl^-. In contrast, it is weaker or absent in some cases when X = Br^-. All of the chloropyridinium cations in the tetrachlorocuprate salts are involved in chlorine···chloride distances within the sum of their r_{vdW}. In the tetrabromocuprate salts it is quite the opposite, only two out five crystallographically different cations are involved in C-Cl···Br^- contacts. Even in the two isomorphous structures, 4CP-Cl(II) and 4CP-Br, the chlorine···chloride distance is 0.117Å less than the sum of the r_{vdW}, while the analogous chlorine···bromide distance is 0.069 Å less. This would indicate that C-Cl···Cl^- synthon is stronger than the C-Cl···Br^- synthon.

Scheme 3. Illustration of π-π stacking for cations and nitrogen-chlorine synthons. Views are from the normal to the planes of the cations. The dashed lines denote for the centroid-centroid connections for the closest two cations inside the crystal.

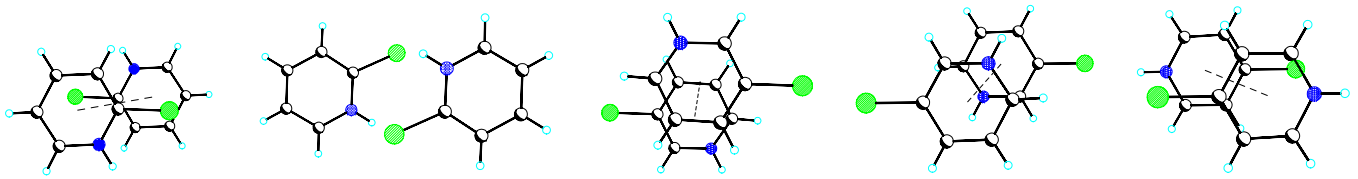

(a) 2CP-Cl-cat1 (b) 2CP-Cl cat2 (c) 3CP-Cl-cat1 (d) 3CP-cat2 (e) 4CP-Cl(I) cat1

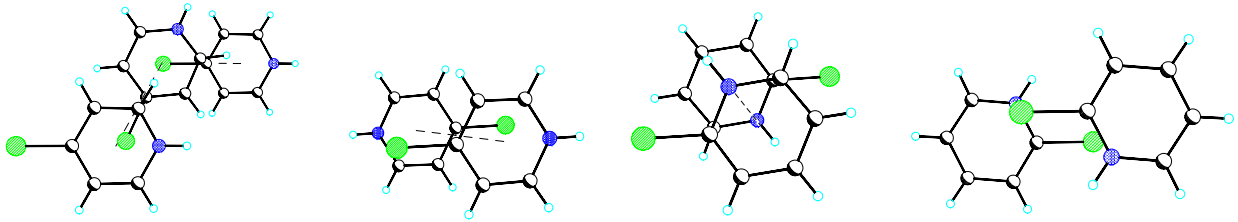

(f) 4CP-Cl(I) cat2 (g) 4CP-Cl(II) (h) 2CP-Br-cat1 (i) 2CP-Br-cat2

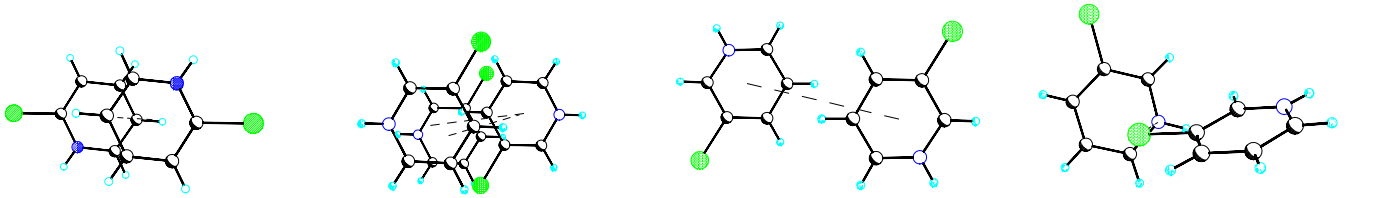

(j) 2CP-Br-cat2 (k) 3CP-Br cat1 (l) 3CP-Br cat2 (m) 3CP-Br cat1 and cat2

Table 4. Packing interactions parameters.

Compound	cation	$d_{\perp}$ (Å)[a]	d_{c-c}(Å)[b]	Φ (º)[c]	d_{Cl-N}[d]	Θ (º)[e]	d_{X-N}[f]	Θ'(º)[g]
2CP-Cl		3.531	4.463	37.71	4.031	28.90		
					3.792	26.20		
3CP-Cl	1	3.504	3.685	18.02				
	2	3.522	3.887	25.02			3.704	7.76
4CP-Cl(I)	1	3.504	4.059	30.31	3.574	12.66	3.452	20.92
	2	3.464	4.634	41.62	3.658	18.97	3.773	22.30
4CP-Cl(II)		3.474	4.433	38.39	3.627	17.33	3.641	25.48
2CP-Br	1	3.490	3.777	22.47			3.578	17.79
	2	3.452	3.868	26.83	3.421	6.01		
3CP-Br.H_2O	1	3.546	4.683	40.78			3.516	10.62
		3.414	4.673	43.06			3.608	13.76
	2	3.090	5.827	57.98	3.527	8.20	3.752	18.84
4CP-Br		3.495	4.460	38.42	3.687	18.50	3.700	21.54

[a] The perpendicular distance between the planes of two adjacent cations.

[b] The centroid- centroid distance between the adjacent pyridinium cations.

[c] The angle between the line connecting the two centroids and the normal to the plane of the cation.

[d] The distance from the nitrogen atom to the chlorine atom of the adjacent cation.

[e] The angle between the N-Cl line between cations and the normal to the plane of pyridinium cation.

[f] The out-of-plane $N-X^-$ distance from the nitrogen atom to the halide anion.

[g] The angle between the $N-X^-$ line and the normal to the plane of the pyridinium cation.

Scheme 4. Illustration of nitrogen-halide interactions. Views normal to the plane of the cations. The dashed lines denote for the nitrogen-halide connections.

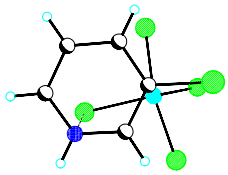

(a) 3CP-Cl-cat2

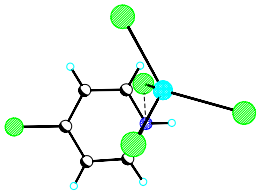

(b) 4CP-Cl(I)- cat1

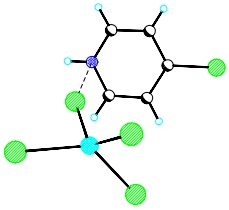

(c) 4CP-Cl(I)-cat2

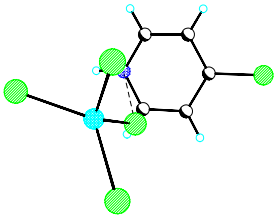

(d) 4CP-Cl(II)

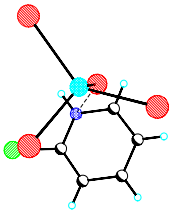

(e) 2CP-Br cat1

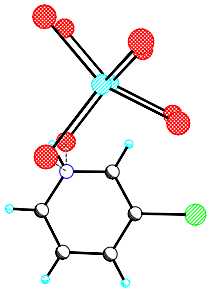

(e) 3CP-Br cat1

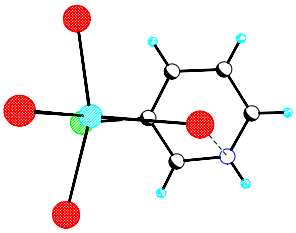

(f) 3CP-Br cat2

The studied structures show that there is a competition between the C-Cl···X^- synthon and N-H···X^- synthon. Three different N-H···X^- hydrogen bond patterns are observed in these structures (linear, asymmetric bifurcated and symmetric bifurcated). In contrast, only two types of hydrogen bond are observed in the analogous methyl structures (linear and symmetric bifurcated). This would indicate that the presence of the C-Cl···Cl^- contacts perturbed the symmetric bifurcated hydrogen bond. This competition can even be seen within the structures of the $(n\text{CP})_2\text{CuX}_4$ compounds. As it has been shown in the previous paragraph, the chlorine···chloride synthon is stronger than the chlorine···bromide synthon. Therefore, in the two isomorphic structures, 4CP-Cl(II) and 4CP-Br, the difference in the length of the two legs of the bifurcated N-H···X^- hydrogen bond is larger in the case of the 4CP-Cl(II) (Table 3).

In our previous study involving the copper halide salts of the *n*-bromopyridinium cations (nBP^+) , it was found that the C-Br···X^- synthon exists in all $(nBP)_2CuBr_4$ structures.[10a] Moreover, the Br···X^- distance is 0.3-0.4 Å less than the sum of the r_{vdW}. In contrast, even in the cases where the chlorine···halide contacts exist, the Cl···X^- distance is only 0-0.24 Å less than the sum of r_{vdW}. This clearly indicates that the C-Br···X^- interaction is stronger than the C-Cl···X^- interaction. Studying the competition between the N-H···X^- hydrogen bonds and the C-Y···X^- interactions in the isomorphic structures in the two structural series strengthens this argument. Three pairs of structures, 3CP-Cl and 3BP-Cl; 4CP-Br and 4BP-Br; 4CP-Cl(I) and 4BP-Cl, are isomorphic structures. Only two pairs of these can be used for the sake of comparison, since the crystal structures of the first pair were not determined at the same temperature. In the second pair, the difference in the length of the two legs of the asymmetric hydrogen bond is 0.12 Å in the former and in the later 0.19 Å. These differences in the last isomorphic pair are 0.27 Å and 0.31 Å for 4CP-Cl and 4BP-Cl respectively. Thus, the bromine···halide synthons distorted the symmetric arrangement of the bifurcated N-H···X^- hydrogen bonds more than chlorine···halide synthons. This again indicates that C-Br ···X^- interaction is stronger than the C-Cl···X^- interaction.

In addition, the chloro-methyl exchange rule predicts that the π-π stacking interactions should play a significant role in developing the $(nCP)_2CuX_4$ structures,[17b] since in the analogous *n*-methyl-pyridinium cation salts $(nMP)_2CuX_4$, it was the π-π stacking interactions which complimented the N-H···X^- hydrogen bonds. In contrast, in the $(nCP)_2CuX_4$ structures, significant π-π overlap is only observed in two cases, 3CP-Cl and 2CP-Br. Therefore, the presence of the C-Cl···X^- synthons causes a perturbation of the structure of the $(nCP)_2CuX_4$ compounds, when compared to the corresponding $(nMP)_2CuX_4$ structures.[17a]

Recently, *ab initio* calculations on iodobenzene and halomethane showed the presence of a positive electrostatic potential cap on the halogen atom.[9b,18] Therefore, the halide anion is expected to confront this positive potential. This explains the linearity of the C-Y···X angle. Moreover, this picture of the halogen atom explains the weakness of the C-Cl···Br^- synthon compared to the C-Cl···Cl^- synthon, since the charge is more condensed in the case of chloride anion. This behavior is in clear contrast with the charge transfer or donor acceptor idea of interaction,[19] and points to the importance of the electrostatic effects. This agrees with our *ab initio* calculations that show the strength of the C-Cl···X^- interactions increase in the order $I^- < Br^- < Cl^- < F^-$.[18] Also most recently, Zordan *et al.* showed that the electrostatic forces play a substantial role in the physical nature of the C-Y···Cl-M synthons (M = Pt(II) Or Pd(II); Y = F, Cl, Br, I).[10e] Other related intermolecular interactions have been proved to be electrostatic in nature.[20] In this context, Lommerse et al, based on theoretical and crystallographic studies, showed that C-Y···El interaction (Y = F, Cl, Br or I, El = N, O or S) is mainly due to electrostatic factors.[20a] More recently, the electron density map revealed that the interactions I···O and I···N are electrostatic in nature.[20b,c]

CONCLUSIONS

The structures in this study show that the C-Cl···Cl^- synthon plays a significant role in determining the structures of the $(n\text{CP})_2CuCl_4$ salts. The role of C-Cl···Br^- synthons is less obvious in determining the structure of $(n\text{CP})_2CuBr_4$ compounds. Chlorine···chloride contacts exist in all of the $(n\text{CP})_2CuCl_4$ structures. In contrast, only two out of the five crystallographically different chloropyridinium cations are involved in chlorine···bromide contacts within the sum of the r_{vdW}. Comparing the role of these synthons, C-Cl···X^- with the analogous C-Br···X^- synthons in the $(n\text{BP})_2CuX_4$ salts shows that the C-Br···X^- interactions

play a more significant role in determining the extended structure of crystalline materials, as indicated by the number of C-Br···X^- contacts and Br···X^- separation distances. C-Br···X^- contacts exist in all the structures of $(n\text{BP})_2CuX_4$. In contrast, the C-Cl···X^- synthon, specifically C-Cl···Br^-, is absent in $(2CP)_2CuBr_4$. Moreover, the bromine···halide distances are 0.3-0.4 Å less than the sum of the r_{vdW}, and even when chlorine···halide contacts exist, the reduction in the Cl···X^- distances is less than 0.25 Å.

ACKNOWLEDGEMENT: Work supported in part by ACS-PRF 34779-AC. The Bruker (Siemens) SMART CCD diffraction facility was established at the University of Idaho with the assistance of the NSF-EPSCoR program and the M. J. Murdock Charitable Trust, Vancouver, WA, USA.

Supporting Information Available: Crystal data for all the seven compounds in CIF format. This materials are available free of charge *via* the Internet at http://pubs.acs.org. Supplemental Figures S8-S10.

REFERENCES

1. (a) Desiraju, G. R. *Nature* **2001**, *412*, 397-400. (b) Desiraju, G. R. *Crystal Engineering, The Design Of Organic Solids,* Elsevier Science Publishers B. V.: Amsterdam, **1989**. (c) Desiraju, R. G. *Angew. Chem. Int. Ed. Engl.* **1995**, *34*, 2311-2327. (d) Brammer, L. *Chem. Soc. Rev.* **2004**, *33*, 476-489. (e) Metrangolo, P.;Neukirch, H.; Pilati, T.; Resnati, G. *Acc. Chem. Res.* **2005**, *38*,386-395.(f) Braga, D.; Brammer, L.; Champness, N. *CrystEngComm.* **2005**, *7*, 1-19.

2. (a) Yamamoto, H. M.; Yamaura, J.; Kato, R. *J. Am. Chem. Soc.* **1998**, 120(24), 5905-5913 and references therein.

3. (a) Hasegawa. M. *Advances in Physical Organic Chemistry*, Academic Press: London, **1995**; vol. 30, pp 117-171. (b) MacGillivray, L. R.;Reid, J. L.; Ripmeester, J. A. *J. Am. Chem. Soc.* **2000,** 122, 7817-7818. (c) Matsumoto, A.; Tanaka, T.; Tsubouchi, T.; Tashiro, K.; Saragai, S.; Nakamoto Sh. *J. Am. Chem. Soc*. **2002**, *124*, 8891-8902.

4. (a) Aakeröy Ch. B.; Beatty A. M. *Aust. J. Chem.* **2001**, *54*, 409-421. (b) Brammer, L.; Bruton, E. A.; Sherwood, P. *Cryst. Growth Des.* **2001**, *1*, 277-290. (c) Lutz, H. D. *J. Mol. Struct*. **2003**, *646*, 227-236.

5. (a) Sinnokrot, M. O.; Sherrill, D. C. *J. Am. Chem. Soc.* **2004**, *126*, 7690-7697. (b) Sinnokrot, M. O.; Sherrill, D. C. *J. Phys. Chem.* **2003**, *107*, 8377-8379. (c) Sinnokrot, M. O.; Valeev, E. F.; Sherrill, D. C. *J. Am. Chem. Soc.* **2002**, *124*, 10887-10893. (d) Hunter, Ch. A.; Sanders, K. M. *J. Am. Chem. Soc.* **1990**, 112, 5525-5534. (e) Desiraju, G. R.; Gavezzotti, A. *J. Chem. Soc. Chem. Commun.* **1989**, 621-623.

6. (a) Desiraju, G. R.; Parthasarathy, R. *J. Am. Chem. Soc.* **1989**, *111*, 8725-8726. (b) Jagarlapudi, A. R.; Sarma, P.; Desiraju G. *Acc. Chem. Res.* **1986**, 19, 222-228.

7. Price, S. L.; Stone, A. J.; Lucas, J.; Rowland, R. S.; Thornley, A. E. *J. Am. Chem. Soc.* **1994,** *116*, 4910-4918.

8. Bondi, A. *J. Phys. Chem.* **1964**, *68*, 441-451.

9. (a) Desiraju, G.R. *Angew. Chem. Int. Ed. Engl.* **1995**, *34*, 2311-2327. (b) Bosch, E.; Barnes, C. L. *Cryst. Growth Des.* **2002**, *2*, 299-302. (c) Thalladi, V. R.; Brasselet, S.; Weiss, H. C.; Blaser, D.; Katz, A. K.; Carrell, H. L.; Boese, R.; Zyss, J.; Nangia, A.; Desiraju, G. R. *J. Am. Chem. Soc.* **1998**, *120*, 2563-2577. (d) Anthony, A.; Desiraju, G. R.; Jetti, R. K. R.; Kuduva, S. S.; Madhavi, N. N. L.; Nangia, A.; Thaimattam, R.; Thalladi, V. R. *Cryst. Engn. 1, Mater. Res. Bull. Suppl. S.* **1998**, 1-18. (d) Broder, Ch. K.; Howard, A. J.; Wilson, Ch. C.; Allen, F. H.; Jetti, R. K.; Nangia A.; Desiraju, G. R. *Acta. Cryst.* **2000,** *B56*, 1080-1084.

10. (a) Willett, R. D.; Awwadi, F. F.; Butcher, R.; Haddad, S.; Twamley, B. *Cryst. Growth Des.* **2003**, *3*, 301-*311*. (b) Brammer, L.; Espallargas, G. M.; Adams, H. *CrystEngComm.* **2003**, *5(60)*, 343-345. (c) Haddad, S.; Awwadi, F.; Willett, R. D. *Cryst. Growth Des***. 2003**, *3(4),* 501-50. (d) Kuhn, N.; Abu-Rayyan, N. A.; Eichele, K.; Piludu, C.; Steimann, M. *Z. Anorg. Allg. Chem.* **2004**, 630*(4)*, 495-497. (e) Zordan, F.; Brammer, L.; Sherwood, P. *J. Am. Chem. Soc*. **2005**, *127*, 5979-5989.

11. (a) Freytag, M.; Jones, P. G. *Zeit. Naturfor. B: Chem. Sci.* **2001**, *56*, 889-896. (b) Freytag, M.; Jones, P. G.; Ahrens, B.; Fischer, A. K. *New J. Chem*. **1999**, *23*, 1137-1139. (c) Logothetis, Th.; Meyer, F.; Metrangolo, P.; Pilati, T; Resnati, G. *New*

J. Chem. **2004**, *28*, 760-763. (d) Kuhn, N.; Abu-Rayyan A.; Eichele, K.; Schwarz, S.; Steimann, M. *Inorg. Chim. Acta* **2004**, *357(6)*, 1799-1804. (f) Awwadi, F. F.; Willett, R. D.; Twamly, B.; *J. Am. Chem. Soc.* (to be submitted). (g) Awwadi, F. F.; Willett, R. D.; Twamly, B.; *unpublished results.*

12. (a) Domercq, B.; Devic, T.; Fourmigue, M.; Auban-Senzier, P.; Canadell, E. *J. Mater. Chem*. **2001**, *11*, 1570-1575. (b) Farina, A.; Meille, S. V.; Messina, T. M.; Metrangolo, P.; Resnati, G.; Vecchio, G. *Angew. Chem. Int. Ed.* **1999**, *38*, 2433-2436.

13. (a) Willett R. D.; *Mol. Cryst. Liq. Cryst.*, *Sect. A*, **1995**, *233*, 227. (b) Turnbull, M.M.; Albrecht, A.S.; Jameson, G.B.; Landee, C.P. *Mol. Cryst. Liq. Cryst.,* Sect. A. **1999**, *335*, 245. (c) Matsumoto, T.; Miyazaki, Y.; Albrecht, A.S.; Landee, C.P.; Turnbull, M.M.; Sorai, M. *J. Phys. Chem. B*., **2000**, *104*, 9993. (d) Blanchette, J. T.; Willett, R. D. *Inorg. Chem.* **1988**, *27*, 843. (e) Rubenacker, G. V.; Waplak, S.; Hutton, S. L.; Haines, D. N.; Drumheller, J. E. *J. Appl. Phys.***1985,** *57*, 3341. (f) Snivley, L. O.; Seifert, P. L.; Emerson, K.; Drumheller, J. E. *Phys. Rev. B,* 1**979**, *20*, 2101. (g) Snivley, L. O.; Tuthill, G.; Drumheller, J. E.. *Phys. Rev. B,* **1981,** *24*, 5349-5355.

14. XSCANS, Siemen Analytical X-ray Instrument, Inc., Version 2.2, Madison, WI, USA.

15. (a)SMART: v.5.626, Bruker Molecular Analysis Research Tool, Bruker AXS, Madison, WI, **2002**. (b) SAINTPlus: v. 6.36a, Data Reduction and Correction Program, Bruker AXS, Madison, WI, **2001**. (c) SADABS: v.2.01, an empirical absorption correction program, Bruker AXS Inc., Madison, WI, **2001**.(d) SHELXTL: v. 6.10, Structure Determination Software Suite, Sheldrick, G.M., Bruker AXS Inc., Madison, WI, **2001**.

16. Halvorson, K. E.; Patterson, C.; Willett, R. D. *Acta Cryst*., **1990**, *B56*, 508-519.

17. (a) Luque, A.; Sertucha, J.; Casillo, O.; Roman, P.; *New J. Chem*. **2001**, *25,* 1208. (b) Desiraju, G. R.; Sarma, R. P. *Proc. Indian Acad. Sci. (Chem. Sci).,* **1986**, *96*, 599-605.

18. Awwadi, F. F. ; Peterson, K ; Willett, R. D. *J. Am. Chem. Soc.* (to be submitted)

19. Ramasubbu, N.; Parthasarathy, R.; Murray-Rust, P. *J. Am. Chem. Soc.* **1986**, *108*, 4308-4314.

20. Lommerse, J. P.; Stone, A. J.; Taylor, R.; Allen, F. H. *J. Am. Chem. Soc.* **1996**, *118*, 3108-3116. (b) Bianchi, R.; Forni, A.; Pilati, T. *Acta Cryst.* **2004**, *B60*, 559-568. (c) Bianchi, R.; Forni, A.; Pilati, T. *Chem. Eur. J.*, **2003**, *9*, 1631-1638.

SYNOPSIS

The Aryl Chlorine-Halide Ion Synthon and Its Role in the Control of the Crystal Structures of Tetrahalocuprate(II) Ions.

Firas F. Awwadi, Roger D. Willett and Brendan Twamley

Crystallographic studies show that The $Cl\cdots Cl^-$ interaction is stronger than $Cl\cdots Br^-$ interactions, which can be explained based on an electrostatic model. The chain structure of $(2CP)_2CuCl_4$ (2CP = 2-chloropyridinium cation) in (a) is extended *via* hydrogen bonds and $Cl\cdots Cl^-$ interactions. In contrast, the $Cl\cdots Br^-$ synthon in (b) is absent in $(2CP)_2CuBr_4$.

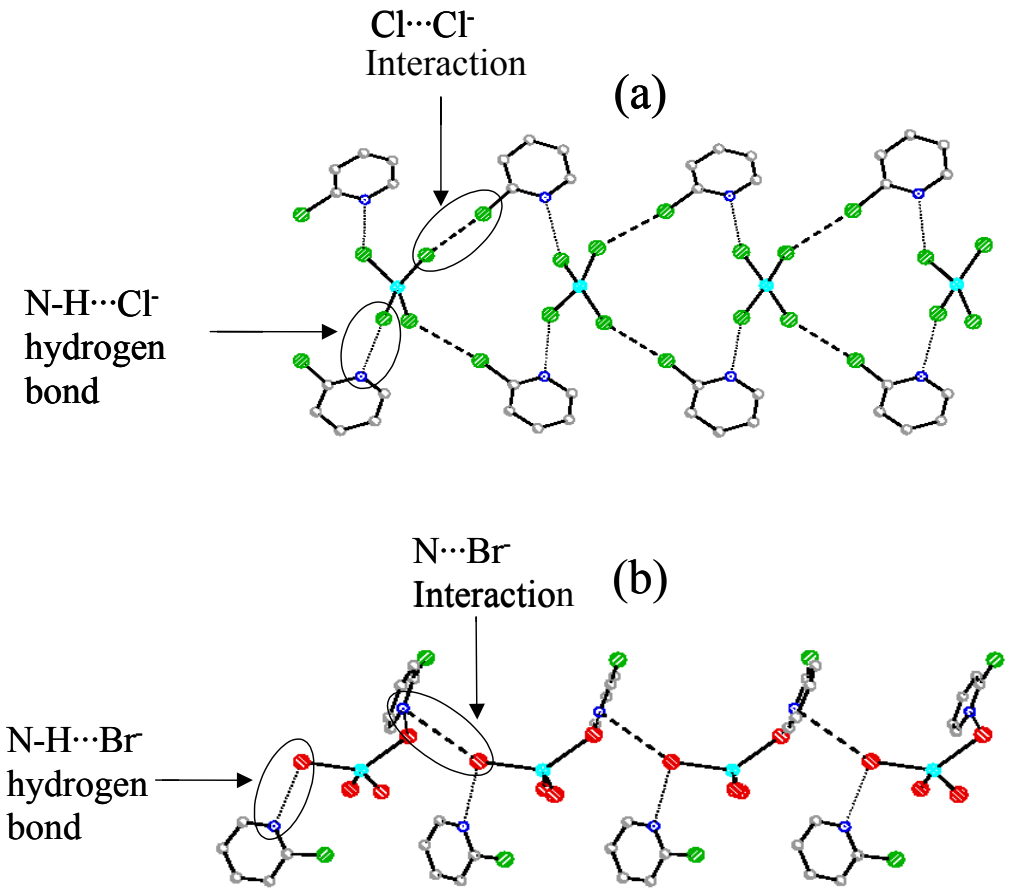

SUPPORTING INFORMATION

The Aryl Chlorine-Halide Ion Synthon and Its Role in the Control of the Crystal Structures of Tetrahalocuprate(II) Ions.

Firas F. Awwadi,[†] *Roger D. Willett*[†,*] *and Brendan Twamley*[‡]

[†]Department of Chemistry, Washington State University, Pullman, WA 99164 USA

[‡]University Research Office, University of Idaho, Moscow, ID 83844 USA

*Department of Chemistry, Washington State University, Pullman, WA 99164, USA, Tel (Office), 509 335 3925, FAX (dept.) 509 335 8867, E-mail rdw@mail.wsu.edu

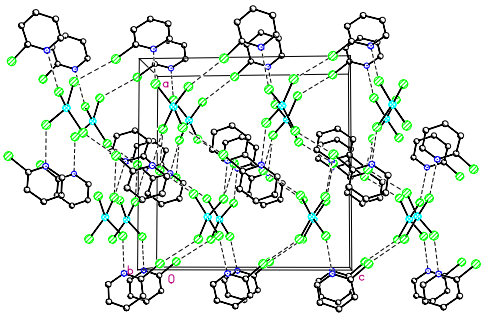

Figure 1S. The three-dimensional structure of 2CP-Cl.

(a)

Nitrogen-chloride synthon

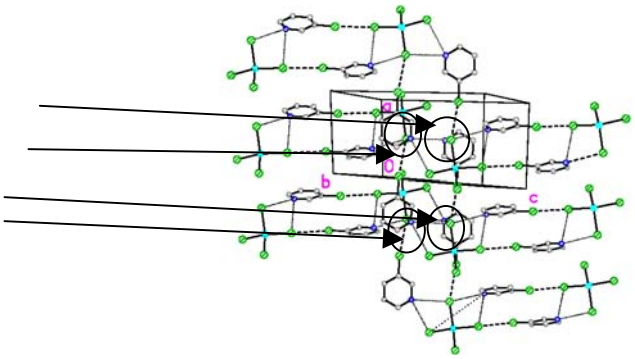

(b)

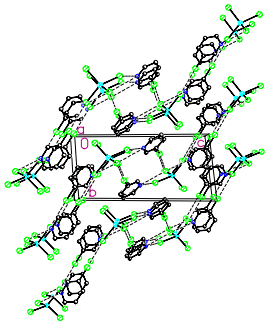

Figure 2S. (a) The layer structure of 3CP-Cl, the layer is located in 0 1 1 plane. The chains aggregate based on N···Cl^- synthons. (b) The layers aggregate to form the three-dimensional structure based on C-H···X^- hydrogen bonds. The view is parallel to the *a* axis.

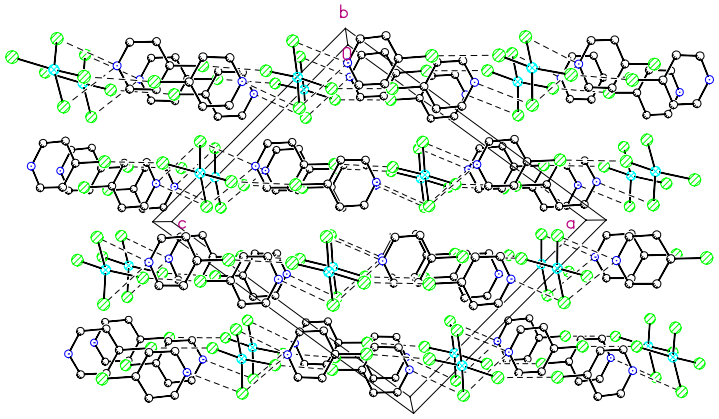

Figure 3S. Three-dimensional structure of 4CP-Cl(II).

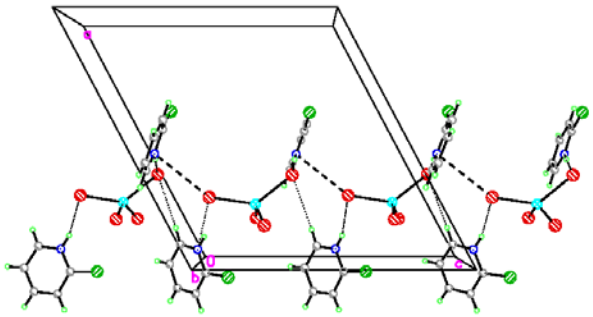

(a)

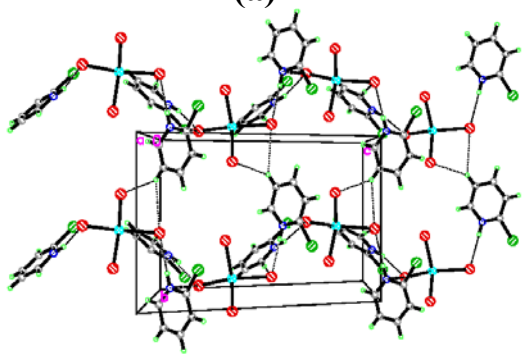

(b)

Figure 4S. (a) The chain network in 2CP-Br, showing the C-H···Br^- hydrogen bonds and nitrogen-bromide synthons. (b) The layer structure in 2CP-Br. The hydrogen bonds and nitrogen-bromide synthons are represented by dotted and dashed lines respectively

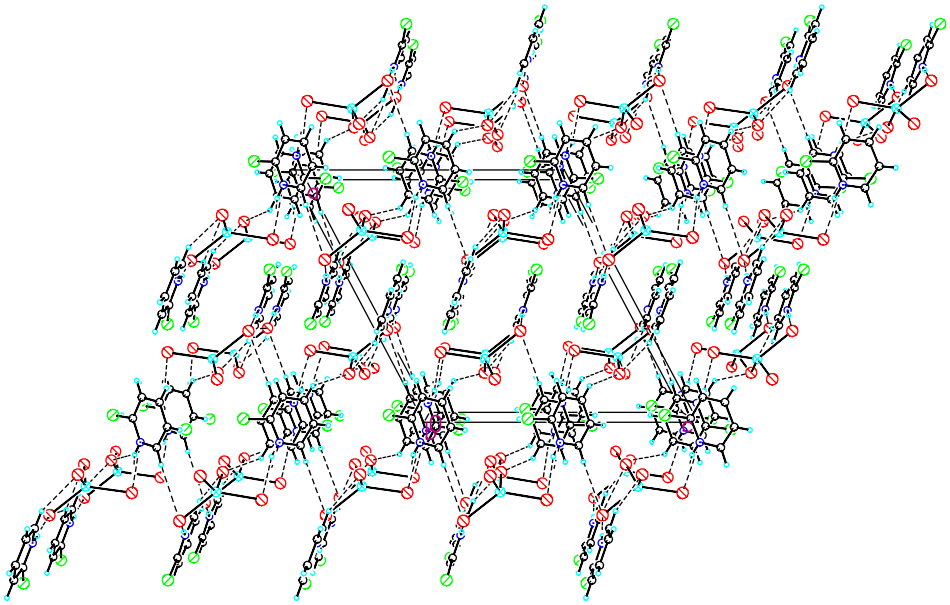

Figure 5S. Illustration of the stacking of the layers in 2CP-Br.

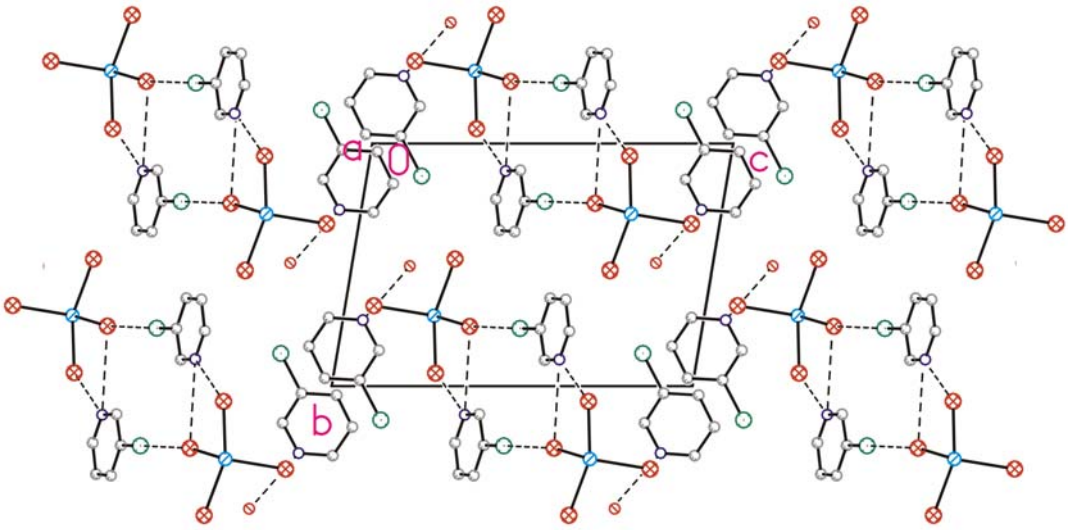

Figure 6S. The three-dimensional structure of $(3CP)_2CuBr_4.H_2O$. The structure viewed parallel to the *a* axis from infinity. The hydrogen atoms are omitted for clarity.

CHAPTER FIVE

The Electrostatic Nature of Aryl-Bromine-Halide Synthons: The Role Of Aryl-Bromine-Halide Synthons in the Crystal Structures of the Trans-bis(2-bromopyridine)dihalocopper(II) and Trans-bis(3-bromopyridine)dihalocopper(II) Complexes.

Firas F. Awwadi[†], Roger D. Willett[†,], Salim F. Haddad[‡]*

and Brendan Twamley[§]

[†]Department of Chemistry, Washington State University, Pullman, WA 99164 USA.

[‡]Department of Chemistry, University of Jordan, Amman 11942, Jordan.

[§]University Research Office, University of Idaho, Moscow, ID 83844 USA.

* rdw@mail.wsu.edu

ABSTRACT The role of C-Br···X synthons in the structures of Cu(*n*bp)$_2$X$_2$, (*n*bp = *n*-bromopyridine; *n* = 2 and 3), are investigated. A comparison of the role of these synthons in these and in the previously published (*n*BP)$_2$CuX$_4$ and (*n*BP)X structures (*n*BP = *n*-bromopyridinium cations; X = Br^- or Cl^-; *n* = 2, 3 or 4) indicate that electrostatic effects - the positive charge on the bromopyridinium cation and the negative charge on the halide anion - play a major role in the strength, and directionality, of C-Br···X synthons. The data indicates that the C-Br···X synthons are stronger in the (*n*BP)$_2$CuX$_4$ and (*n*BP)X salts compared to the Cu(*n*bp)$_2$X$_2$ compounds. The supramolecular assembly of these Cu(*n*bp)$_2$X$_2$ complexes, is dominated by non-traditional C-Br···X synthons and Cu···X semi-coordinate bonds. The bromine-halide distances are almost equal to the sum of their van der Waals radii (r_{vdW}) in Cu(3bp)$_2$X$_2$ but less than the sum of the r_{vdW} by ~0.24 Å in Cu(2bp)$_2$X$_2$. The C-Br···X angles are close to linear, ranging from 158.15(8)° to 167.90(8)° for Cu(3bp)$_2$Cl$_2$ and Cu(2bp)$_2$Cl$_2$ respectively. The Cu(2bp)$_2$X$_2$ units form chain structures based on the C-Br···X synthons. These chains interact *via* C-H···X and π-π stacking to form the three dimensional structure. In contrast, the chain structures in Cu(3bp)$_2$X$_2$ compounds are based on the Cu···X semi-coordinate bond. These chains interact *via* C-Br···X synthons to form the three dimensional structure.

INTRODUCTION

Intermolecular forces have received much interest in the recent years due to their importance in determining the three dimensional structure of many important molecules e.g. proteins, DNA, enzyme-substrate complexes, and their possible use in designing new materials.[1] These forces range from strong forces like classical hydrogen bonds,[2,1b] to weaker ones like halogen bonds,[3] non-classical hydrogen bonds,[4] halogen···halogen interactions[5] and π-π stacking.[6]

Halogen···halide synthons of the type $(R\text{-}Y)^{+}\cdots X^{-}$ (X and Y = Cl, Br or I) have not been studied in as much detail as the traditional halogen···halogen synthons R-Y···Y-R. It has been found that these synthons (halogen···halide synthons) are characterized by nearly linear $C\text{-}Y\cdots X^{-}$ arrangements with $Y\cdots X^{-}$ distances significantly less than the sum of the van cer Waals radius r_{vdW} of the halogen atom and the ionic radius of the halide anion.[7] These synthons, referred to as charge assisted halogen···halide interactions, play an important role in the crystal structure of halogenated pyridinium salts and other crystal structures.[7,8] For example, chlorine···chloride interactions stabilize the structure of diphenyldichlorophosphonium trichloride-chlorine solvate mixture, with the presence of several short chlorine···chloride distances (ranging from 3.171-3.300 Å).[9] We and others have found that the arylbromine-halide ion synthons play a crucial role in determining the crystal structure of tetrahalometallate(II) ions.[10a,b,c] Domercq *et al.* used these synthons to develop organic based conducting materials.[11a] In another study, Farina *et al.* used the bromine···bromide synthon for the resolution of racemic 1,2-dibromohexafluoropropane.[15b] More recently, we have also found that the bromine-metal bromide synthons, along with hydrogen bonding interactions, could be used to dissect the infinite bibridged chains in cupric

bromide into decamers of ($Cu_{10}Br_{22}^{2-}$) stoichiometry,[10c] the longest known copper halide oligomeric species.

Very recently, Zordan *et al.* have shown that the attractive electrostatic effects play a dominant role in controlling the M-X···X`-C synthons.[10d] In this paper, we are proposing an electrostatic model to describe the physical nature of these synthons based on investigation of Cambridge Structural Data Base (CSD), the previously published (nBP)$_2$CuX$_4$ and (nBP)X crystal structures and the Cu($n$bp)$_2$X$_2$ structures reported in this paper, (nBP= n-bromopyridinium, $n$bp = bromopyridine, n = 2, 3 or 4 and X^- = Br^- or Cl^-). Several studies have shown that the bromine-halide synthons are strong when the halide anion carries a full negative charge and the bromine atom is attached a positively charged species.[7] Recently, we found that the arylbromine-halide interaction is strong in tetrahalocuprate salts,[10a] even though the halide anion does not carry a full negative charge but is coordinated to a copper(II) anion. To complement these studies, we have undertaken the synthesis and structure determinations of the complexes Cu($n$bp)$_2$X$_2$, with n = 2 or 3. Here, neither the halide anion carries a full negative charge nor is the bromine atom attached directly to a positively charged species. In addition, these structures will help us to study these interactions in the absence of strong hydrogen bonds, which are prevalent in previously studied models.[7,10a,b,c]

EXPERIMENTAL SECTION

Synthesis and Crystal Growth.

(a) Dibromobis(2-bromopyridine)copper(II), Cu(2bp)$_2$Br$_2$. 2 mmol of 2bp were added to1 mmol of $CuBr_2$ dissolved in 20 mL methanol. The mixture was heated for 30 minutes, and the solution left to evaporate slowly. After 2 days, dark brown cubic crystals formed. A crystal of a suitable size was selected and used for X-ray data collection. *(b)*

Bis(2-bromopyridine)dichlorocopper(II), $Cu(2bp)_2Cl_2$. 1 mmol of 2bp was added to 0.5 mmol of $CuCl_2.2H_2O$ dissolved in 30 mL of acetonitrile. The solution was stirred while it was being heated for 30 minutes. The solution was left to slowly evaporate until blue crystals formed. A crystal of a suitable size was selected and used for X-ray data collection. *(c) Dibromobis(3-bromopyridine)copper(II), $Cu(3bp)_2Br_2$.* 1 mmol of $CuBr_2$ was dissolved in 10 mL of ethanol and put in an Erlenmeyer flask fitted with air-cooled reflux condenser. 2 mmol of 3bp, dissolved in 20 mL of ethanol, were added to the hot solution. A green precipitate formed. The solution was filtered. The solid was re-dissolved in hot ethanol (20 mL) and 8 mL of H_2O were added. Thin green needle-like crystals formed within 1 day. A crystal of a suitable size was selected and used for X-ray data collection. *(d) Bis(3-bromopyridine)dichlorocopper(II), $Cu(3bp)_2Cl_2$.* 0.5 mmol of $CuCl_2.2H_2O$ was added to 1 mmol of the 2bp, dissolved in 20mL of butanol, which was heated and stirred for 30 minutes. A blue-white precipitate formed. The solution was filtered, and the precipitate was transferred to a test tube, and was then filled with acetonitrile. The test tube was incubated in a temperature gradient crystal growth apparatus and after 1 week, blue needle like crystals formed. One of these crystals was used for data collection.

Crystal Structure Determination.

The diffraction data sets for four complexes were collected at 81-85 K on a Bruker 3-circle platform diffractometer equipped with SMART APEX CCD detector. Frame data were acquired with the SMART[12a] software, and the frames were processed using SAINT[12b] software to give hkl file corrected for Lp/decay. Absorption corrections were performed using SADABS.[12c] The SHELXTL[12d] package was used for the structure solution, refinement and the Figure preparation. The structures were refined by least square method on F^2. Hydrogen

atoms were placed at the calculated positions. The structure of $Cu(3bp)_2Br_2$ was solved as a rotational twinned structure with a twin ratio of 81:19. The twin law is 1, 0, 0.004, 0, 1, 0, 0, 0, -1. Data collection parameters and refinement results are given in Table 1.

Table 1. Summary of data collection and refinement parameters for the $Cu(nbp)_2X_2$ complexes.

Crystal	**$Cu(2bp)_2Cl_2$**	**$Cu(2bp)_2Br_2$**	**$Cu(3bp)_2Cl_2$**	**$Cu(3bp)_2Br_2$**
Formula	$C_{10}H_8Br_2Cl_2CuN_2$	$C_{10}H_8Br_4CuN_2$	$C_{10}H_8Br_2Cl_2CuN_2$	$C_{10}H_8Br_4CuN_2$
Formula Weight	450.44	539.36	450.44	539.36
Diffractometer	SMART	SMART	SMART	SMART
D_{calc} (Mg/m^3)	2.184	2.590	2.352	2.671
T(K)	85	85	83	81
Crystal system	Monoclinic	Triclinic	Monoclinic	Monoclinic
Space group	$P2_1/n$	P-1	$P2_1/c$	$P2_1/c$
a (Å)	8.490(2)	6.066(1)	3.818(1)	3.936(2)
b (Å)	6.386(1)	7.370(2)	13.831(3)	13.929(6)
c (Å)	12.712(3)	8.639(2)	12.050(2)	12.236(5)
α (º)	90	100.94(3)	90	90
β (º)	96.46(3)	95.16(3)	91.53(3)	90.337(9)
γ (º)	90	112.10(3)	90	90
V ($Å^3$)	684.8(3)	345.8(2)	636.1(2)	670.7(5)
μ mm^{-1}	7.796	13.113	8.394	13.519
Ind. reflections	1235	1250	1157	1199
R(int)	0.0284	0.0263	0.0363	0.0441
Z	2	1	2	2
Goodness of fit	1.084	1.064	1.075	1.037
R_1[a] [I > 2σI]	0.0249	0.0346	0.0229	0.0661
wR_2[b] [I > 2σI]	0.0614	0.0915	0.0566	0.1961

[a] $R_1 = \sum| |F_o| - |F_c| | / \sum|F_o|$.

[b] $wR_2 = \{\sum[w(F_o^2 - F_c^2)^2] / \sum[w(F_o^2)^2]\}^{1/2}$

RESULTS.

Description of the Molecular Structure of $Cu(nbp)_2X_2$.

The structure of the $Cu(2bp)_2X_2$ and $Cu(3bp)_2X_2$ series are all based on the presence of *trans* planar CuN_2X_2 geometries, as seen in Figure 1. However the 2bp and 3bp compounds show a distinctly different development of their three dimensional architecture, due to factors related to the isomeric nature of the bromopyridine ligands. Thus the 2bp compounds form isolated CuL_2X_2 species that are linked into chains by C-Br···X interactions. In contrast, in the 3bp structures, the monomeric species expand their coordination sphere *via* Cu···X semi-coordinate bonds to form $[Cu(3bp)_2X_2]_n$ chains. These chains are subsequently linked into a three dimensional framework *via* the C-Br···X synthons.

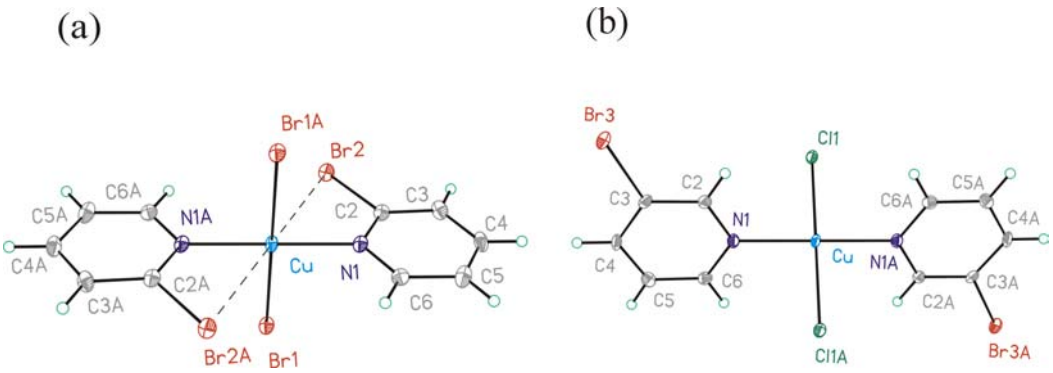

Figure 1. The molecular units of two complexes; (a) $Cu(2bp)_2Br_2$ and (b) $Cu(3bp)_2Cl_2$. The molecular structure of $Cu(2bp)_2Cl_2$ and $Cu(3bp)_2Br_2$ are similar to $Cu(2bp)_2Br_2$ and $Cu(3bp)_2Cl_2$ respectively. Thermal ellipsoids are shown at 50% probability.

These differences in the development of the supramolecular architectures can be traced to the orientation of the planes of the pyridine rings relative to the coordination planes that is found in the two series. In the 3bp complexes, the pyridine rings are rotated out of the coordination plane by $\Phi_{AB} = 60.7°$ (Table 2), due to repulsion between the halide ions and the protons on the 2 and 6 positions of the ring. However, despite this rotation, the 5th and 6th

coordination sites remain accessible and a stacked monomer chain structure (Figure 2b) is formed *via* formation of the semi-coordinate Cu···X bonds. For the 2bp complexes, in contrast, apparent attractive interactions exist between the Cu^{2+} centers and the bromine atoms on the rings, causing the coordination planes and the pyridine rings to be essentially perpendicular (Figure 1a). This leads to short Cu···Br contacts (3.187(1) and 3.071(1) Å for the Cl and Br complexes respectively), although the geometric restrictions of the 2bp ligands causes the N-Cu···Br angles to be roughly 60°. The influence of the attractive nature of this interaction can be seen in the Cu-N-C2 and Cu-N-C6 angles, where the former is smaller than the latter. However, the Cu-X and Cu-N bond lengths are shorter in the 2bp complexes than in the 3bp series (Table 2), indicating these semi-coordinate type interactions are weaker than the Cu···X interactions in the 3bp complexes.

Table 2. Selected angles (º) and distances (Å) in the Cu(*n*bp)$_2$X$_2$ structures.

Compound	$Cu(2bp)_2Cl_2$	$Cu(2bp)_2Br_2$	$Cu(3bp)_2Cl_2$	$Cu(3bp)_2Br_2$
Cu-N (Å)	1.988(3)	1.979(3)	2.011(3)	2.002(16)
Cu-X (Å)	2.248 (1)	2.422(1)	2.301(1)	2.437(2)
X-Cu-N (º)	90.08(7)	89.90(10)	90.16(7)	90.9(4)
C-Br (Å)	1.891(3)	1.897(4)	1.895(3)	1.900(18)
Cu···X (Å)	3.187(1)	3.071(1)	3.008(1)[a]	3.144(2)[a]
Cu-X···Cu (º)	-	-	90.98(3)[a]	88.76(6)[a]
Br···X (Å)	3.358(1)	3.460 (1)	3.622 (1)	3.627 (3)
C-Br···X (°)	167.89(9)	163.36 (13)	158.09 (9)	160.86 (57)
Br···X-Cu (°)	103.38 (3)	104.68 (3)	120.64 (3)	118.01 (7)
Φ_{AB} (º) [b]	91.6	90.1	60.7	60.4

[a] Symmetry transformations used to generate equivalent atoms; –1+x, y, z.

[b] Angle between the CuN_2X_2 coordination plane and the plane of the pyridine rings.

Description of the Supramolecular C-Br···X-Cu Synthons and the Supramolecular Structure in $Cu(nbp)_2X_2$ Crystals.

Based on the bromine···halide interactions, two of the complexes, $Cu(2bp)_2Cl_2$ and $Cu(2bp)_2Br_2$, form chain structures that extend along the *b* axis for the former and along *a* axis for the latter (Figure 2). Though structurally different, the two chain structures are topologically similar. The bromine···halide synthons are characterized by bromine···halide distance ~0.24 Å less than the sum of the r_{vdW} (Table 2, r_{vdW} in Å; Cl = 1.75 and Br = 1.85).[13] In both compounds, these chains form a layer structure in the *ab* plane. For $Cu(2bp)_2Cl_2$, the chains are linked *via* C-H···X hydrogen bonds as well as π-π stacking, while, in the case of $Cu(2bp)_2Br_2$, the chains are connected *via* hydrogen bonds only (Figure 3). The layers of $Cu(2bp)_2Cl_2$ pack *via* C-H····X hydrogen bonds, while in $Cu(2bp)_2Br_2$, the layers pack using π-π interactions to form the 3D structure.

The $Cu(3bp)_2X_2$ chains are formed *via* the Cu···X semi-coordinate bond. Their three dimensional structure is created *via* bromine···halide contacts as illustrated in Figure 4. In contrast to $Cu(2bp)_2X_2$, the bromine···halide synthons in the $Cu(3bp)_2X_2$ are characterized by bromine···halide distances almost equal to the sum of r_{vdW}. Significantly the C-Br···X angles remain essentially linear as in $Cu(2bp)_2X_2$ (Table 2). The role of π-π stacking and C-H····X hydrogen bond is to facilitate the packing of these chains into the final three dimensional structure.

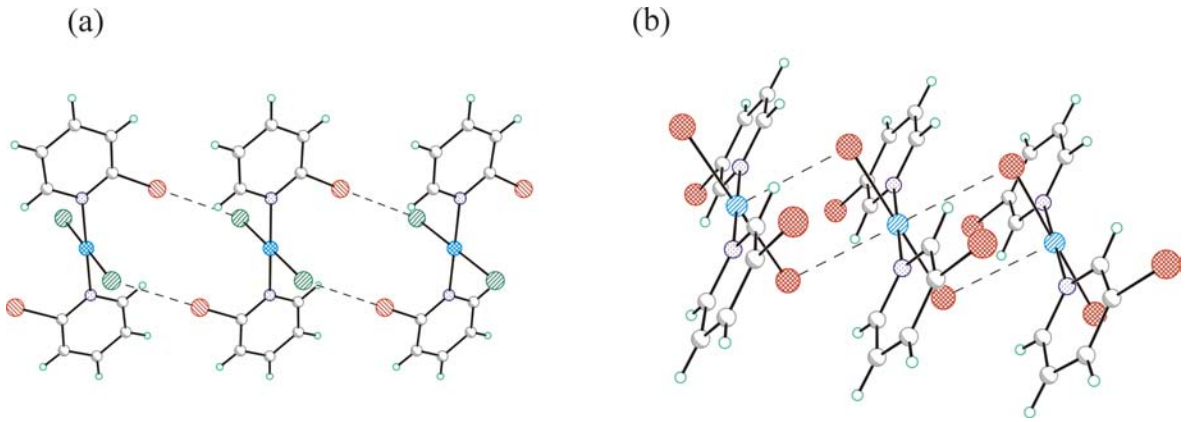

Figure 2. The network chain structures in (a) $Cu(2bp)_2Cl_2$, where the chains run parallel to the *b* axis, and (b) $Cu(3bp)_2Br_2$, where the chains run parallel to the *a* axes. $Cu(3bp)_2Cl_2$ and $Cu(3bp)_2Br_2$ have isomorphous structures.

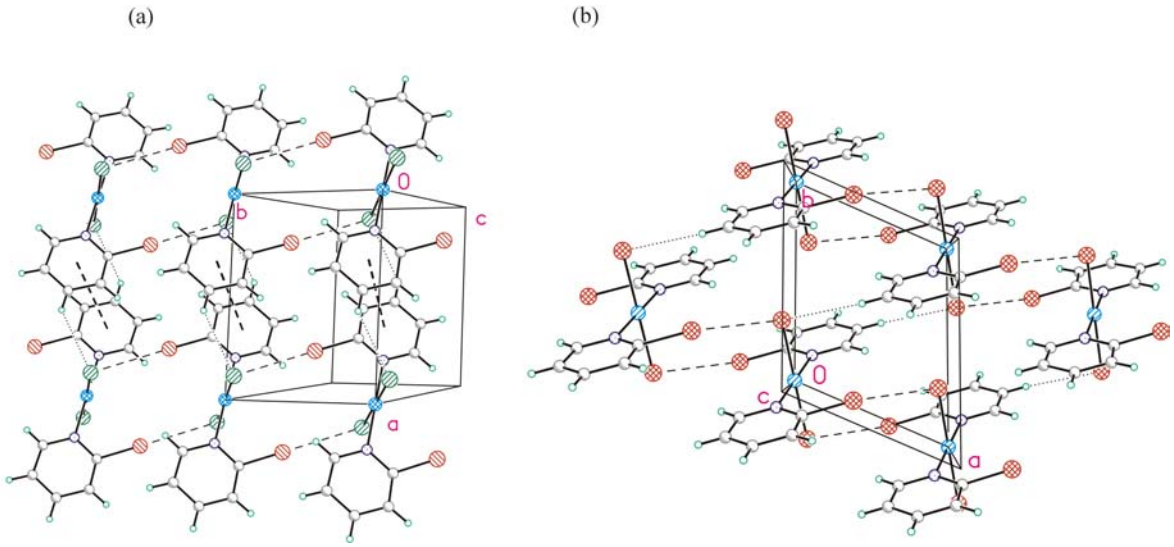

Figure 3. The layer structures; (a) $Cu(2bp)_2Cl_2$, where the layers lie parallel to the ab plane. (b) $Cu(2bp)_2Br_2$, where the layers also lie parallel to the ab plane. The bromine···halide synthons, hydrogen bond and the connection between the two centroids are represented by dashed, dotted and heavier dashed lines respectively.

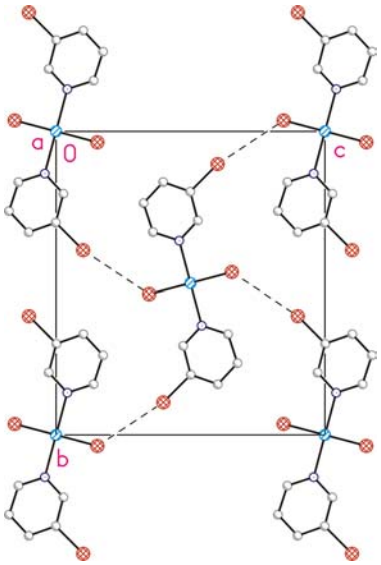

Figure 4. The stacking diagram of $Cu(3bp)_2Br_2$ viewed down the *a* axis. The chains, described in Figure 2b, interact *via* bromine···halide contacts to form the three dimensional crystal structure. The structures of $Cu(3bp)_2Br_2$ and $Cu(3bp)_2Cl_2$ are isomorphous. Hydrogen atoms are omitted for clarity.

The bromine···halide contacts are weaker in the $Cu(3bp)_2X_2$ complexes than in $Cu(2bp)_2X_2$ as indicated by the distances between the bromine atom and halide ion and the synthon angles. The bromine···halide distances are ~0.24 Å less than and almost equal to the sum of their r_{vdW} for $Cu(2bp)_2X_2$ and $Cu(3bp)_2X_2$ (Table 2). The Cu-X···Br angle is ~15° larger in $Cu(3bp)_2X_2$ than in $Cu(2bp)_2X_2$. In contrast, the C-Br···X angles in the four complexes are close to linear, with those in $Cu(2bp)_2X_2$ closer to linearity than for $Cu(3bp)_2X_2$,with an average difference ~6°.

DISCUSSION

The Electrostatic Model.

The properties of the C-Br···X synthon in these, and other structures can be explained on the basis of an electrostatic model. Theoretical calculations have shown that the charge

distribution on the halogen atom in the R-X bond (R = phenyl, methyl, pyridyl; X = Cl, Br, I) is distributed so that there is a positive electrostatic potential end cap on the halogen atom.[14, 16] Therefore, the electrostatic model predicts the negatively charged halide anion, or any negatively charged species, to face this positive potential. Consequently, a linear C-Br···X directionality is expected. Investigation of Cambridge Structural Data Base (CSD)[§] for C-Br···X-M and C-Br···X^- contacts, where M = transition metal, C = sp^2 hybridized carbon atom and X = halide anion, showed that the C-Br···X contacts are essentially characterized by almost linear geometry (i.e. most of contacts have C-Br···X angle between 150-180°) (Figure 5). For the C-Br···X^- contacts, a general trend is clear where the contact distances are shortest for the angles closest to 180°. No contacts of the types C-Br···F-M and C-Br···F^- were found.

The electrostatic model can be generalized to explain related synthons and to explain C-X interactions with negatively charged atoms other than the halide anions. In this context, Lommerse *et al*., based on *ab initio* quantum mechanical calculations, showed that C-X···El synthons, (El = N, O, and S), (X = Cl, Br, or I) are mainly controlled by electrostatic interactions.[14a] Recently, the experimental electron density showed that the C-I···O and C-I···N are essentially electrostatic in 4,4'-dipyridyl-N,N'-dioxide and 1,4-diiodotetrafluorobenzene, and the complex of (E)-1,2-bis(4-pyridyl)ethylene with 1,4-diiodotetrafluorobenzene.[15b,15c] This modeling agrees with the proposed electrostatic model for the aryl-Br···X synthon. More recently, Zordan *et al.* showed that the electrostatic effects plays a significant role in determining the crystal structure of $M(3bp)_2Cl_2$ (M = Pd and Pt).

[§] CSD version 5.25 November 2003. Six filters were applied to the searches; crystallographic R factor < 0.075, no errors in the crystal structures, not disordered, not polymeric, 3D coordinate determined and no powder structures.

Factors Affecting the C-Br···X Synthons Strength.

The three structure sets (*n*BP)X, $(n\text{BP})_2CuX_4$ and $Cu(n\text{bp})_2X_2$ will be investigated to characterize the effect of electrostatic charge on the bromine···halide synthons.[10a,16] Two methods will be used to analyze electrostatic effects on the bromine···halide interaction by (a) looking at the bromine···halide distances and using these distances as a parameter to determine the relative strength of these interactions- as these distances get shorter, the bromine···halide synthons get stronger; (b) looking at the perpendicular distance between the bromine atom that is attached to the pyridine ring and the plane that is defined by the plane of the aromatic system. If the bromine···halide interaction is weak or absent, the bromine atom will be located in the plane of the aromatic system and the position of the halide anion will be arbitrary. In contrast, if the bromine···halide synthons are strong and the halide atom is located out the plane, the bromine atom is expected to be located out of the plane of the aromatic system and displaced from the plane toward the halide anion. This distortion will give information about the relative strength of the interaction. The advantage of this method over the first one is that this method prevails over complications due to the anisotropy in the r_{vdW}.

(a) The $Br\cdots X^-$ distances are (avg. = 0.28 Å, range 0.24-0.29 Å; avg. = 0.28 Å, range 0.24-0.33 Å; avg. = 0.13 Å, range –0.02-0.24 Å)[1] less than the sum of the r_{vdW} in the (*n*BP)X, $(n\text{BP})_2CuX_4$ and $Cu(n\text{bp})_2X_2$ structures, respectively. Thus, the shortening of the $Br\cdots X^-$ distances is significantly less in the neutral compounds. This is understood on the basis of the electrostatic model, since the former two salts involve charged donors and acceptors, while in the latter both complexes are neutral.

[1] only room temperature structures are used because $Br\cdots X^-$ is temperature dependent.

The electrostatic model also depicts the Br···X shortening in the $Cu(2bp)_2X_2$ structures over the $Cu(3bp)_2X_2$ structures. The halide anions in $Cu(3bp)_2X_2$ structures carry a smaller negative charge since it is bonded to two copper cations through a coordination and semi-coordinate bond. In contrast, the halide anion in $Cu(2bp)_2X_2$, is only involved in one coordination bond (i.e. it is not involved in any semi-coordinate bond) and so will carry a larger negative charge. Thus, the electrostatic attraction in $Cu(2bp)_2X_2$ is expected to be higher.

(b) In all of the studied structures, with one exception[†], the bromine atom is displaced from the plane toward the halide anion. This means the same synthon is present in all of them but with varying strength. The average ratio of deviation of the bromine atom to that of the halide anion follow the order $Cu(n\text{bp})_2X_2$ < $(n\text{BP})_2CuX_4$[10a] < $(n\text{BP})X$.[16] Only room temperature structures have been used in the study to eliminate temperature effects on intermolecular bond lengths. These perecent average deviation ratios are 1.75, 6.9, and 9.75 for $Cu(n\text{bp})_2X_2$, $(n\text{BP})_2CuX_4$[10a], $(n\text{BP})X$[16], respectively. This indicates that the Br···X^- interactions are weaker in the $Cu(n\text{bp})_2X_2$ structures that in $(n\text{BP})_2CuX_4$[10a] and $(n\text{BP})X$[16] structures.

In the two structural series ($(nBP)_2CuX_4$ and (nBP)X)), these synthons are perturbed due to the competition between these synthons with strong N-H···X^- hydrogen bonds. Thus, no conclusive statement could be said about the relative strength of these synthons in the $(n\text{BP})_2CuX_4$[10a] and $(n\text{BP})X$ structural series.

[†]This is the only case, $(4BP)_2CuBr_4$, where the bromine atom is directed toward the side of the plane of the pyridine ring that is opposite to the halide anion. This is due to the fact that the bromide anion is almost located on the plane of the pyridine ring (Table 3).

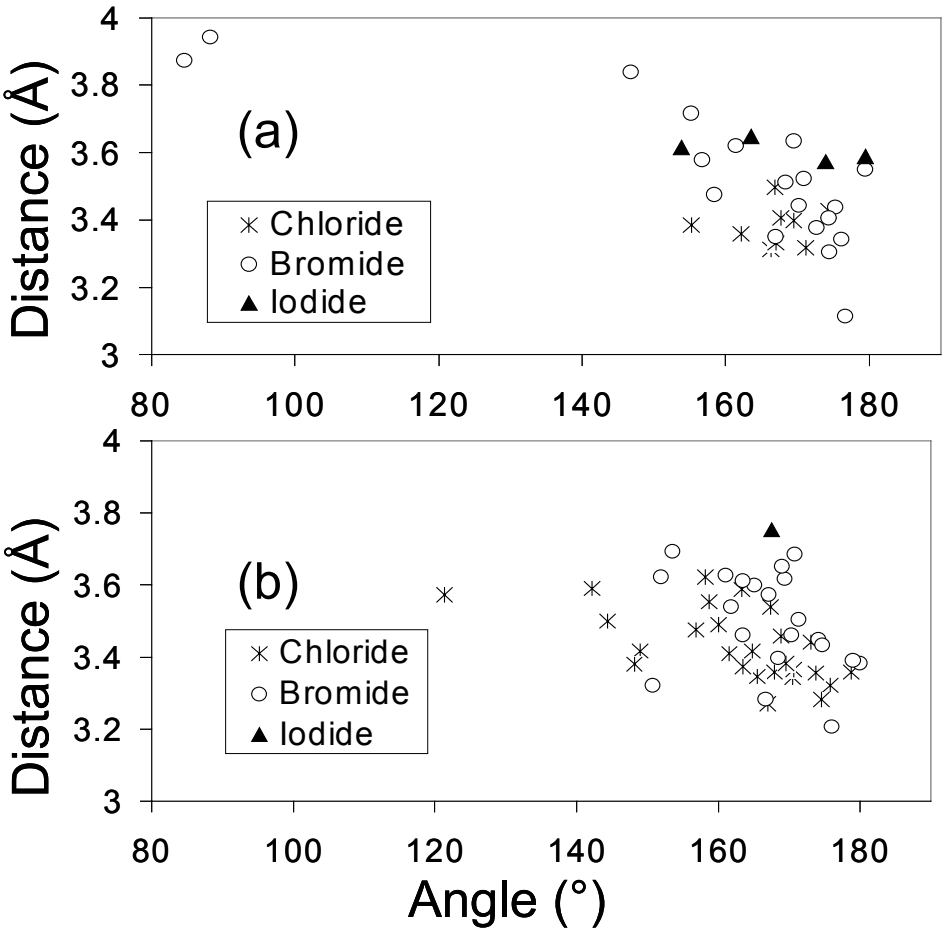

Figure 5. A scatter plot of the C-Br···X angle *vs.* (a) Br···X distance within the sum of the r_{vdW} of the bromine atom and the ionic radius of the corresponding halide anion for C-Br···X^- synthons; (b) Br···X distance within the sum of the r_{vdW} for C-Br···X-M synthons. The plots include, in addition to those obtained from CSD, the C-Br···X contact parameters in the (*n*BP)X, $(nBP)_2CuX_4$ and $Cu(nbp)_2X_2$ compounds. Ionic radii in Å; F^- = 1.33, Cl^- = 1.81, Br^- = 1.96 and I^- = 2.2.

Table 3. C-Br···X synthons distances, angles and deviations from the plane of the aromatic ring for the (*n*BP)X, $(nBP)_2CuX_4$ and Cu(*n*bp)X_2 structures.

Compound	Y···X^- (Å)	C-Y···X^- (°)	Br deviation (Å)	Halide-anion deviation (Å)	Temperature K	%Ratio Br/X^-	Reference
(2BP)Cl	3.310	171.4	0.0401	0.5912	297	6.8	16
(2BP)Br	3.407	172.4	0.0379	0.5496	297	6.9	16
(3BP)Cl	3.359	162.2	0.1735	1.4664	295	11.8	16
(3BP)Br	3.407	174.3	0.0574	0.4125	173	13.9	7a
(4BP)Cl	3.313	166.4	0.1599	1.1818	295	13.5	16
(4BP)Br	3.350	167.3	0.1763	1.1785	173	15.0	7b
$(2BP)_2CuCl_4$	3.322	175.8	0.0017	0.1096	295	1.6	10a
$(2BP)_2CuBr_4$	3.449	174.2	0.0092	0.1268	295	7.2	10a
$(3BP)_2CuCl_4$	3.283	174.5	0.0162	0.3355	295	4.8	10a
	3.271	167.0	0.0757	0.8028	295	9.4	10a
$(3BP)_2CuBr_4$	3.390	179.0	0.0959	0.2699	81	36	10a
	3.397	168.5	0.0701	0.0677	81	104	10a
$(4BP)_2CuCl_4$	3.356	173.8	0.0033	0.2048	295	1.6	10a
	3.358	178.8	0.0031	0.0184	295	16.8	10a
$(4BP)_2CuBr_4$	3.435	174.7	-0.0205	0.0641	295		10a
$Cu(2bp)_2Cl_2$	3.358	167.9	0.0122	0.7072	85	1.7	This work
$Cu(2bp)_2Br_2$	3.460	163.4	0.0381	0.8760	85	4.3	This work
$Cu(3bp)_2Cl_2$	3.622	158.1	0.0129	1.2494	83	1	This work
$Cu(3bp)_2Br_2$	3.627	160.9	0.0000	1.0686	81	0	This work

CONCLUSIONS

The above analysis indicates that the bromine···halide synthon is electrostatic in nature. The electrostatic model can be used to explain both the relative strength of the halogen···halide synthons and the linear C-Br···X angles. The importance of this model is that it helps chemists to easily predict the directionality of these synthons in the crystals and design new solid-state materials. Moreover, the similarity between the electrostatic model of C-Br···X and the C-X···El (El = N, O, and S), (X = Cl, Br, or I) model makes the electrostatic model valid to include other negatively charged atoms other than halide anions.

Both the bromine···halide distances and the distances between the bromine atom and the plane of the pyridine ring indicate that the strength of the bromine···halide synthon in the studied structures have the following order $Cu(3bp)_2X_2$ < $Cu(2bp)_2X_2$ < $(n\text{BP})_2CuX_4$ ≈ (*n*BP)X. This can be explained based on the electrostatic model of these interactions taking into account two parameters; (1) the negative charge on the halide anion and (2) the positive charge on the bromopyridinium cation. The positive electrostatic potential cap on the bromine atom explains the directionality of these synthons (C-Br···X angles (~180°)). The halide anions are located in a position to meet this positive potential head-on and hence form a linear arrangement. Even in the uncharged species $Cu(3bp)_2X_2$ and $Cu(2bp)_2X_2$, the strength of C-Br···X is correlated to the induced charges on the halide anion. Although electrostatic differences cause C-Br···X distances to vary systematically, the same linear directionality is observed in all. This demonstrates that the same synthon is present in all despite the varying strength. Thus, even the weakest C-Br···X interaction can be used to influence the crystal structure and in crystal engineering. But, it should be

kept in mind that many other factors play a major role in determining the crystal structure and distances between atoms in crystals e.g. the shape of the molecules, the stacking interactions, the relative orientations of the atoms with respect to each other (angles), the anisotropy in r_{vdW} and other intermolecular forces.

To test if the electrostatic model of the bromine···halide synthon can be generalized to halogen···halide synthons, we are performing an *ab initio* quantum mechanical calculations to model the halogen···halide interactions in the simple salts of (*n*YP)X, Y = F, Cl or Br, X= F, Cl, Br or I, and to calculate their relative strength. The results indicated the strength of the C-Br···X synthons follow the order $I^- < Br^- < Cl^- < F^-$ which in agreement with our proposed electrostatic model. These calculations will be compared to the real crystal structures in an effort to predict the structure of similar compounds and will be presented at a later date.

Supporting Information Available: The stacking interactions parameters, the hydrogen bond C-H···X parameters, stacking diagram of (a) $Cu(2bp)_2Cl_2$ and (b) $Cu(2bp)_2Br_2$ and crystal data for all the four compounds in CIF format. These materials are available free of charge the Internet at http://pubs.acs.org.

Acknowledgement: Work supported in part by ACS-PRF 34779-AC. The Bruker (Siemens) SMART CCD diffraction facility was established at the University of Idaho with the assistance of the NSF-EPSCoR program and the M. J. Murdock Charitable Trust, Vancouver, WA, USA.

REFERENCES.

1. (a) Desiraju, G. R. *Nature* **2001**, *412*, 397-400. (b) Desiraju, G. R. *Crystal Engineering, The Design Of Organic Solids,* Elsevier Science Publishers B. V. **1989**. (c) Desiraju, R. G. *Angew. Chem. Int. Ed. Engl.* **1995**, *34*, 2311-2327. (d) Brammer, L. *Chem. Soc. Rev.* **2004**, *33*, 476-489. (e) Braga, D.; Brammer, L.; Champness, N. *CrystEngComm.* **2005**, *7*, 1-19.

2. (a) Aakeröy Ch. B.; Beatty A. M. *Aust. J. Chem.* **2001**, *54*, 409-421. (b) Brammer, L.; Bruton, E. A.; Sherwood, P. *Cryst. Growth Des.* **2001**, *1*, 277-290. (c) Lutz, H. D. *J. Mol. Struct*. **2003**, *646*, 227-236.

3. (a) Walsh, R. B.; Padgett, C. W.; Metrangolo, P.; Resnati, G.; Hanks, T. W.; Pennington, W. T. *Cryst. Growth Des.* **2001,** *1*, 165-175. (b) Ouvrard, C.; Questel, J.; Berthelot, M.; Laurence, Ch. *Acta Cryst.* **2003**, *B59*, 512-526. (c) Forni, A.; Metrangolo, P.; Pilati, T.; Resanti, G. *Cryst. Growth Des.* **2004**, *4*, 291-295. (d) Berski, S.; Ciunik, Z.; Drabent, K.; Latajka, Z.; Panek, J. *J. Phys. Chem. B.* **2004**, 108, 12327-12332. (e) Santis, A.; Forni, A.; Liantonio, R.; Metrangolo, P.; Pilati, T.; Resnati, G. *Chem. Eur. J.* **2003**, *9*, 3974-3983. (f) Wang, W.; Wong, N.; Zheng, W.; Tian, A. *J. Phys. Chem. A*. **2004**, *108*, 1799-1805**.** (g) Metrangolo, P.;Neukirch, H.; Pilati, T.; Resnati, G. *Acc. Chem. Res.* **2005**, *38*,386-395.

4. Braga, D.; Grepioni, F. *New J. Chem*. **1998**, *22*, 1159-1161. (b) Desiraju, G. R.; Stiener, T. *The Weak Hydrogen Bond in Structural Chemistry and Biology* (Oxford Univ. Press. Oxford **1990**). (c) Langley, P. J.; Hulliger, J.; Thaimattam. R.; Desiraju, G. R. *New J. Chem*., **1998**, *22*, 1307-1309.

5. (a) Desiraju, G. R.; Parthasarathy, R. *J. Am. Chem. Soc.* **1989**, *111*, 8725-8726. (b) Jagarlapudi, A. R.; Sarma, P.; Desiraju G. *Acc. Chem. Res.* **1986**, 19, 222-228.

6. (a) Sinnokrot, M. O.; Sherrill, D. C. *J. Am. Chem. Soc.* **2004**, *126*, 7690-7697. (b) Sinnokrot, M. O.; Sherrill, D. C. *J. Phys. Chem.* **2003**, *107*, 8377-8379. (c) Sinnokrot, M. O.; Valeev, E. F.; Sherrill, D. C. *J. Am. Chem. Soc.* **2002**, *124*, 10887-10893. (d) Hunter, Ch. A.; Sanders, K. M. *J. Am. Chem. Soc.* **1990**, 112, 5525-5534. (e) Desiraju, G. R.; Gavezzotti, A. *J. Chem Soc. Chem. Commun*. **1989**, 621-623.

7. (a) Freytag, M.; Jones, P. G. *Zeit. Naturfor. B: Chem. Sci.* **2001**, *56*, 889-896. (b) Freytag, M.; Jones, P. G.; Ahrens, B.; Fischer, A. K. *New J. Chem.* **1999**, *23*, 1137-1139.

8. (a) Logothetis, Th.; Meyer, F.; Metrangolo, P.; Pilati, T; Resnati, G. *New. J. Chem.* **2004**, *28*, 760-763. (b) Kuhn, N.; Abu-Rayyan A.; Eichele, K.; Schwarz, S.; Steimann, M. *Inorg. Chim. Acta* **2004**, *357(6)*, 1799-1804. (c) Kuhn, N.; Abu-Rayyan, N. A.; Eichele, K.; Piludu, C.; Steimann, M. *Z. Anorg Allg. Chem.* **2004**, *630(4)*, 495-497.

9. Taraba, J.; Zak, Z. *Inorg. Chem.* **2003**, *42*, 3591-3594.

10. (a) Willett, R. D.; Awwadi, F. F.; Butcher, R.; Haddad, S.; Twamley, B. *Cryst. Growth Des.* **2003**, *3*, 301-311. (b) Brammer, L.; Espallargas, G. M.; Adams, H. *CrystEngComm*. **2003**, *5(60)*, 343-345. (c) Haddad, S.; Awwadi, F.; Willett, R. D.

Cryst. Growth Des. **2003**, *3(4),* 501-505. (d) Zordan, F.; Brammer, L.; Sherwood, P. *J. Am. Chem. Soc*. **005**, *127*, 5979-5989.

11. (a) Domercq, B.; Devic, T.; Fourmigue, M.; Auban-Senzier, P.; Canadell, E. *J. Mater. Chem*. **2001**, *11*, 1570-1575. (b) Farina, A.; Meille, S. V.; Messina, T. M.; Metrangolo, P.; Resnati, G.; Vecchio, G. *Angew. Chem. Int. Ed.* **1999**, *38*, 2433-2436.

12. (a) SMART, Version 5.625, Bruker AXS Inc. Madison, WI, USA, **2002**. (b) SAINTPlus V. 6.22, Bruker AXS, Inc. Madison, WI, USA, **2001**. (c) SADABS Version 2.03, Bruker AXS Inc. Madison WI, USA, **2001**. (d) SHELXTL (XCIF, XL, XP, XPREP, XS), Version 6.10, Bruker AXS Inc. Madison, WI, USA **2002**.

13. Bondi, A. *J. Phys. Chem.* **1964**, *68*, 441-451.

14. Bosch, E.; Barnes, C. L. *Cryst. Growth Des.* **2002**, *2*, 299-302.

15. Lommerse, J. P.; Stone, A. J.; Taylor, R.; Allen, F. H. *J. Am. Chem. Soc.* **1996**, *118*, 3108-3116. (b) Bianchi, R.; Forni, A.; Pilati, T. *Acta Cryst.* **2004**, *B60*, 559-568. (c) Bianchi, R.; Forni, A.; Pilati, T. *Chem. Eur J*, **2003**, *9*, 1631-1638.

16. Willett, R. D.; Awwadi, F.; Twamley, B. *J. Am. Chem. Soc.* (to be submitted).

SYNOPSIS

The Electrostatic nature of Aryl-Bromine···Halide Synthons: The Role Of Aryl-Bromine···Halide Synthon in the Crystal Structures of the *Trans*-bis(2-bromopyridine)dihalocopper(II) and *Trans*-bis(3-bromopyridine)dihalocopper(II) Complexes.

Firas F. Awwadi, Roger D. Willett, Salim F. Haddad, and Brendan Twamley.

The role of the bromine···halide synthons in the crystal structures of the *trans*-bis(*n*-bromopyridine)dihalocopper(II) salts is described, and an electrostatic model is proposed to quantify this C-Br···X synthon in these and other compounds. Two parameters are used to characterize its strength: the Br···X distance and the deviation of the Br atom from the plane of the pyridine ring.

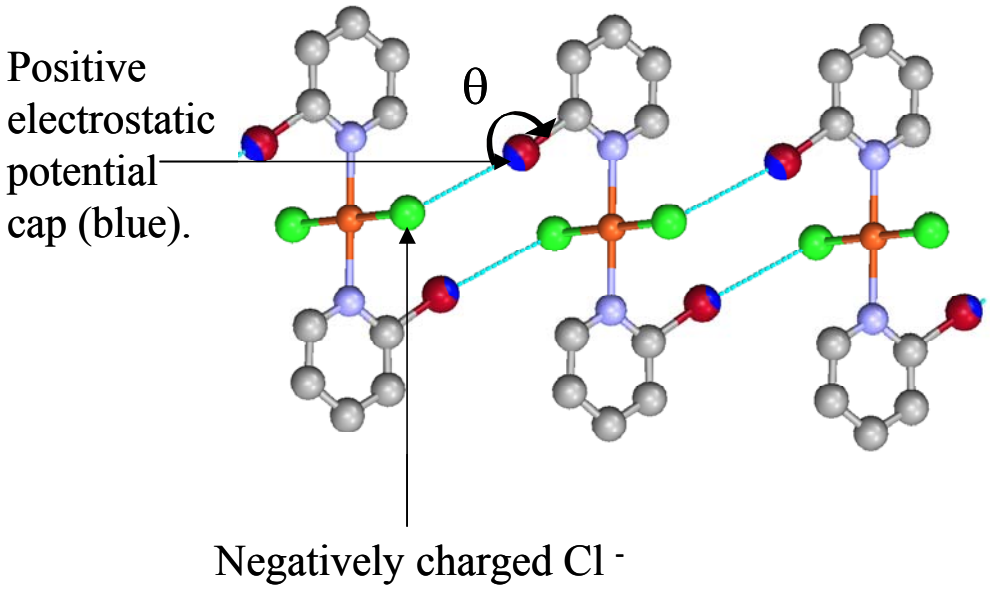

SUPPORTING INFORMATION

The Electrostatic nature of Aryl-Bromine···Halide Synthons; The Role Of Aryl-Bromine···Halide Synthon in the Crystal Structure of the Trans-bis(2-bromopyridine)dihalocopper(II) and Trans-bis(3-bromopyridine)dihalocopper(II) Complexes.

Firas F. Awwadi[†], *Roger D. Willett**[†], *Salim F. Haddad*[‡]

and Brendan Twamley[§]

[†]Department of Chemistry, Washington State UniversityPullman, WA 99164 USA.

[‡]Department of Chemistry, University of Jordan, Amman 11942, Jordan, University

[§]Research Office, University of Idaho, Moscow, ID 83844 USA

*rdw@mail.wsu.edu

(a)

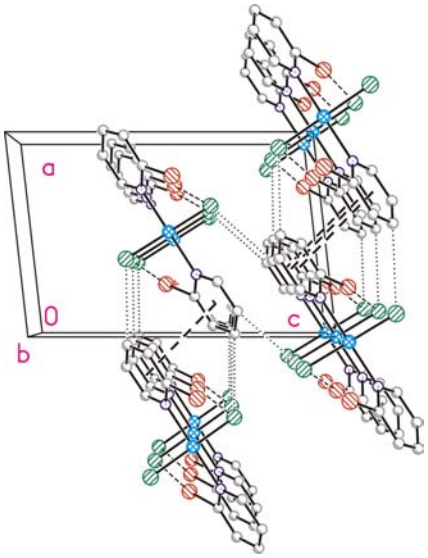

(b)

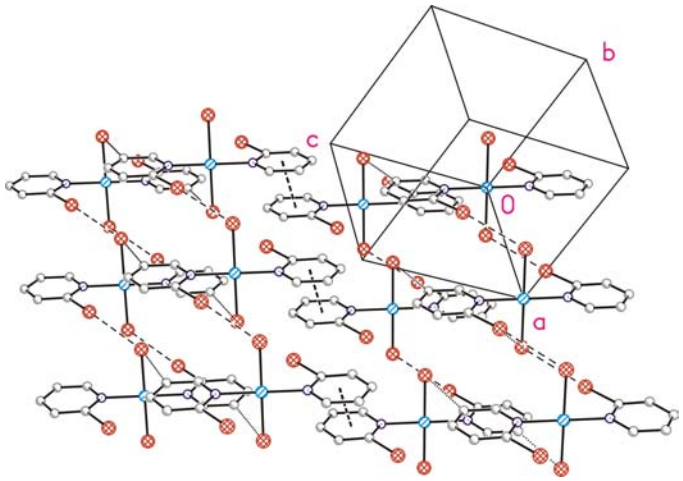

Figure S. Stacking diagram of (a) $Cu(2bp)_2Cl_2$ and (b) $Cu(2BP)_2Br_2$. The previously described layers in Figure 3 stacks *via* hydrogen for the former and π-π stacking for the latter to form the 3d dimensional structure. Hydrogen atoms are not shown for clarity.

Table 1S. Stacking interaction parameters of $Cu(nbp)_2X_2$ crystal structures.

Parameter / Compound	d_{x-x}(Å)[a]	$d_{\perp}$(Å)[b]	θ°
$Cu(2bp)_2Cl_2$	3.890	3.385	27.23
$Cu(2bp)_2Br_2$	4.435	3.487	38.17
$Cu(3bp)_2Cl_2$	3.818	3.521	22.75
$Cu(3bp)_2Br_2$	3.939	3.606	23.72

[a] d_{x-x} is the centroid to centroid distance between the pyridine aromatic systems.

[b] $d\perp$ is the perpendicular distances between the planes.

[c] θ is the angle between the line connecting the two centroids and the normal to the plane of the aromatic system.

Table 2S. The hydrogen bond C-H···X parameters of $Cu(nbp)_2X_2$ crystal structures.

parameter / Compound	Hydrogen bond	d(H...X) (Å)	d(C...X) (Å)	<(CHX)°
$Cu(2bp)_2Cl_2$	C(4)-H(4A)···Cl(1)[a]	2.83	3.538(3)	131.9
	C(5)-H(5A)···Cl(1)[b]	2.82	3.508(3)	130.0
$Cu(2bp)_2Br_2$	C(5)-H(5A)···Br(1)[c]	2.91	3.831(5)	162.3
	C(3)-H(3A)···Br(2)[d]	3.01	3.933(4)	163.5
$Cu(3bp)_2Cl_2$	C(5)-H(5A)···Cl(1)[e]	2.91	3.607(3)	132.5
	C(2)-H(2A)···Cl(1)[f]	2.76	3.397(3)	126.4
	C(6)-H(6A)···Cl(1)[g]	2.79	3.427(3)	126.9
$Cu(3bp)_2Br_2$	C(5)-H(5)···Br(1)[h]	2.93	3.649(15)	133.7
	C(2)-H(2)···Br(1)[f]	2.79	3.460(15)	128.7
	C(6)-H(6)···Br(1)[g]	2.79	3.495(15)	131.6

Symmetry transformations used to generate equivalent atoms:

[a] -x+1, -y, -z. [b] x+1/2, -y+1/2, z-1/2 . [c] x+1, y+1, z. [d] -x-1, -y,-z-1. [e] x, -y-1/2, z+1/2 . [f] x-1, y, z . [g] x+1, -y, -z. [h] x, -y-1/2, z-1/2.

CHAPTER SIX

CONCLUSIONS

Our studies on the nature of halogen···halogen and halogen···halide synthons, both theoretical and crystallographic, indicate that these synthons are controlled by electrostatics. An electrostatic model was proposed to describe these synthons. This model was based on two ideas; (a) the calculated electrostatic potential shows the presence of a positive potential end cap and a negative electrostatic potential ring on the π region of the halogen atom in C-Y bond where (Y = Cl, Br, I); (b) the electron density is anisotropically distributed around the halogen atom. Therefore, the halogen atom has two different radii; a short one along the C-Y bond and a longer one perpendicular to it.

In chapter one, we showed that the above electrostatic model describes the observed arrangement in halogen···halogen contacts. According to the electrostatic model, the presence of the energy minimum in the potential energy diagram of two interacting halogen atoms (R-Y···Y-R) dictates that the negative electrostatic ring should face the positive electrostatic end cap. In view of this, two energy minima are expected between the halogen atoms. These minima occur at the following geometries; (i) $\theta_1 = \theta_2$ = ca. 150° with a torsion angle of (C-Y···Y-C) Φ = 180° (ii) θ_2 = 180° and θ_1 = 90°. Hereafter the former will be called type (i) and the latter type (ii) interactions. Type (ii) interactions were ignored in our study due to the

fact that in this arrangement, the interaction of the halogen atom with the organic moiety of the other molecule cannot be ignored. In type(i) interactions the value of $\theta_1 = \theta_2$ = ca. 150° was determined using the calculated potential energy diagram and experimental data within the sum of the van der Waals radii (r_{vdW}). The calculated energy diagram shows an energy minimum at 150°; the number of contacts within r_{vdW} shows a maximum between 140-160 for all halogen···halogen contacts except fluorine.

The effects of several factors on the relative strength of halogen···halogen contacts have been studied using type (i) interactions;

(a) The type of the halogen atom. Halogen···halogen contacts are stronger in the heavier congener halogens. For example, in halomethane dimers, chlorine···chlorine contacts are weak (energy of interaction ca. - 2.6 kJ/mol), iodine-iodine interactions are stronger (ca. – 7.6kJ/mol).

(b) The hybridization of the *ipso* carbon. Halogen···halogen interactions are strongest when the halogen atom is attached to sp^2 hybridized atom and weakest when attached to sp^3 hybridized one. The energy of two interacting chlorobenezene molecules is ca. -5.2KJ/mol. Theoretical calculations show that, as the hybridization of the *ipso* carbon changes from sp^3 to *sp*, θ becomes more acute. This trend is confirmed experimentally for sp^3 and sp^2. However, no halogen···halogen contacts of the type C(*sp*)-Y···Y-C(*sp*) has been observed (C(*sp)* = *sp* hybridized carbon atom).

(c) Adding extra electronegative atoms to the *ipso* carbon can reinforce the halogen···halogen contact.

The electrostatic model also explains halogen···halide contacts. In Chapter 2, these interactions are characterized by a linear C-Y···X^- geometry and Y···X^- separation distance

less than the sum of r_{vdW} of the halogen atom and the ionic radii of the halide anion. The presence of a positive electrostatic potential end cap on all halogen atoms except fluorine, explains the linear arrangement of the halogen···halide contact. The halide anion confronts the positive cap and forms a linear arrangement. The strength of these synthons varies from weak or non-existing (C-F···X^- and H_3C-Cl···X^-) to very strong (e.g. 3dF^-, energy of interaction ca. -153kJ/mol). Four main factors are found to influence the strength of the halogen···halide contacts;

(a) The type of halogen atom. The calculated energies show that the strength of the C-Y···X^- interaction follows the order I > Br > Cl > F for the halogen Y. Experimentally, this trend is supported by crystallographic data.

(b) The type of the halide anion. Calculations show that the lighter the halide anion the stronger C-Y···X^- contacts. Based on the studied structures it is not possible to confirm this trend experimentally.

(c) The hybridization of the *ipso* carbon. Theoretical calculations show that, as the hybridization of the carbon atom changes from sp^3 to *sp*, the energy of the interaction increases. Experimentally, r_{exp}* values support this behavior, and r_{exp} values follow the order C(sp^3)-Y···X^- > C(sp^2)-Y···X^- > C(*sp*)-Y···X^-.

(d) Addition of greater electronegative substituents to the organic group. From calculations, replacing the phenyl group with a pyridyl group increases the strength of these contacts. Calculations also show that charge assisted halogen···halide synthons are of comparable strength to simple halogen···halide interactions.

---

* r_{exp} = [(Y···X distance, exp) / (Σ r_{vdW} of the halogen atom and the ionic radii of the halide anion)]×100%

In chapter one and two we proved that halogen···halogen and halogen···halide interactions are electrostatic in nature. These two synthons represent two extreme cases; in the former, both halogen atoms carry the same electronic charge; in the latter synthon, the halide anion carries a full negative charge. Therefore, our study has been extended by bonding the halide anion to a more electropositive atom (e.g., a metal cation) thereby decreasing the negative charge on the halide. This results in C-Y···X-M synthons.

In Chapter 3 and Chapter 4, C-Y···X-M synthons are characterized by a linear C-Y···X angle. These types of synthons are investigated in two type of complexes; in the first type ($(n\text{BP})_2\text{CuX}_4$ and $(n\text{CP})_2\text{CuX}_4$)) ($n\text{CP}^+$ = *n*-chloropyridinium; ($n\text{BP}^+$ = *n*-bromopyridinium; n = 2, 3, or 4; X = Cl^- or Br^-), the halogen atom is bonded to positively charged species and the halide anion is bonded to a negatively charged species. In the second type ($Cu(n\text{bp})_2X_2$) ($n$bp = *n*-bromopyridine; n = 2 or 3) , the halogen atom and the halide anion are bonded to a neutral species. Experimental results indicate that halogen···halide synthons are stronger in $(n\text{BP})_2\text{CuX}_4$ compared to $Cu(n\text{bp})_2X_2$. Also, these contacts are more prevalent with the heavier halogen congeners. There are many contacts in $(n\text{BP})_2\text{CuX}_4$ (X = Br) compared to $(n\text{CP})_2\text{CuX}_4$ (X = Br). This lends additional support to our electrostatic model.

Pericyclic organic reactions have been controlled using hydrogen bonding and halogen···halogen interactions. Our study shown the halogen···halide interaction is of comparable strength to a strong hydrogen bond. These metal complexes can potentially be used as a template for pericyclic reactions. The synthon can also potentially be used to direct fundamental crystallization and can impact crystal engineering methods as much as directed hydrogen bonding has done over the years. In conclusion, the electrostatic model we propose,

can be utilized in the *a priori* prediction of the directionality of these contacts in crystal structures. This can be another useful tool in the crystal engineer's toolkit.